
Characterization of the Dpb11-Slx4 Complex and its Role in DNA Repair

DISSERTATION DER FAKULTÄT FÜR BIOLOGIE
DER LUDWIG-MAXIMILIANS-UNIVERSITÄT MÜNCHEN



vorgelegt von
Dalia Gritenaite, M.Sc. Biologie

Februar 2015

EIDESSTATTLICHE ERKLÄRUNG

Hiermit erkläre ich an Eides statt, dass ich die vorliegende Dissertation selbstständig und ohne unerlaubte Hilfe angefertigt habe. Ich habe weder anderweitig versucht, eine Dissertation einzureichen oder eine Doktorprüfung durchzuführen, noch habe ich diese Dissertation oder Teile derselben einer anderen Prüfungskommission vorgelegt.

Dalia Gritenaite

München, den 25.02.2015

Promotionsgesucht eingereicht:

25.02.2015

Tag der mündlichen Prüfung:

18.05.2015

Erster Gutachter:

Prof. Dr. Stefan Jentsch

Zweiter Gutachter:

Prof. Dr. Wolfgang Enard

Die vorliegende Arbeit wurde zwischen Mai 2011 und Juni 2014 unter Anleitung von Dr. Boris Pfander am Max-Planck-Institut für Biochemie in Martinsried durchgeführt.

Wesentliche Teile dieser Arbeit sind in folgenden Publikationen veröffentlicht:

Gritenaite D.*, Princz L.N.*, Szakal B., Bantele S.C.S., Wendeler L., Schilbach S., Habermann B.H., Matos J., Lisby M., Brnzei D. and Pfander B. (2014). A cell cycle-regulated Slx4-Dpb11 complex promotes the resolution of DNA repair intermediates linked to stalled replication. *Genes Dev.* 28, 1604-19 *equal contribution

Princz L.N.*, **Gritenaite D.***, Pfander B. (2014). The Slx4-Dpb11 scaffold complex: coordinating the response to replication fork stalling in S-phase and the subsequent mitosis. *Cell Cycle*. 14, 488-494 *equal contribution

Note on results obtained in collaboration:

Analysis of data and generation of graphs depicted in Fig. 4.14 were performed by our collaborators B. Szakal and D. Brnzei (Istituto FIRC do Oncologia Molecolare, Milan, Italy), and in Fig. 4.3b, 4.4, 4.5, 4.17b,c, 4.25 by L. N. Princz (Max Planck Institute of Biochemistry, Martinsried, Germany).

Methods, reagents and machines used by L. N. Princz, B. Szakal and D. Brnzei are not described in this thesis but referenced in Gritenaite et al., 2014.

TABLE OF CONTENTS

1 SUMMARY	1
2 INTRODUCTION	2
2.1 Cell cycle regulation of the DNA damage response	2
2.1.1 The DNA damage response	2
2.1.2 Cell cycle kinases and their relation to DNA damage response	5
2.2 S-phase-specific DNA damage	8
2.2.1 The S-phase DNA damage.....	8
2.2.2 Bypass mechanisms of damaged DNA in S-phase	11
2.3 Mechanisms to process X-shaped DNA structures	14
2.3.1 The RecQ DNA helicases and dissolution mechanism.....	14
2.3.2 Structure-specific endonucleases and resolution mechanism	16
2.3.3 Regulation of X-shaped DNA structure resolution.....	18
2.4 The scaffold proteins in DNA damage response	20
2.4.1 Dpb11 and its complexes	20
2.4.2 Slx4 and its role in DNA repair	21
2.4.3 Rtt proteins and their role in DNA repair	22
3 AIMS OF THIS STUDY	25
4 RESULTS	26
4.1 Cdk1 regulates the interaction between Dpb11 and Slx4.....	26
4.1.1 Dpb11 BRCT3/4 are important for the interaction with Slx4.....	26
4.1.2 Phosphorylated S486 of Slx4 is important for the interaction with Dpb11	27
4.2 The Dpb11-Slx4 complex is required for the response to replication fork stalling	32
4.2.1 The <i>slx4-S486A</i> mutant is particularly sensitive to MMS	32
4.2.2 The Dpb11-Slx4 complex is crucial after replication fork stalling in S-phase..	33
4.3 The Dpb11-Slx4 complex promotes Mus81-Mms4-dependent X-shaped DNA structure resolution.....	37
4.3.1 The Dpb11-Slx4 complex is not exclusively involved in PRR or HR	38
4.3.2 The Dpb11-Slx4 complex functions in the Mus81-Mms4 pathway	44
4.3.3 Dpb11-Slx4 physically interacts with Mus81-Mms4	48
4.4 The DNA damage checkpoint regulates Dpb11-Slx4-dependent Mus81-Mms4 function	53
4.4.1 Reduced DNA damage checkpoint activation promotes DNA repair in the absence of Dpb11-Slx4 interaction.....	53

TABLE OF CONTENTS

4.4.2 Reduced DNA damage checkpoint activation promotes DNA repair by activating Mus81-Mms4	56
4.5 Dpb11-Slx4 belongs to a multi-protein complex	59
4.5.1 The Slx4-Dpb11-Mms4-Mus81 complex involves additional proteins.....	59
4.5.2 Rtt proteins have a role in the recruitment of Slx4-Dpb11-Mms4-Mus81	62
5 DISCUSSION	66
5.1 Dpb11 forms a complex with Slx4 and Mus81-Mms4	66
5.2 The Slx4-Dpb11-Mms4-Mus81 complex is regulated by the cell cycle	67
5.3 The Dpb11-Slx4 complex is important for X-shaped DNA structure resolution	69
5.4 The DNA damage checkpoint has a role in the resolution of X-shaped DNA structures	73
5.5 Dpb11-Slx4 is a part of a multi-protein complex	75
5.6 The Dpb11-Slx4 complex exists in mammalian cells	77
6 MATERIALS AND METHODS	79
6.1 Computational analyses	79
6.2 Microbiological and genetic techniques	80
6.2.1 <i>E. coli</i> techniques	80
6.2.2 <i>S. cerevisiae</i> techniques	81
6.3 Molecular biology techniques	93
6.3.1 Isolation of DNA.....	94
6.3.2 Molecular cloning	95
6.3.3 Polymerase chain reaction	97
6.3.4 Separation and visualization of yeast chromosomes	100
6.4 Biochemistry techniques.....	101
6.4.1 Preparation of yeast protein extracts.....	101
6.4.2 Gel electrophoresis and immunoblot techniques	102
7 REFERENCES.....	104
8 ABBREVIATIONS	118
9 ACKNOWLEDGEMENTS	121
10 CURRICULUM VITAE.....	122

1 SUMMARY

Stable propagation of the genetic information is a necessity for all living organisms, but DNA is vulnerable to DNA damage. DNA replication in particular is affected by DNA damage, as it requires an intact template. DNA damage during S-phase therefore causes stalling of replication forks, which can lead to the occurrence of mutations or chromosomal aberrations. To uphold genome integrity cells evolved an error-free DNA repair mechanism by which DNA repair intermediates called X-shaped DNA structures are generated. These structures must be resolved before anaphase since unresolved X-shaped DNA structures block chromatid segregation and can lead to chromosome alterations and rearrangements. Two distinct mechanisms are used to resolve X-shaped DNA structures: dissolution carried out by Sgs1 helicase and resolution that engages structure-specific endonucleases like Mus81-Mms4. However, despite the extensive studies of the function of resolution enzymes, the regulation of X-shaped DNA structure resolution is poorly understood.

This study characterizes the Dpb11-Slx4 complex as a regulator of resolution of X-shaped DNA structures by Mus81-Mms4 in *Saccharomyces cerevisiae*. The Dpb11-Slx4 complex is formed in S-phase after Slx4 phosphorylation by cyclin-dependent kinase Cdk1. A phosphorylation deficient Slx4 mutant is sensitive to the DNA alkylating agent MMS and shows slow S-phase progression. Furthermore, an impaired Slx4 interaction with Dpb11 leads to slower resolution of X-shaped DNA structures, accumulation of anaphase bridges and increased crossover rates. This suggests that the Dpb11-Slx4 complex is involved in resolution and through an epistatic relationship with the *mus81* and *mms4* mutants the Dpb11-Slx4 complex can be assigned to the Mus81-Mms4-dependent resolution pathway. Moreover, biochemical data show that Mus81-Mms4 binds Dpb11-Slx4 in M-phase. Formation of Slx4-Dpb11-Mms4-Mus81 is dependent on Polo-like kinase Cdc5 phosphorylation of Mms4. Intriguingly, this phosphorylation is delayed when Dpb11-Slx4 interaction is impaired. Notably, partially inactive DNA damage checkpoint promotes Mms4 phosphorylation and the formation of the Slx4-Dpb11-Mms4-Mus81 complex.

Taken together, this study describes a new Slx4-Dpb11-Mms4-Mus81 complex that is involved X-shaped DNA structures resolution and is regulated by Cdk1, Cdc5 and the DNA damage checkpoint.

2 INTRODUCTION

2.1 Cell cycle regulation of the DNA damage response

The cell cycle is an ordered series of events that ultimately leads to cell division. The generation of two genetically identical cells from one mother cell requires two fundamental processes: the faithful duplication of the genetic information (DNA replication) and its accurate distribution between the two daughter cells (mitosis). However, a cell's genome is constantly being damaged. Various DNA damaging agents originating from endogenous and exogenous sources introduce DNA lesions, which interfere with the integrity of the genomic information. To prevent cell death or the transmission of mutations to the daughter cells, it is crucial for a cell to cope with DNA damage efficiently at every time during the cell cycle.

2.1.1 The DNA damage response

Unrepaired DNA lesions are toxic for a cell and can lead to mutations, malignant cell transformation or cell death. Consequently, cells have evolved a set of DNA damage response (DDR) mechanisms, which help to cope with DNA damage and efficiently repair DNA lesions. The DDR consists of different pathways that act in concert to stall the cell cycle, thereby providing time to repair the lesion specifically or allow damaged DNA to be replicated.

The cellular response to a DNA double strand break (DSB) could serve as an example for DDR mechanism, in particular DNA damage checkpoint activation (Longhese et al., 1998). When a DSB is formed, the MRX complex is recruited to the site of the lesion. The MRX complex consists of three members - Mre11, Rad50 and Xrs2. The binding of the MRX complex to a DNA break site leads to the recruitment of the protein kinase Tel1 (Lisby et al., 2004). At the break Tel1 is activated by the MRX complex and DNA ends (Fukunaga et al., 2011). After processing of DSB by resection, single-stranded DNA (ssDNA) ends are generated. ssDNA at the break site is covered by the replication protein A (RPA). RPA is known to physically interact with the Mec1 kinase, which is recruited together with its binding factor Ddc2 (Rouse and Jackson, 2002; Zou and Elledge, 2003; Ball et al., 2005; Jazayeri et al., 2006; Ball et al., 2007).

INTRODUCTION

For full activation of the DNA damage checkpoint the 9-1-1 complex is additionally required as co-sensor (Delacroix et al., 2007; Lee et al., 2007; Puddu et al., 2008). The 9-1-1 complex consists of three protein subunits, Ddc1, Mec3 and Rad17, which form a trimeric ring that is loaded onto ssDNA and double-stranded DNA (dsDNA) junction by RFC-like clamp loader (Kondo et al., 1999), which consists of Rad24 and Rfc2-5. The 9-1-1 complex subunit Ddc1 interacts with the scaffold protein Dpb11 and recruits Dpb11 to the DNA damage site (Wang and Elledge, 2002). Dpb11 was shown to stimulate the protein kinase Mec1 (Kumagai et al., 2006; Mordes et al., 2008; Navadgi-Patil and Burgers, 2008). The activated protein kinases Tel1 and Mec1 directly phosphorylate the adaptor proteins Rad9 and Mrc1 (Alscasabas et al., 2001; Schwartz et al., 2002). Consequently, the DNA damage checkpoint signal is transferred to the kinases Rad53 and Chk1. Rad53 and Chk1 function as effector kinases of the DNA damage checkpoint and mediate the phosphorylation of a variety of checkpoint target proteins, which turn the signal into a biological outcome (Sanchez et al., 1999).

The activated DNA damage checkpoint often regulates DNA repair pathways. Importantly, depending on the type of DNA damage different repair mechanisms are engaged to repair the lesion. For example, DSBs are repaired by the homologous recombination (HR) or non-homologous end joining (NHEJ) mechanisms. The main enzyme in HR repair is the Rad51 recombinase. Rad51 is involved in homology search and catalysis of strand exchange to prime for DNA synthesis to repair DSB. In contrast to HR, the NHEJ mechanism is rather simple. The Ku70/Ku80 complex captures and brings DNA ends together. After little or no end processing the ends are directly ligated by the ligase IV (Lieber, 2010; Jasin and Rothstein, 2013).

The most simple and most accurate way of DNA repair is the direct reversal of DNA damage. An example is the repair of UV-induced damage, which is reversed by the photolyase Phr1 (Sebastian et al., 1990). Moreover, yeast cells express the DNA repair methyltransferase Mgt1, which removes methyl groups from alkylated DNA bases (Sassanfar and Samson, 1990; Sassanfar et al., 1991).

The majority of endogenous DNA damage is caused by oxidation, spontaneous hydrolysis or deamination reactions. DNA lesions originating from these sources are usually repaired by base excision repair (BER) mechanisms. BER involves five groups of DNA modifying enzymes that release the base from deoxyribose (Ung1, Mag1, Ntg1, Ntg1, Ogg1), nick the DNA backbone (Apn1, Apn2), remove the

remaining deoxyribose backbone phosphate (Rad27), fill the gap (Pol2) and ligase the remaining DNA ends (Lig1) (Hoeijmakers, 2001).

Lesions that interfere with base pairing are repaired by nucleotide excision repair (NER), which additionally can act on BER substrates (Torres-Ramos et al., 2000). The first step in NER is the excision of 25-30 nucleotides, which surround the lesion (Guzder et al, 1995). Subsequently, the single-stranded gap is filled by the action of a DNA polymerase followed by ligation (Budd and Campbell, 1995; Ogi et al., 2010). Crucial factors functioning in NER are Rad4-Rad23, Rad14, Rad1-Rad10, Rad2 (Schärer, 2013).

In case lesions are not repaired by BER or NER before encountered by the DNA replication machinery, they can be bypassed by post-replication repair (PRR) mechanisms (di Caprio and Cox, 1981; Prakash, 1981). PRR is also known as Rad6 pathway and is carried by ubiquitin ligase complexes and specialized DNA polymerases (see 2.2.2) (Ulrich and Jentsch, 2000; Waters et al., 2009).

DNA mismatch repair (MMR) is important when erroneous insertion, deletion or misincorporation of bases occur during DNA synthesis. Relevant proteins in this pathway are Msh1-6, Pms1, Mlh1-3, Pol30, Exo1 (Harfe and Jinks-Robertson, 2000; Kunkel and Erie, 2005; Hsieh and Yamane, 2008). In case of the erroneous incorporation of ribonucleotide monophosphates (rNMPs) into the genome, the mistake is corrected by ribonucleotide excision repair. rNMPs are incised by Rad27 and RNase H2 (Cerritelli and Crouch, 2009).

Interstrand crosslinks, which covalently link both strands of the DNA helix, are processed by Pso2-family proteins and various proteins, which have a role in other DNA repair pathways like homologous recombination as well as nucleases and DNA translesion polymerases (McVey, 2010).

After DNA repair, in order to allow cell cycle progression, the DNA damage checkpoint has to be inactivated. Checkpoint recovery takes place at different levels. As initiators of checkpoint signaling, DNA repair and DNA damage checkpoint proteins have to be removed from the site of damage (Vaze et al., 2002). Furthermore, protein phosphatases are required to revert phosphorylation marks, which were introduced by checkpoint effector kinases (Keogh et al., 2006). Moreover, the central effector kinase Rad53 is degraded or dephosphorylated. It was shown that the Ptc2, Ptc3 and Pph3 phosphatases work in dephosphorylation of the DNA damage

checkpoint effector kinase Rad53, thus inactivating DNA damage checkpoint (Leroy et al., 2003; O'Neill et al., 2007).

2.1.2 Cell cycle kinases and their relation to DNA damage response

While DNA damage can occur at any time and independently of the cell cycle phase, the chromosomal structure and thereby the DNA repair pathways, which are dependent on a certain chromosome state, are tightly coupled to the different cell cycle phases. Hence, to adapt to structural changes of chromosomes, DNA damage repair mechanisms are regulated by the cell cycle in hand of the cell cycle kinases.

Cyclin-dependent kinases (CDKs) are a family of kinases, which are characterized by the binding of a kinase subunit to a specific non-catalytic cyclin. CDKs are highly conserved proteins and six cyclin-dependent kinases are expressed in the yeast *Saccharomyces cerevisiae*: Cdk1 (also known as Cdc28), Pho85, Kin28, Ssn3, Ctk1 and Bur1. Cdk1 is necessary and sufficient during all cell cycle phases. Pho85 acts in G1-phase when Cdk1 activity is low. All other cyclin-dependent kinases have roles in transcription regulation (Lőrincz and Reed, 1984; Simon et al., 1986; Toh-e et al., 1988; Lee and Greenleaf, 1991; Liao et al., 1995; Liu and Kipreos, 2000; Yao et al., 2000).

Cdk1 kinase levels are constant during the cell cycle. The expression of different cyclins at the particular cell cycle stage regulates Cdk1. Cdk1 is inactive in G1-phase due to the low concentration of cyclins and the presence of cyclin-dependent kinase inhibitors Sic1 and Far1 (Schwob et al., 1994; Alberghina et al., 2004). Cdk1 kinase activity increases at late G1-phase, when the cyclin expression reaches a level sufficient for the activation of Cdk1 and the Sic1 and Far1 inhibitors are degraded (Mendenhall and Hodge, 1998). Active Cdk1 phosphorylates various proteins on the consensus site for Cdk1 phosphorylation S/T-P-x-K/R (x is any amino acid, S/T-P constituting the minimal consensus (Nigg, 1993)).

The cyclin-Cdk1 complexes have specific target proteins and thereby affect different cellular processes. A recent study combining Cdk1 inhibition experiments with mass spectrometry (MS) analysis led to the identification of more than 300 Cdk1 target proteins (Holt et al., 2009). Among the variety of processes regulated by CDKs

are DNA replication, chromosome segregation, transcription and cell morphogenesis. Moreover, proteins of the DNA damage response are targets of CDK signaling.

To date, mainly studies on DNA double strand break repair have provided insights into how cell cycle regulation of DNA repair processes is achieved (Aylon et al., 2004; Ira et al., 2004). Early studies indicated that in G1-phase cells tend to repair DSBs by NHEJ, whereas homologous recombination is preferred in S/G2/M-phase, when a sister chromatid is present and can serve as homologous repair template (Kadyk and Hartwell, 1992; Johnson and Jasin, 2001).

HR proteins have been shown to be direct targets of Cdk1-mediated phosphorylation (Ira et al., 2004). Cdk1 phosphorylates the endonuclease Sae2 to initiate DNA resection, which is a crucial step to initiate homologous recombination (Huertas et al., 2008). For subsequent homology search the nucleases Exo1 and Dna2 generate single-stranded 3' ends (Zhu et al., 2008). Strikingly, this step in HR is also regulated by the cell cycle via phosphorylation of the nuclease Dna2 (Ubersax et al., 2003; Kosugi et al., 2009). This suggests that Cdk1 regulation is crucial for making the choice, which pathway - NHEJ or HR - to choose for DSB repair. In addition, Cdk1 phosphorylates the helicase Srs2 that has been implicated to regulate HR (Saponaro et al., 2010).

Moreover, late steps of homologues recombination repair such as X-shaped DNA structure resolution are also regulated by the cell cycle. This control mechanism is based on phosphorylation of the Mms4 subunit of the structure-specific Mus81-Mms4 endonuclease and inhibitory phosphorylation of the resolvase Yen1 (Matos et al., 2011; Gallo-Fernandez et al., 2012; Matos et al., 2013; Szakal and Branzei, 2013; Blanco et al., 2014).

In addition to DNA repair, CDK-dependent phosphorylation also regulates the DNA damage checkpoint. For instance the checkpoint mediator protein Rad9 harbors several Cdk1 sites (Ubersax et al., 2003). Rad9 phosphorylation on S462 and T474 are important for the interaction with Dpb11, which boosts the DNA damage checkpoint activation cascade (Pfander and Diffley, 2011).

Interestingly, the signals from the DNA damage checkpoint and the cell cycle kinases converge on specific targets. In particular, Srs2 and Sae2 are the targets of Cdk1 as well as Mec1/Tel1-mediated phosphorylation. Mutating either Cdk1 or Mec1/Tel1-phosphorylation sites results in increased sensitivity after DNA damage (Libreri et al., 2000; Baroni et al., 2004; Huertas et al., 2008). Similar regulation

mechanisms combining influence of the cell cycle as well as DNA damage checkpoint also impact on the proteins Swi6, Cdc5, Cdc20 and Pds1 (Enserink and Kolodner, 2010). However, it is still unclear, why overlap between targets exists. Presumably, this helps to coordinate the DNA damage response with the cell cycle.

Another important class of cell cycle regulators is Polo-like kinases (PLKs). These serine-threonine kinases are conserved from yeast to human. There are five PLKs in mammalian cells, while budding yeast have only one Polo-like kinase (Cdc5), which is the orthologous protein of human PLK1 (Glover et al., 1998; Barr et al., 2004; Lowery et al., 2005). The domain in PLKs, which coordinates protein-protein interaction, is called Polo-box domain (PBD) and recognizes S(pS/pT)-P/x (x is any amino acid) motifs on target proteins (Elia et al., 2003). Intriguingly, the PBD binding motif is similar to the CDK phosphorylation sequence. It is hypothesized that a priming phosphorylation by CDK is important for protein recognition and subsequent phosphorylation by PLKs (Golan et al., 2002; Yamaguchi et al., 2005).

Main functions of PLKs are the regulation of mitotic entry, the spindle pole and cytokinesis (Glover et al., 1998; Barr et al., 2004; Strebhardt, 2010). However, the precise role of PLKs in the DDR is not completely understood. Interestingly, after activation of the DNA damage checkpoint PLK1 is inactivated, which leads to cell cycle arrest in mammalian cells (Smits et al., 2000; Taylor and Stark, 2001). Furthermore, PLKs have been implicated in checkpoint adaptation, when cells proceed in the cell cycle in the presence of unrepaired DNA (Toczyski et al., 1997). In budding yeast, Cdc5 was shown to regulate Sae2 and overexpression of Cdc5 interferes with checkpoint target phosphorylation in response to DSBs. It has been proposed that Cdc5 acts on different levels to interfere with the checkpoint signaling and at the resection step of DSB repair (Donnianni et al., 2010). Moreover, Cdc5 regulates X-shaped DNA structure resolution by phosphorylating Mms4 and activating structure-specific endonuclease Mus81-Mms4 (Matos et al., 2011; Gallo-Fernandez et al., 2012; Matos et al., 2013; Szakal and Branzei, 2013).

Taken together, CDKs and PLKs are crucial during the cell cycle and their function in regulating the cellular processes by phosphorylation is tightly related to DNA damage response.

2.2 S-phase-specific DNA damage

The S-phase of the cell cycle is characterized by the duplication of genetic information. During S-phase accurate DNA replication and functional DNA damage response are critical to assure cell survival, avoidance of replication fork breakdown and completion of DNA replication. At this cell cycle stage DNA strands are being unwound by the DNA replication machinery, therefore ssDNA might be exposed to DNA damage.

Replication fork stalling is a consequence of a lesion that damages only one of two DNA strands. Therefore, DNA damaging agents such as methyl methanesulfonate (MMS) create a barrier for the DNA polymerase. Importantly, cells developed DNA damage bypass mechanisms to cope with DNA damage, which stalls DNA replication. DNA repair mechanisms during DNA replication together with the S-phase-specific DNA damage checkpoint are critical to maintain the integrity of genomic DNA.

2.2.1 The S-phase DNA damage checkpoint

The S-phase DNA damage checkpoint is activated under conditions of perturbed DNA replication and affects a variety of processes in a cell to efficiently repair stalled replication forks (Paulovich and Hartwell, 1995; Zhou and Elledge, 2000).

DNA lesions stall the replicative DNA polymerase, while the MCM helicase continues unwinding double stranded DNA (Sogo et al., 2002; Byun et al., 2005; Nedelcheva et al., 2005). This creates long stretches of ssDNA, which is recognized and covered by the RPA protein (You et al., 2002; Zou et al., 2003; Zou and Elledge, 2003; Binz et al., 2004). Consequently, single-stranded DNA bound by RPA recruits checkpoint kinase Mec1 via its regulatory subunit Ddc2 (Rouse and Jackson, 2002; Zou and Elledge, 2003; Ball et al., 2005; Jazayeri et al., 2006; Ball et al., 2007). Activated Mec1 phosphorylates the mediator protein Mrc1, which transduces Mec1 signal to the effector kinase Rad53 (Alcasabas et al., 2001). Another mediator protein Rad9 is thought to act downstream of the checkpoint kinase Tel1 (Gilbert et al., 2001). In both cases, the effector kinases Rad53 and Chk1 are phosphorylated and activated (Putnam et al., 2009).

INTRODUCTION

Once activated, the S-phase DNA damage checkpoint signaling prevents late origin firing, stabilizes replication forks, restores DNA replication, regulates transcription of DNA damage response genes, coordinates DNA repair pathways and inhibits mitosis (Figure 2.1) (Allen et al., 1994; Desany et al., 1998; Santocanale and Diffley, 1998; Shirahige et al., 1998; Santocanale et al., 1999; Lopes et al., 2001; Tercero and Diffley, 2001; Kai et al., 2007; Szyjka et al., 2008).

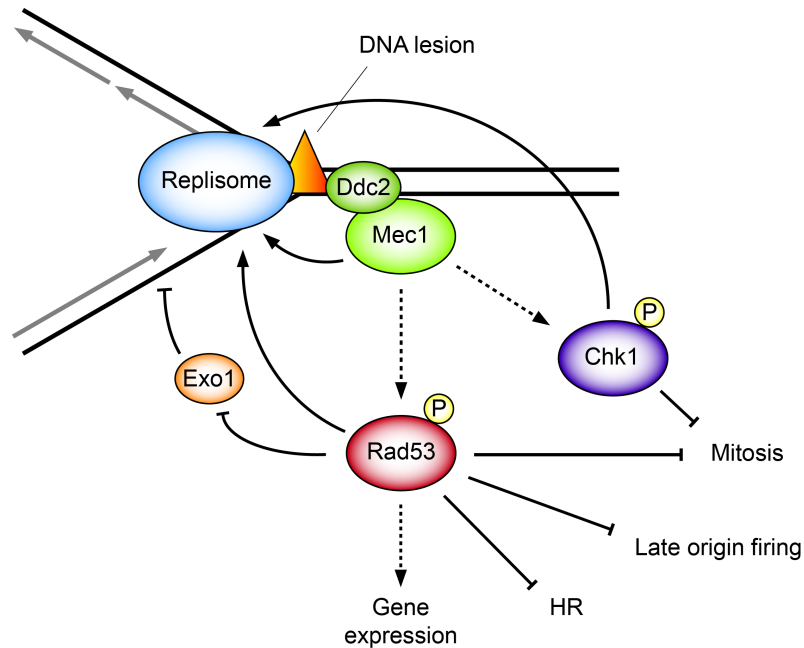


Figure 2.1. The S-phase DNA damage checkpoint is activated after replication fork stalling.

When DNA lesions stall the replicative DNA polymerase, the S-phase DNA damage checkpoint is activated. First, Mec1-Ddc2 is recruited to the lesion. Next the DNA damage signal is transferred to the effector kinases Rad53 and Chk1 via mediator proteins. Activated DNA damage checkpoint prevents late origin firing, stabilizes replication forks, regulates transcription, inhibits mitosis, Exo1 and homologous recombination (adapted from Segurado and Tercero, 2009).

A central outcome of the S-phase DNA damage checkpoint is slowed down replication and cell cycle arrest in subsequent mitosis in order to provide time for a cell to respond to stalled replication. Importantly, Rad53 phosphorylates Sld3 and Dbf4 and therefore prevents late origin firing by disrupting the assembly of the replication initiation complex (Lopez-Mosqueda et al., 2010; Zegerman and Diffley, 2010). Moreover, Rad53 slows down cell cycle progression by blocking cohesion cleavage. It does so by stabilizing Pds1, which is an inhibitor of the separase Esp1. Anaphase is activated by the action of Esp1, which then cleaves cohesion. Therefore,

the onset of anaphase is delayed, when Pds1 is phosphorylated by Rad53 (Sanchez et al., 1999; Agarwal et al., 2003).

Stabilization of stalled replication forks is also of great importance since collapsed replication forks cause DSBs (Kuzimov, 1995; Kogoma, 1996; Cox et al., 2000). However, the exact mechanism, how the S-phase DNA damage checkpoint stabilizes replication forks, is not clear even though some checkpoint targets have been suggested. One reasonable candidate could be RPA. The RPA protein not only triggers S-phase DNA damage checkpoint initiation but also is phosphorylated by the Mec1 kinase (Brush et al., 1996). Nevertheless the direct connection of RPA phosphorylation to replication fork stabilization is not clear.

In contrast, the function of Mrc1 phosphorylation in stabilizing replication forks is partially uncovered. Phosphorylated Mrc1 interacts with a replication pausing checkpoint complex subunit Tof1, which is essential to keep replication machinery components together (Alcabas et al., 2001; Katou et al., 2003).

Interestingly, the MCMs are phosphorylated by the ATR/ATM (Mec1/Tel1 in budding yeast) in metazoans (Ishimi et al., 2003; Cortez et al., 2004; Yoo et al., 2004; Shi et al., 2007; Trenz et al., 2008). Moreover, MCMs dissociate from the damaged forks when Rad53 is absent in budding yeast (Cobb et al., 2005). These observations support the idea that MCMs could be a direct target important for the stabilization of stalled replication forks.

Another mechanism of the S-phase DNA damage checkpoint to stabilize stalled replication forks is the blocking of unscheduled recombination (Meister et al., 2005; Lambert et al., 2007). For example, in fission yeast the structure-specific endonuclease Mus81 is phosphorylated by Cds1 (Rad53 in budding yeast) after DNA damage (Kai et al., 2005). This might prevent Mus81 from cleavage of DNA intermediates at stalled replication forks and formation of DNA breaks. Thus, the Cds1 regulation by phosphorylation of Mus81 might protect genomic DNA from unscheduled recombination events.

Interestingly, the activity of the nuclease Exo1 is also down-regulated by DNA damage checkpoint (Morin et al., 2008). While during DSB repair Exo1 generates ssDNA for recombination initiation and is involved in the excision step of DNA mismatch repair, Exo1 activity at stalled replication forks may be harmful. The exact mechanism how Exo1 could negatively affect stalled replication forks is unknown. On the one hand it is possible that in the absence of Rad53 after replication fork

stalling some pathological structures, which could be targeted by Exo1, are generated (Szankasi and Smith, 1995; Sogo et al., 2002; Cotta-Ramusino et al., 2005; Zhu et al., 2008). On the other hand Exo1 might process normal DNA replication intermediates. Therefore, to prevent Exo1-dependent processing of stalled replication forks after DNA damage, the activity of Exo1 is reduced after its phosphorylation by Rad53 (Smolka et al., 2007).

The S-phase DNA damage checkpoint also phosphorylates chromatin remodelers and histone regulating enzymes, which contribute to maintenance of functional DNA replication forks. One of the targets is the Ino80 complex, which accumulates at the stalled replication forks facilitating replication fork recovery (Papamichos-Chronakis and Peterson, 2008; Shimada et al., 2008). It was shown that the Ino80 complex subunit Ies4 is phosphorylated by Mec1/Tel1 after DNA damage (Morrison et al., 2007). Moreover, the Hst3 deacetylase is also a target of the Mec1 kinase. Mec1-phosphorylation of Hst3 results in accumulation of acetylated histone H3, which could contribute to the recruitment of proteins required for the signaling of a lesion or stabilization of stalled replication forks (Thaminy et al., 2007).

2.2.2 Bypass mechanisms of damaged DNA in S-phase

Damaged DNA in a cell is repaired by the different conserved mechanisms shortly summarized in 2.1.1. However, cells face a special situation in S-phase when DNA replication takes place. At this stage, DNA lesions, which are not detected and repaired by NER or BER pathways, cause replication fork stalling. Nevertheless, after exposure to DNA damage like UV light cells are still able to replicate DNA just with a short delay suggesting that there is a mechanism to bypass the lesions in S-phase (Khidhir et al., 1985; Witjin et al., 1987; Courcelle et al., 2005; Belle et al., 2007; Rudolph et al., 2007).

DNA damage tolerance (DDT, also known as post-replication repair or Rad6 pathway) is a term to describe a collection of mechanisms important to replicate DNA even in the presence of DNA damage (Lawrence, 1994). The lesions introduced by UV or MMS on one DNA strand serve as a block to the replisome. Because the lesion site cannot be used as template for replicative polymerases, the DNA replication fork stalls. Interestingly, at least during lagging-strand replication, DNA replication

continues after repriming downstream of a lesion. This allows not only to finish DNA replication but also to generate a complementary undamaged DNA strand, which can serve as template for BER or NER (Yeeles et al., 2013).

Importantly, a lesion in the lagging-strand of DNA is thought to be less severe comparing to a lesion in the leading-strand. The main difference of the damage in one or another DNA strand is that the repriming step in the lagging-strand is most likely quicker (McInerney and O'Donnell, 2004; Nelson and Benkovic, 2010). The lagging DNA strand is replicated via Okazaki fragments (DePamphilis and Wassarman, 1980). When the replicative DNA polymerase faces a lesion in the lagging DNA strand, it continues the replication downstream of a lesion starting from a newly synthesized primer.

The situation is different when DNA polymerase faces a lesion in the leading DNA strand. It has long been believed that the DNA replication machinery is not able to proceed over the damage on the leading-strand until the lesion is removed. Strikingly, the discovery that at least in bacteria primase is able to prime on the leading DNA strand outside of the replication origin provided mechanistic evidence that the leading-strand synthesis can be reinitiated (Heller and Marians, 2006). However, it is still unclear whether leading-strand repriming is active in eukaryotes.

The repriming process generates single stranded DNA gaps as unfinished Okazaki fragments (Lopes et al., 2006). These ssDNA gaps can be later repaired post-replicatively by translesion synthesis (TLS) polymerases or recombination-dependent template switch (Lehmann and Fuchs, 2006; Branzei and Foiani, 2010).

The post-replication repair pathway consists of different ubiquitin ligases with the main player - the Rad6-Rad18 complex (Bailly et al., 1994). For this reason, this lesion bypass pathway is also called Rad6 pathway. The Rad6 pathway allows to bypass a lesion by two ways. One way is via recruiting the TLS polymerases and thereby channeling the repair into the error-prone sub-pathway of PRR (Lemontt, 1971). Alternatively, HR-like mechanisms result in an error-free bypass of the lesion (Broomfield et al., 1998).

The switch between error-free and error-prone sub-pathways of PRR is achieved by the modification of the replicative sliding clamp PCNA (encoded by *POL30* in budding yeast) (Moldovan et al., 2007). PCNA is a main target of the ubiquitin ligase complexes of PRR (Hoege et al., 2002). After DNA damage, lysine 164 of PCNA is monoubiquitinated by the Rad6-Rad18 enzymes. This modification

promotes TLS (Stelter and Ulrich, 2003). The same residue of PCNA is modified further by the Ubc13-Mms2-Rad5 ubiquitin ligase complex, therefore providing a signal for the error-free mechanisms of PRR (Broomfield et al., 1998; Hofmann and Pickart, 1999; Brusky et al., 2000; Ulrich and Jentsch, 2000; Hoege et al., 2002).

The error-prone pathway is well studied and the mechanism seems to be rather simple. After DNA damage, the replicative DNA polymerase-bound PCNA is monoubiquitinated. This modification stimulates PCNA interaction with translesion synthesis polymerases. TLS polymerases have a nonrestrictive active site and lack 3'-5' proofreading exonuclease activity, which allows to replicate over a lesion site (Figure 2.2). Most of the eukaryotic TLS polymerases harbor PCNA- and ubiquitin-binding domains. There are three known TLS polymerases in budding yeast, namely Rev1, Rev3-Rev7 and Rad30 (Yang and Woodgate, 2007; Goodman and Woodgate, 2013). After the damage is passed, TLS polymerases are replaced with replicative polymerases (Kannouche et al., 2004; Moldovan et al., 2007). Interestingly, the cell cycle regulation of TLS polymerases was proposed because there is more Rev1 in G2/M, however, Rev3-Rev7 levels are constant during the cell cycle (Waters and Walker, 2006; D'Souza and Walker, 2006). Thus, there might be temporal separation of error-prone and error-free pathways.

In contrast to error-prone pathway, the error-free PRR mechanism is not very well understood. To date it is obvious that this mechanism requires Rad18, Rad5, Ubc13-Mms2 and Rad51 (Branzei et al., 2008; Minca and Kowalski, 2010). Interestingly, the newly synthesized sister chromatid is used as a template for synthesis of the complementary strand of damaged DNA. There are two models for the molecular mechanism of error-free PRR: template switch and replication fork regression (Broomfield et al., 2001). The template switch mechanism involves the invasion of the homologous sister chromatid followed by high fidelity DNA synthesis and the resolution of the resulting Holliday junction (Higgins et al., 1979). The fork regression model is characterized by the formation of a particular DNA structure known as "chicken foot", in which newly synthesized DNA strands are paired (Figure 2.2) (Robu et al., 2001).

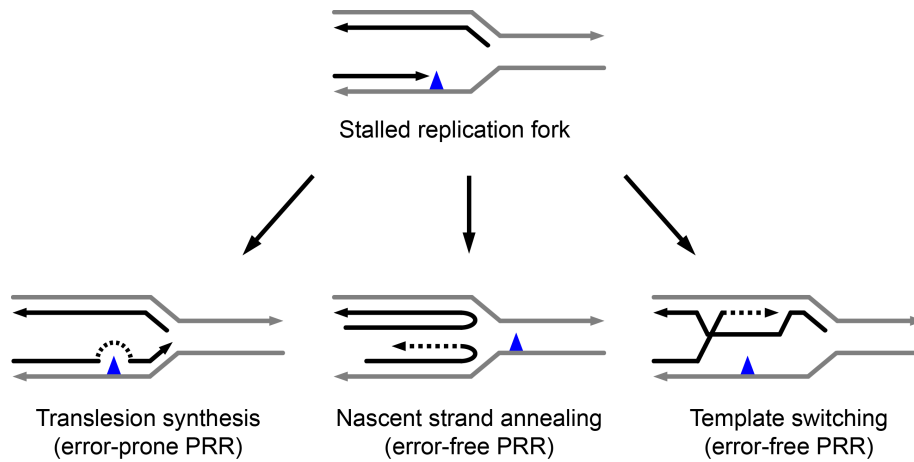


Figure 2.2. Post-replication repair mechanism allows the bypass of a lesion during S-phase.

When replication fork stalls, a lesion can be bypassed by three different mechanisms. First, translesion synthesis polymerases can replicate damaged DNA. Second, nascent strands can be paired to form a “chicken foot” structure. Third, homologous sister chromatid can be invaded by the template switch (adapted from Andersen et al., 2008).

2.3 Mechanisms to process X-shaped DNA structures

The error-free PRR by template switching or HR repair of DSB after collapse of stalled replication forks result in formation of X-shaped DNA structures (also known as joined molecules (JMs)). These DNA repair intermediates have to be processed before the metaphase to anaphase transition. If not repaired, X-shaped DNA structures interfere with sister chromatid segregation and result in the formation of anaphase bridges, and consequently to chromosome breakage, deletions and translocations. There are two mechanisms to process X-shaped DNA structures. One pathway known as dissolution involves the RecQ helicase together with a topoisomerase. The other mechanism is called resolution and requires the action of structure-specific nucleases.

2.3.1 The RecQ DNA helicases and dissolution mechanism

The dissolution mechanism for resolving X-shaped DNA structures is completely dependent on the RecQ family of proteins, named after the RecQ helicase in *E. coli* (Umezumi et al., 1990). The RecQ DNA helicases are conserved from bacteria to human. There are five known RecQ proteins in humans: BLM, RECQ1, RECQL4, RECQ5 and WRN (Puranam and Blacjshear, 1994; Seki et al., 1994; Yu et al., 1996;

Kitao et al., 1998). However, just one RecQ DNA helicase namely Sgs1 is present in budding yeast. Structurally and functionally Sgs1 is most similar to human BLM (Ashton and Hickson, 2010).

The role of Sgs1 in resolution can be easily studied by two dimensional gel electrophoresis, which allows to detect X-shaped DNA structures (Liberi et al., 2005). As expected, the processing of X-shaped DNA structures after MMS damage is slowed down in the absence of the helicase Sgs1 (Bernstein et al., 2009). Moreover, the accumulation of X-shaped DNA structures in the absence of Sgs1 is dependent on the Rad51 recombinase and on Rad18, a member of the Rad6 pathway. These results suggest that Sgs1 processes DNA repair intermediates arising from HR-like mechanisms to bypass DNA lesion at damaged replication forks (Liberi et al., 2005; Branzei et al., 2008).

Sgs1 action in resolution is not possible without two other proteins - topoisomerase 3 (Top3) and Rmi1 - that form a complex with Sgs1 (TOPOIII α and RMI1 in mammalian cells) (Bennett et al., 2000; Mullen et al., 2005). This complex is called STR (BTR in human cells) complex or dissolvasome (Mankouri and Hickson, 2007). In the dissolution process Sgs1 first unwinds the complementary strands of DNA and the topoisomerase Top3 removes the resulting hemicatenate, while the Rmi1 protein stimulates the enzymatic activity of Sgs1-Top3 (Bachrati and Hickson, 2003; Chen and Brill, 2007; Cejka et al., 2010; Yang et al., 2010). Importantly, inactivation of any member of the STR complex leads to the accumulation of X-shaped DNA structures (Liberi et al., 2005; Mankouri and Hickson, 2006; Mankouri et al., 2007).

The STR complex is proficient in the processing of X-shaped DNA structures such as double Holiday junction (HJ) DNA intermediates. Interestingly, the studies in mammalian cells provide evidence that one dissolvasome binds one HJ at a time and move the HJs towards each other to promote dissolution. STR-mediated dissolution results in the formation of non-crossover (NCO) (Figure 2.3) (Ira et al., 2003; Wu and Hickson, 2003; Cejka et al., 2010).

2.3.2 Structure-specific endonucleases and resolution mechanism

In addition to the dissolution pathway cells are able to process X-shaped DNA structures by a resolution mechanism. The principle of the resolution mechanism relies on an endonuclease activity. Structure-specific endonucleases introduce nicks in X-shaped DNA structures in a symmetrical fashion. The outcome of the process depends on the position of the cut sites. If the nick in a pair of HJs is introduced along the same axis the resolution product is a non-crossover. In the case of resolution along different axes, crossover products are formed (Figure 2.3) (Szostak et al., 1983; Connolly et al., 1991; Iwasaki et al., 1991).

To date, there are three different enzymes in eukaryotes known to be capable of acting in the repair of X-shaped DNA structures by resolution. These enzymes are named Mus81-Mms4, Slx1-Slx4 and Yen1 (MUS81-EME1, SLX1-SLX4 and GEN1 in mammalian cells) (Rass, 2013).

The structure-specific endonuclease Mus81-Mms4 (also known as Slx3-Slx2) was discovered as a factor necessary for cell viability in the absence of the helicase Sgs1 (Mullen et al., 2000). Mus81-Mms4 belongs to the XPF family of nucleases (Ciccica et al., 2008). Both subunits of Mus81-Mms4 have an endonuclease domain, however, this domain is inactive in Mms4, and Mms4 acts as a regulatory subunit of the Mus81-Mms4 resolvase. *In vitro* studies have shown that Mus81-Mms4 processes a variety of DNA structures like 3'-flaps, double-stranded three way junctions, HJ precursors and HJs (Boddy et al., 2001; Chen et al., 2001; Kaliraman et al., 2001; Constantinou et al., 2002; Doe et al., 2002; Ciccica et al., 2003). Importantly, the activity of purified Mus81-Mms4 towards HJs is relatively weak and increases if the HJ contains a ssDNA break (Osman et al., 2003; Fricke et al., 2005; Ehmsen and Heyer, 2008, 2009).

Slx1-Slx4 was identified in the same screen as Mus81-Mms4 for proteins required for cell viability in the absence of Sgs1 (Mullen et al., 2000). Slx1 is an active member of the Slx1-Slx4 nuclease, while Slx4 is a scaffold protein (Fricke and Brill, 2003). Slx1 belongs to the GIY-YIG family of nucleases (Dunin-Horkawicz et al., 2006). The substrates of Slx1-Slx4 are DNA duplexes with unpaired 3' and 5' overhangs on one side, 5' flaps, replication forks and Holiday junctions. Budding yeast Slx1-Slx4 acts relatively inefficiently on HJ substrates and cuts them with low specificity at multiple, non-symmetric sites (Fricke and Brill, 2003).

INTRODUCTION

Interestingly, in contrast to the situation in the yeast *S. cerevisiae*, in human cells a direct interaction of SLX4 with MUS81-EME1 was identified (Fekairi et al., 2009; Munoz et al., 2009; Svendsen et al., 2009; Schwartz et al., 2012). Formation of the SLX-MUS complex by binding of SLX1-SLX4 to MUS81-EME1 increases the endonuclease activity (Wyatt et al., 2013). This observation raises the interesting possibility that similar complexes of endonucleases, which promote X-shaped DNA structure resolution, may exist also in yeast.

The Yen1 protein was identified in the screen for HJ resolvases in the yeast *S. cerevisiae* (Ip et al., 2008). Yen1 belongs to the XPG nuclease family. This type of nucleases harbors the super family specific N-terminal domain and internal XPG nuclease motifs (Tomlinson et al., 2010). The Yen1 enzyme has been shown to process similar DNA substrates as Mus81-Mms4, suggesting a possible overlapping role. Yen1 acts on the 5' flaps, replication fork DNA structures and Holiday junctions (Ip et al., 2008; Rass et al., 2010).

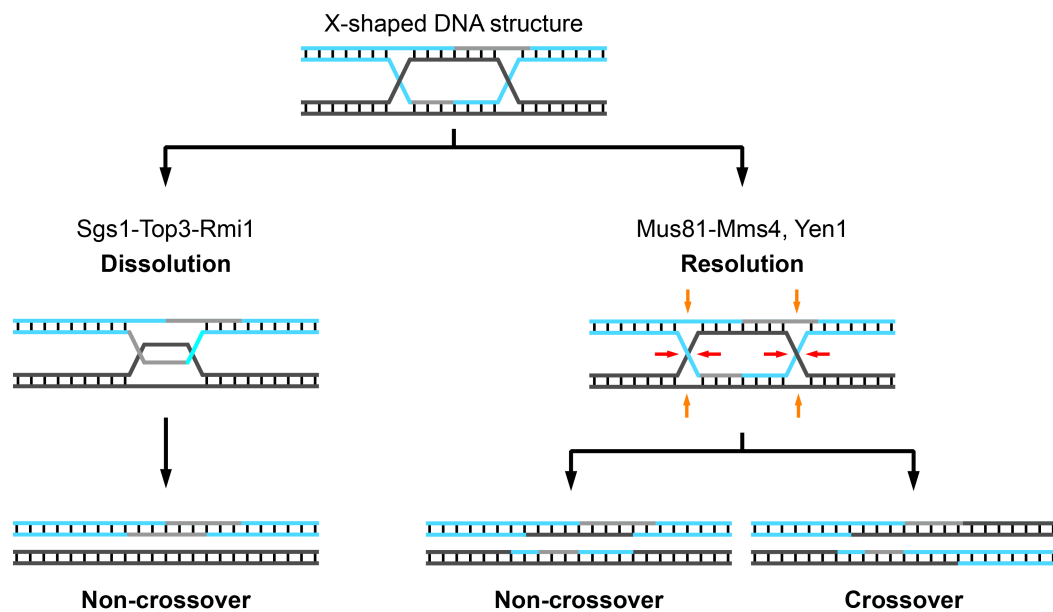


Figure 2.3. There are two mechanisms to process X-shaped DNA structures. Dissolution mechanism involves the activity of Sgs1-Top3-Rmi1 and resolves X-shaped DNA structures to non-crossover products. Resolution mechanism involves Mus81-Mms4 or Yen1 and resolves X-shaped DNA structures to non-crossover or crossover products (adapted from Matos and West, 2014).

2.3.3 Regulation of X-shaped DNA structure resolution

In recent years, the enzymatic mechanism and substrate specificity of X-shaped DNA structure processing enzymes were intensively studied. In comparison to the dissolution pathway, which in principle initiates the migration of two X-shaped DNA structures and consequently decatenates them through topoisomerase activity resulting in NCO formation, the resolution mechanism introduces a cut in DNA repair intermediates and mediates the formation of NCO and CO products (Figure 2.3) (Iwasaki et al., 1991; Wu and Hickson, 2003)

In theory, the dissolution and resolution mechanisms can compensate each other; however, dissolution appears to be the preferred way to deal with X-shaped DNA structures since Sgs1 is active in all cell cycle stages. One possible explanation for the cell's preference for dissolution is the final products of the recombination reaction. The NCO outcome of the dissolution process is silent. In contrast, CO formation after recombination events between two homologous chromosomes or two homologous sequences at different genomic loci may lead to loss of heterozygosity or gross chromosomal rearrangements, respectively (Matos et al., 2013; Szakal and Branzei, 2013).

Most importantly, the low substrate specificity of structure-specific nucleases may threaten genome stability. Mus81-Mms4, Yen1 and Slx1-Slx4 are able to cut the replication fork structures (Osman and Whitby, 2007). This activity of structure-specific nucleases might lead to unscheduled homologous recombination followed by gross chromosomal rearrangements in a cell.

Although the function of Sgs1 has been studied extensively, the aspect of cell cycle regulation of the dissolution pathway seems to be not important. Interestingly, in mammalian cells BLM concentration is the highest during DNA replication (Dutertre et al., 2000). In budding yeast the expression of the Sgs1 helicase also peaks in S-phase (Frei and Gasser, 2000). On the other hand, Sgs1 is active at all cell cycle stages (Liberi et al., 2005; Karras and Jentsch, 2010). Recent studies suggest that the Rmi1 subunit of the dissolvasome might be the main regulator of the STR complex formation and function (Cejka et al., 2010). Thus, more detailed mechanistic analyses of STR complex regulation would be informative to uncover the cell cycle's role in dissolution.

Previous studies of resolution already provided some evidence that processing of X-shaped DNA structures might be regulated by the cell cycle. The reason for this hypothesis was the discovery that Mus81-Mms4 activity is restricted to mitosis, and that Yen1 nuclease is active at an even later stage of the cell cycle. Strikingly, during last years it was shown that the resolution machinery is cell cycle-regulated by Cdk1-phosphorylation of Mms4 and Yen1 (Matos et al., 2011; Gallo-Fernandez et al., 2012; Matos et al., 2013; Szakal and Brnzei, 2013; Blanco et al., 2014).

In M-phase of budding yeast, Mms4 is phosphorylated by Cdk1, followed by hyperphosphorylation by Polo-like kinase Cdc5. Together these phosphorylations induce the activity of Mus81 and allow it to resolve X-shaped DNA structures (Matos et al., 2011; Gallo-Fernandez et al., 2012; Matos et al., 2013; Szakal and Brnzei, 2013; Blanco et al., 2014). In fission yeast the regulation of Mus81-Eme1 appears slightly different. In addition to Cdk1 phosphorylation of Eme1, the DNA damage checkpoint also plays a regulatory role by phosphorylating Eme1 and activating Mus81-Eme1 (Dehe et al., 2013). In human cells, the control of MUS81-EME1 is even more complex. At the onset of mitosis, CDK1-mediated phosphorylation brings together the MUS81-EME1 and SLX1-SLX4 endonucleases forming the SLX-MUS complex and consequently increasing the endonuclease activity (Wyatt et al., 2013). Although PLK1 was found to interact with SLX4, the importance of Polo-like kinase for the activity of the SLX-MUS complex is still unclear (Svendsen et al., 2009).

In contrast to Mus81-Mms4 activation, Yen1 is inhibited by Cdk1 phosphorylation. At the G1/S transition, Cdk1 phosphorylates the NLS of the Yen1 protein, thereby preventing Yen1 entry into the nucleus (Kosugi et al., 2009). Furthermore, phosphorylated Yen1 has reduced binding affinity to DNA (Blanco et al., 2014). Only in anaphase, when the phosphatase Cdc14 promotes Yen1 dephosphorylation, Yen1 is able to enter the nucleus and reach its DNA substrates (Blanco et al., 2014; Eissler et al., 2014). In mammalian cells, GEN1 is also located in the cytoplasm and thereby held inactive. In M-phase CDK1 mediates nuclear envelope breakdown providing access to GEN1 to reach X-shaped DNA structures (Guttinger et al., 2009).

2.4 The scaffold proteins in DNA damage response

Molecular scaffolds are proteins without enzymatic activity. Interestingly, such proteins are of great significance in regulating different processes in a cell. Scaffold proteins work, for example, as the readers of post-translational modifications (PTMs) like CDK phosphorylation. Moreover, molecular scaffolds can also undergo modifications themselves. Scaffold proteins can form molecular bridges in order to bring particular proteins together and mediate the formation of the functional transient complexes.

2.4.1 Dpb11 and its complexes

Fundamental features of Dpb11 (TopBP1 in human cells) are its BRCA1 carboxy terminal (BRCT) domains. BRCT motifs are frequently found in DNA replication and repair proteins (Rodrigues et al., 2003; Stucki et al., 2005; Delacroix et al., 2007). BRCT domains generally bind phosphorylated S/T motifs of particular proteins (Manke et al., 2003; Yu et al., 2003). Interestingly, structural studies revealed that two BRCT repeats are needed to form the binding surface for one phosphorylated peptide (Botuyan et al., 2004; Clapperton et al., 2004).

Dpb11 contains four BRCT domains (Araki et al., 1995). BRCT1/2 is located in N-terminal part of the protein, while BRCT3/4 is in the middle domain (Garcia et al., 2005). Therefore Dpb11 contains two platforms for phosphorylated protein binding (Botuyan et al., 2004; Clapperton et al., 2004). BRCT1/2 and BRCT3/4 of Dpb11 enable the binding of two interaction partners at a time forming a functional complex. Moreover, the C-terminus of Dpb11, which harbors ATR-activating domain (AAD), can also serve as a platform for binding of a third member. To date, three individual Dpb11 complexes were described (Tanaka et al., 2007; Zegerman and Diffley, 2007; Pfander and Diffley, 2011; Ohouo et al., 2013).

First, Dpb11 has been identified as a crucial regulator of the DNA replication initiation. CDK phosphorylates the replication proteins Sld2 and Sld3 for binding to Dpb11. Phosphorylated Sld3 interacts with the N-terminal pair of BRCT repeats, while phosphorylated Sld2 binds the two BRCT repeats in the middle domain of Dpb11. As cell enters S-phase, Cdk1 phosphorylates Sld2. Phosphorylated Sld2, which is in complex with Pol2, a subunit of DNA polymerase ϵ , and GINS, binds to

Dpb11 to form pre-loading complex. Next, DDK phosphorylates the MCM complex thereby mediating Cdc45 and Sld3 recruitment. Subsequently, the pre-initiation complex is formed after Dpb11 and thereby the pre-loading complex bind to CDK-phosphorylated Sld3. Finally, after the active helicase consisting of MCM, Cdc45 and GINS is formed and DNA polymerases α and δ are recruited, DNA replication is initiated. Thus, CDK-mediated Sld3-Dpb11-Sld2 interaction is essential for DNA replication initiation (Tanaka et al., 2007; Zegerman and Diffley, 2007; Araki, 2010).

The second Dpb11 complex is important for the activation of the DNA damage checkpoint. In this complex all three domains of Dpb11 are required for the Dpb11-dependent checkpoint complex function and bind to Rad9, Ddc1 and Mec1-Ddc2. The CDK-phosphorylated DNA damage adaptor protein Rad9 interacts with BRCT1/2 in the N-terminus of Dpb11. Mec1-phosphorylated Ddc1 interacts with the BRCT3/4 repeats in the middle domain of Dpb11. Moreover, the AAD domain of Dpb11 plays a role in Mec1 recruitment and activation. In all, formation of the Rad9-Dpb11-Ddc1-Mec1-Ddc2 complex at a lesion activates the DNA damage checkpoint kinase Rad53 and boosts DNA damage response (Kumagai et al., 2006; Mordes et al., 2008; Navadgi-Patil and Burgers, 2008; Pfander and Diffley, 2011).

Recently, the third Dpb11 complex, which regulates DNA damage checkpoint, was identified. In the checkpoint dampening complex Dpb11 interacts with the Cdk1-phosphorylated Slx4 protein, which in turn binds to Rtt107. Within the complex Rtt107 and Slx4 were proposed to dampen DNA damage checkpoint activation. According to this model Slx4 competes with the checkpoint protein Rad9 for the binding to Dpb11. Furthermore, Rtt107 inhibits the DNA damage checkpoint via interaction with Mec1-phosphorylated histone H2A. As a result Slx4-Rtt107 counteracts the checkpoint adapter Rad9 by acting on Dpb11 and phosphorylated H2A, which are two positive regulators of Rad9-dependent DNA damage checkpoint activation (Ohouo et al., 2013).

2.4.2 Slx4 and its role in DNA repair

Slx4 was initially identified in the screen for proteins required for cell viability in the absence of Sgs1 (Mullen et al., 2001). Slx4 is a scaffold protein, which is required for the function of the structure-specific heterodimeric endonuclease Slx1-

Slx4 (Fricke and Brill, 2003). While Slx1 is not active without Slx4, Slx4 seems to have more functions independent of Slx1 (Chang et al., 2002; Hanway et al., 2002; Fricke and Brill, 2003; Flott and Rouse, 2005; Flott et al., 2007). These Slx4 functions are performed together with different interaction partners, particularly Rad1-Rad10 and Rtt107 (Rouse, 2009).

By the interaction with the heterodimeric endonuclease Rad1-Rad10, Slx4 is engaged in HR. Here, Slx4 physically interacts with the Rad1 subunit for cleavage of 3'-non homologous tails (3'-flaps), which are generated during mating type switching in yeast or repair of DSB by single strand annealing. The Slx4 role in 3'-flap cleavage is most likely to stimulate the activity of the Rad1-Rad10 endonuclease (Flott et al., 2007; Li et al., 2008; Lyndaker et al., 2008).

By the interaction with the scaffold protein Rtt107, Slx4 has a specific role at stalled replication forks (Roberts et al., 2006). It was shown that Slx4 is important for Rtt107 phosphorylation by Mec1 after MMS damage (Rouse, 2004; Roberts et al., 2006). However, it is still unclear how mechanistically Slx4-Rtt107 influences cell recovery after MMS damage. One possibility is that the Slx4-Rtt107 complex might recruit DNA repair proteins onto damaged DNA sites (Zappulla et al., 2006). The other possibility is that Slx4-Rtt107 might regulate DNA damage checkpoint after replication fork stalling (see above Ohouo et al., 2013).

Like yeast Slx4, the mammalian SLX4 protein has several interactors as well. The complex domain structure of SLX4 allows the binding of different DNA repair proteins, namely the mismatch repair complex MSH3-MSH2, endonucleases XPF-ERCC1, SLX1 and MUS81-EME1, the telomere binding protein TRF2 as well as the cell cycle control kinase PLK1. Thus, it was proposed that SLX4 might have a regulatory role in controlling DNA repair pathways in mammalian cells (Kim et al., 2013; Sarbajna et al., 2014).

2.4.3 Rtt proteins and their role in DNA repair

Rtt stands for regulators of Ty1 transposition. The *RTT* genes were identified by a genetic screen for factors regulating the mobility of the Ty transposon. In this study, there were 21 *RTT* genes characterized. All of the Rtt proteins have a function in genome maintenance (Scholes et al., 2001).

Rtt107 also known as Esc4 and Yhr154w is a scaffold protein, which contains six BRCT repeats. Four BRCT motifs are located in the N-terminal part of Rtt107 while the other two BRCT repeats lie in the C-terminus of the protein.

Even in the absence of exogenous DNA damage a lack of Rtt107 causes genomic instability like chromosomal rearrangements (Yuen et al., 2007). Deletion of Rtt107 furthermore reduces the viability in the presence of drugs that interfere with DNA replication. In the absence of Rtt107 cells are sensitive to replication stalling agents like MMS, HU and CPT (Chang et al., 2002; Hanway et al., 2002; Roberts et al., 2007). However, it is not clear how Rtt107 contribute to recovery after replication fork stalling.

One possibility is that Rtt107 may promote the repair of stalled replication forks via interaction with Slx4. The interaction surface between Slx4 and Rtt107 lies in the N-terminus of Rtt107. After DNA damage the C-terminus of Rtt107 is phosphorylated by the checkpoint kinase Mec1. This phosphorylation of Rtt107 is dependent on Slx4 (Rouse, 2004; Roberts et al., 2006).

Rtt107 also interacts with the recombination repair protein Rad55, the Smc5/6 complex, phosphorylated histone H2A and the ubiquitin ligase subunit Rtt101 (Chin et al., 2006; Roberts et al., 2008; Leung et al., 2011; Li et al., 2012). At DSBs Rtt107 recruits the Smc5/6 complex via the binding of the N-terminus of Rtt107 to the Nse6 subunit of the Smc5/6 complex (Leung et al., 2011). The C-terminal part of Rtt107 with BRCT5 and BRCT6 is important for the binding of phosphorylated histone H2A and could be involved in the recruitment of Rtt107 to chromatin (Li et al., 2012). Importantly, the presence of the ubiquitin ligase subunit Rtt101 and the histone acetyltransferase Rtt109 were shown to be required for Rtt107 recruitment to chromatin when DNA replication stalls (Roberts et al., 2008).

Rtt109 is a histone acetyltransferase that modifies the newly synthesized histones (Han et al., 2007; Li et al., 2008). Rtt109 activity is low but the histone chaperones increase the ability of Rtt109 to acetylate lysines (K) on histone H3. The histone chaperone Vsp75 stimulates Rtt109 activity for acetylation of H3K9, H3K23 and H3K27, whereas the histone chaperone Asf1 promotes H3K56 modification by Rtt109 (Schneider et al., 2006; Recht et al., 2006; Berndsen et al., 2008; Fillingham et al., 2008; Burgess et al., 2010). H3K56 acetylation plays not only a role in DNA synthesis-dependent nucleosome assembly during DNA replication but also in DNA repair (Driscoll et al., 2007; Chen et al., 2008). Budding yeast which lack acetyltable

lysine 56 are sensitive to DNA damaging agents like CPT supporting the key role of H3K56 modification and the requirement of Rtt109 after DNA damage (Masumoto et al., 2005; Ozdemir et al., 2005).

Rtt101 was also implicated to work at replication forks when DNA is damaged. Rtt101 is a cullin subunit of the ubiquitin ligase complex (Michel et al., 2003). Depending on its interaction partners Rtt101 forms slightly different complexes responsible for particular tasks in a cell. The RING finger protein Hrt1 interacts with Rtt101 and recruits an ubiquitin-conjugating enzyme, which is likely to be Cdc34 as was shown *in vitro*. The Mms1 protein also binds Rtt101 and has an adaptor role for the specific substrate of the ubiquitin ligase complex. Mms1 interacts with Mms22 and together with Rtt101 and Hrt1 forms a complex, which is included in the repair of stalled replication forks (Luke et al., 2006; Suter et al., 2007; Zeidi et al., 2008; Han et al., 2010). Recently, the substrate of the Mms22-Mms1-Rtt101-Hrt1 was identified. It has been shown that the Rtt101 ubiquitin ligase modifies acetylated H3K56 for degradation, thus working downstream of Rtt109 at damaged replication forks (Han et al., 2013).

2 AIMS OF THIS STUDY

The Dpb11 protein is a molecular scaffold that acts as a key regulator of different cellular pathways regulating genome stability. Interestingly, Dpb11 mostly binds Cdk1-phosphorylated proteins suggesting a possible role as a downstream reader of Cdk1 signaling and mediator of cell cycle regulation. Dpb11 interacts with different proteins and forms two distinct complexes that act in DNA replication initiation and the DNA damage checkpoint.

Slx4 is a scaffold protein as well and is known to have different roles in DNA repair, which depend on its interaction partners. Intriguingly, Slx4 interacts with Dpb11 suggesting the existence of the third Dpb11 complex most likely involved in DNA repair.

The initial aim of this study was to characterize the Dpb11-Slx4 complex in *S. cerevisiae*. Using biochemical methods we intended to describe the cellular conditions under which Dpb11 and Slx4 interact. Moreover, we aimed to identify a separation of function mutant on Slx4, which renders Slx4 unable to bind specifically to Dpb11. Such a mutant would then be employed for functional studies of the Dpb11-Slx4 complex, particularly in order to define in which DNA repair pathway the Dpb11-Slx4 complex is involved. To this end, we also aimed to identify additional proteins in the complex, which would confer enzymatic activity in the Dpb11-Slx4 complex.

After we discovered a genetic interaction of Dpb11-Slx4 with the structure-specific endonuclease Mus81-Mms4, we aimed to evaluate the requirements for the formation of the Slx4-Dpb11-Mms4-Mus81 complex. Importantly, since previously the function of Mus81-Mms4 was studied extensively, this study became then focused on the regulation of X-shaped DNA structure resolution by Mus81-Mms4 positioning Dpb11-Slx4 as a regulator of the resolution process.

Finally, since the Slx4-Dpb11-Mms4-Mus81 complex consists of three scaffold proteins we hypothesized that additional interaction partners might be involved in the complex. Here, the aim was to test whether there are more essential components required for orchestrated function of the Slx4-Dpb11-Mms4-Mus81 complex and to get insights into the chromatin recruitment of the Slx4-Dpb11-Mms4-Mus81 complex.

4 RESULTS

4.1 Cdk1 regulates the interaction between Dpb11 and Slx4

Dpb11 is a scaffold protein that harbors several BRCT repeats for phosphoprotein binding. To date, the interaction of Dpb11 with several phosphorylated proteins such as Sld2, Sld3, Rad9, Ddc1 and Mec1-Ddc2 is well described (Tanaka et al., 2007; Zegerman and Diffley, 2007; Pfander and Diffley, 2011). Additional Dpb11 interactors were found in a yeast two-hybrid (Y2H) screen by B. Pfander (unpublished). Interestingly, most of the observed Dpb11 binders have S/TP residues that are putative CDK-phosphorylation sites (Nigg, 1993). This suggests that Dpb11 might work as a reader of Cdk1-phosphorylation.

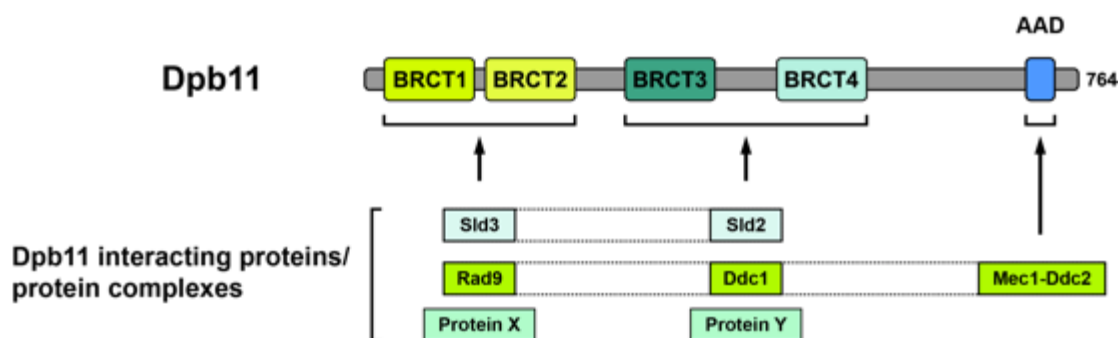


Figure 4.1. Dpb11 interacts with several proteins involved in DNA replication initiation and DNA damage checkpoint activation.

The diagram represents *S. cerevisiae* Dpb11 with its component domains and well-described interaction partners. The protein X and Y stand for the additional proteins, which were found to interact with Dpb11 in a Y2H screen by B. Pfander (adopted from Wardlaw et al., 2014).

4.1.1 Dpb11 BRCT3/4 are important for the interaction with Slx4

In the initial Y2H screen within other Dpb11 binding proteins, the Slx4 protein was found to interact with BRCT3/4 of Dpb11. To confirm the primary result, Y2H experiment was performed using the full-length Slx4 protein and the Dpb11 fragments. Already known Dpb11 interactors namely Rad9 and Ddc1, which bind BRCT1/2 and BRCT3/4 of Dpb11, respectively, were used as a control. In this experimental setup, we confirmed Slx4 interaction with Dpb11. Importantly, Slx4

RESULTS

binds the full-length Dpb11 protein as well as the Dpb11 fragment with BRCT3/4 but not BRCT1/2 of Dpb11 (Figure 4.2).

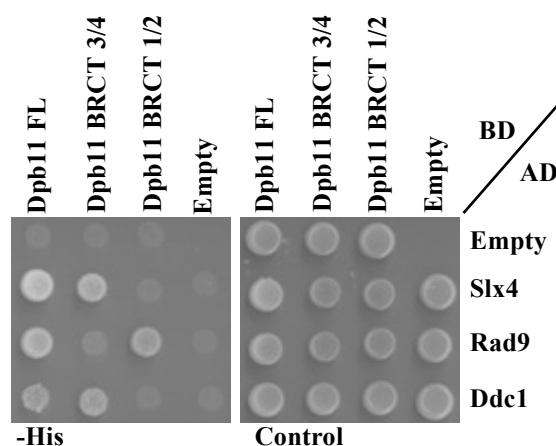


Figure 4.2. Slx4 interacts with BRCT3/4 of Dpb11.

Y2H experiment showing Dpb11, Dpb11 BRCT1/2 and Dpb11 BRCT3/4 binding to Slx4, Rad9 and Ddc1. AD-fusions of *SLX4*, *RAD9* and *DDC1* were co-transformed with BD-fusions of *DPB11* full length or fragments containing BRCT1/2 or BRCT3/4. Cells were spotted on control and selective plates and evaluated after 3 days growth at 30°C.

4.1.2 Phosphorylated S486 of Slx4 is important for the interaction with Dpb11

Dpb11 has four BRCT repeats and is known to bind phosphorylated proteins (Araki et al., 1995). Therefore, we hypothesized that Slx4 might be also phosphorylated for the interaction with Dpb11. To test this idea, we mutated CDK consensus S/TP sites in *SLX4* to alanine, which cannot be phosphorylated. Using various mutated *SLX4* and the *DPB11* construct, Y2H experiment was performed. As figure 4.3a illustrates, we observed that Slx4 that had serine 486 replaced by alanine was not able to interact with full length Dpb11. This result was confirmed using the fragment of Dpb11 with BRCT3/4 and Slx4-S486A in Y2H experiment. From this we conclude that S486 of Slx4 is crucial for the interaction with Dpb11.

There are two ways to explain the reduced Slx4-S486A and Dpb11 interaction. First, mutating serine 486 to alanine might alter the structure of the protein. Second, S486A mutation of *SLX4* may lead to a failure of the kinases to phosphorylate Slx4-S486A.

To test the first hypothesis, we took an advantage of the SILAC-based mass spectrometry (MS) approach. In this experiment the Slx4 interaction partners, which were pulled-down from the lysates of the wild type cells and the mutant expressing

RESULTS

Slx4-S486A, were compared. We found that Slx4-S486A was still able to bind its known interaction partners Slx1 and Rtt107 to the same extent as endogenous Slx4. In contrast, Slx4-S486A binding to Dpb11 was impaired (Figure 4.3b). This suggests that S486A of Slx4 is a specific mutation that leads to impaired interaction exceptionally with Dpb11 but not with Slx1 and Rtt107.

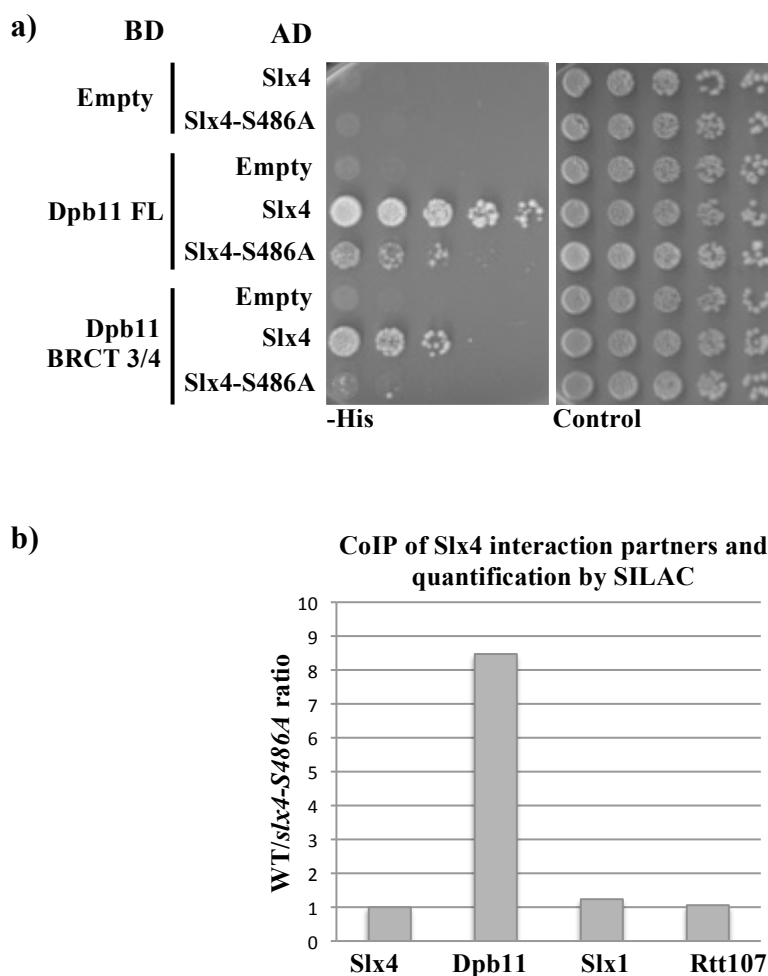


Figure 4.3. S486 of Slx4 is crucial for the interaction with Dpb11 but not for Slx1 and Rtt107.

a) Y2H experiment showing Slx4 and Slx4-S486A binding to Dpb11 and Dpb11 BRCT3/4. AD-fusions of *SLX4* and *slx4-S486A* were co-transformed with BD-fusions of full length *DPB11* or fragment containing BRCT3/4. Cells were spotted on control and selective plates and evaluated after 3 days growth at 30°C; b) SILAC-based MS experiment of Slx4 interactors. Co-immunoprecipitation samples from FLAG-tagged Slx4 and Slx4-S486A were prepared for MS. On the vertical axis WT to Slx4-S486A ratio is plotted. Values higher than one indicate a reduce binding to Slx4-S486A compared to Slx4. Experiment by L. N. Princz.

Second hypothesis was based on the fact that S486 of Slx4 matches CDK consensus site. Moreover, Dpb11 was previously shown to interact mainly with the

RESULTS

Cdk1-phosphorylated proteins (Tanaka et al., 2007; Zegerman and Diffley, 2007; Pfander and Diffley, 2011). For these reasons we hypothesized that Slx4 might be phosphorylated on S486 by Cdk1 for specific interaction with Dpb11. Following this idea, Slx4 peptides from the G1- and G2/M-arrested cells were compared using SILAC-based MS. Slx4 peptide, which contained phosphorylated S486, was enriched in the G2/M-phase sample. The enrichment of other detected Slx4 peptides remained constant in the G1- and G2/M-phase cells (Figure 4.4a). Therefore, we conclude that phosphorylation of S486 of Slx4 is cell cycle regulated.

To test the idea of Slx4 as a target of Cdk1 phosphorylation, SILAC-based MS experiment was performed. The abundance of Slx4 peptides was compared from WT cells with those from the strain where Cdk1 activity was inhibited. To control Cdk1 activity, we used the *cdc28-as1* allele. This allows the inhibition of Cdk1 by adding mutant kinase inhibitor 1NM-PP1 to the medium. The cells carrying *cdc28-as1* allele were arrested in G2/M-phase and treated with the inhibitor or left untreated. After comparison of the samples from the cells with active and inactive Cdk1, we measured the increased amounts of the Slx4 peptide containing phosphorylated S486 in the sample, which did not contain the 1NM-PP1 inhibitor (Figure 4.4b). Thus, we conclude that S486 of Slx4 is phosphorylated by Cdk1.

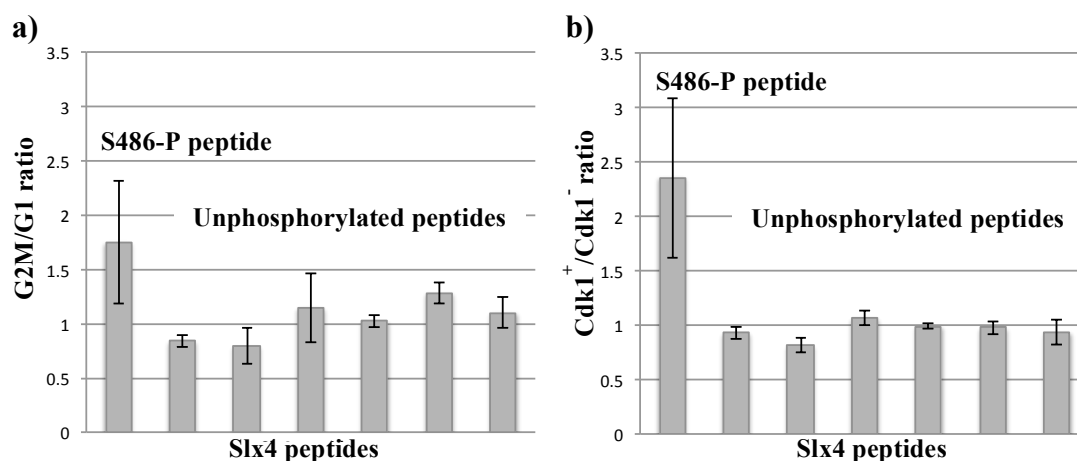


Figure 4.4. Phosphorylation of S486 of Slx4 is cell cycle regulated by Cdk1.

a) SILAC-based MS experiment of Slx4 phosphopeptides. Co-immunoprecipitation samples from G2/M- and G1-arrested cells using FLAG-tagged Slx4. On the vertical axis G2/M to G1 ratio is plotted. Values higher than one show enrichment of a peptide in G2/M. Experiment by L. N. Princz; b) SILAC-based MS experiment of Slx4 phosphopeptides. Co-immunoprecipitation samples from Cdk1 active (Cdk1⁺) and Cdk1 inactive (Cdk1⁻) cells using FLAG-tagged Slx4. On the vertical axis Cdk1⁺ to Cdk1⁻ ratio is plotted. Values higher than one show enrichment of a peptide in the presence of active Cdk1. Experiment by L. N. Princz.

RESULTS

To further strengthen the cell cycle role in phosphorylation of Slx4 S486 for Slx4 binding to Dpb11, we investigated Slx4 and Dpb11 physical interaction. Since the DNA damage checkpoint and the cell cycle can function in parallel to regulate the specific pathways in a cell (Libreri et al., 2000; Baroni et al., 2004; Huertas et al., 2008), we also wondered whether DNA damage has an influence on the Dpb11-Slx4 complex formation. Therefore, we first compared wild type Slx4 and Slx4-S486A ability to interact with Dpb11. Second, to our analysis we included treatment with MMS to evaluate the DNA damage checkpoint influence on the Dpb11 binding to Slx4. For this particular experiment the strains, which had FLAG-tagged Slx4 or Slx4-S486A were generated. Co-immunoprecipitation was performed from the asynchronous cells, which were treated or untreated with MMS. Interestingly, the increase of slower migrating species of Slx4 were observed in WT cells after MMS damage (Figure 4.5a, lane 4). Also, using FLAG-tagged Slx4 more Dpb11 was pulled down from the MMS treated compared to untreated sample (Figure 4.5a, lanes 4 and 3). When we compared the samples from the *slx4-S486A* mutant cells, the Slx4-S486A interaction with Dpb11 was not detected even after treatment with MMS (Figure 4.5a, lane 6). Just after longer exposure of Western blot, faint band corresponding to Dpb11 was identified suggesting that there is some residual Dpb11 binding to Slx4-S486A (Figure 4.5a). These data confirms the requirement of S486 for binding of Slx4 to Dpb11. Moreover, it seems that the Dpb11-Slx4 interaction is promoted by the DNA damage checkpoint.

To verify the importance of Cdk1 phosphorylation to the Dpb11-Slx4 interaction, we compared the samples from G1 and G2/M cells after co-immunoprecipitation using FLAG-tagged Slx4. In this experiment cells were synchronized in G1 or in G2/M and treated with phleomycin. As observed in previous experiment (Figure 4.5a, lane 4), more Dpb11 was pulled-down from the samples where DNA damage was induced (Figure 4.5b, lanes 2 and 4). Moreover, the Slx4 interaction with Dpb11 was reduced in G1-phase comparing to G2/M-phase (Figure 4.5b, lanes 1 and 3). Interestingly, even treatment with phleomycin increased Dpb11 binding to Slx4 in G1 and G2/M, the amount of pulled-down Dpb11 after DNA damage was grater from G2/M sample compared to G1 sample (Figure 4.5b, lanes 2 and 4). This demonstrates that the Dpb11-Slx4 complex formation is dependent on two regulators - cell cycle and DNA damage checkpoint.

RESULTS

The cell cycle influence to Dpb11 binding to Slx4 was also evaluated using *cdc28-as1* allele. The *cdc28-as1* expression enables to manipulate the activity of the kinase by adding analog 1NM-PP1. In our experiment the cells expressing Slx4-3FLAG with active or inactivated Cdk1 were compared. Interestingly, Dpb11 was enriched in the wild type Cdk1 sample compared with the cells where Cdk1 was inhibited (Figure 4.5c, lanes 2 and 3).

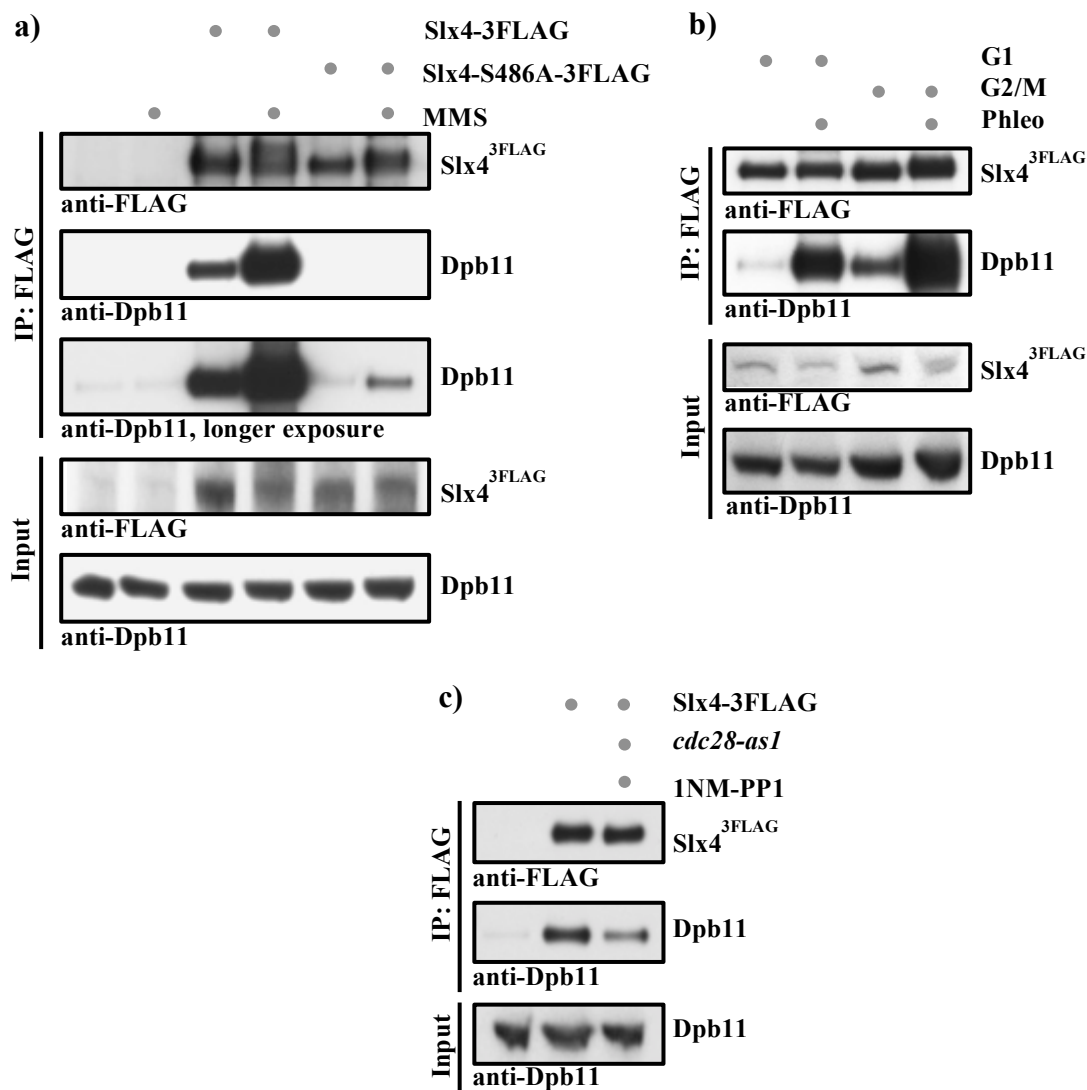


Figure 4.5. Cdk1-dependent Dpb11-Slx4 interaction is impaired in the *slx4-S486A* mutant.

a) CoIP experiment showing Dpb11 interaction with Slx4 and Slx4-S486A. FLAG-tagged Slx4 and Slx4-S486A were pulled-down from MMS-treated or untreated cells. Experiment by L. N. Princz; b) CoIP experiment showing Dpb11-Slx4 interaction at different cell cycle stages. FLAG-tagged Slx4 and Slx4-S486A were pulled-down from G1 or G2/M cells, which were treated or untreated with phleomycin (Phleo). Experiment by L. N. Princz; c) CoIP experiment showing Dpb11-Slx4 interaction dependence on Cdk1. FLAG-tagged Slx4 was pulled-down from Cdk1 active and Cdk1 inactive (*cdc28-as1* + 1NM-PP1) cells. Experiment by L. N. Princz.

All together, these experiments show that Slx4 is a target of Cdk1 and that Cdk1-phosphorylation of S486 in Slx4 is important for the interaction with Dpb11.

4.2 The Dpb11-Slx4 complex is required for the response to replication fork stalling

Having found the requirements for the interaction of Dpb11-Slx4, we were prompted to define the function of the Dpb11-Slx4 complex. The Slx4 protein is known to have several functions in DNA repair depending on its interaction partners Rad1, Slx1 and Rtt107 (Rouse, 2009). For that reason, we speculated that the Dpb11-Slx4 complex might also have a function in DNA repair.

Cells experience variety of DNA damage and have different mechanisms to repair a specific lesion (summarized in 2.1.1). So we aimed to find the conditions when the interaction of Dpb11 and Slx4 is important using the *slx4-S486A* mutant.

Different DNA damaging agents cause specific type of lesion. For example, phleomycin and zeocin give rise to single-strand and double-strand DNA brakes. UV light introduces thymidine dimers. A natural alkaloid camptothecin (CPT) inhibits the topoisomerase I thereby introducing single strand brakes. Cisplatin is known to induce inter-strand DNA crosslinking. Hydroxyurea (HU) is featured in decreasing dNTP levels in a cell. Methyl methanesulfonate alkylates DNA. 4-Nitroquinoline 1-oxide (4-NQO) mimics the effect of UV light and also might induce DNA damage indirectly by the production of the reactive oxygen species.

4.2.1 The *slx4-S486A* mutant is particularly sensitive to MMS

To find the type of the lesion that requires the action of the Dpb11-Slx4 complex, the *slx4-S486A* mutant sensitivity to UV, phleomycin, HU, CPT, cisplatin, 4-NQO and MMS was tested. Interestingly, similar to WT, the *slx4-S486A* mutant was not sensitive to UV, phleomycin, HU, CPT and cisplatin induced DNA damage (Figure 4.6a). However, a slight sensitivity to 4-NQO was observed in the *slx4-S486A* mutant cells (Figure 4.6a, lowest panel). Strikingly, the viability of the *slx4-S486A* mutant on MMS was markedly decreased compared to the WT cells (Figure 4.6b). This experiment suggests that the Dpb11-Slx4 complex is important after MMS induced DNA damage.

RESULTS

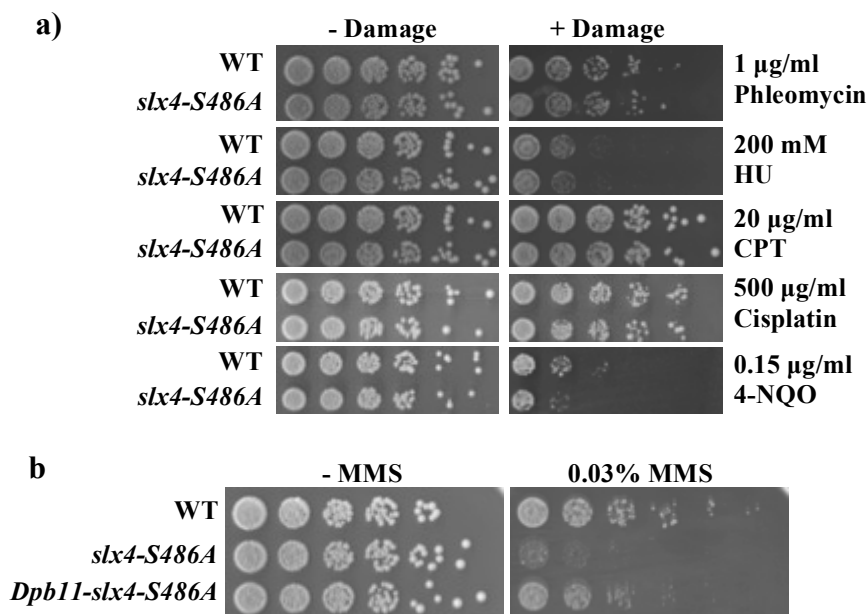


Figure 4.6. Dpb11-Slx4 interaction is important after DNA damage by MMS but not UV, phleomycin, HU, CPT, cisplatin and 4-NQO.

a) The *slx4-S486A* mutant sensitivity was tested using UV, phleomycin, HU, CPT, cisplatin and 4-NQO. Cells were spotted in serial dilutions and analyzed after 2 days growth at 30°C; b) The *slx4-S486A* and *Dpb11-slx4-S486A* mutants sensitivity was tested using MMS. Cells were spotted as in a.

Slx4-S486A is not able to fully interact with Dpb11, suggesting that the *slx4-S486A* mutant sensitivity to MMS comes from the reduced binding to Dpb11. To confirm this hypothesis, we created a fusion protein where Dpb11 was covalently fused to Slx4-S486A. When the *Dpb11-slx4-S486A* mutant sensitivity to MMS was tested, we observed that the mutant expressing Dpb11-slx4-S486A fusion is not sensitive to MMS, suggesting the rescue of the *slx4-S486A* mutant phenotype. These data strongly indicate that MMS sensitivity of the *slx4-S486A* mutant is due to the loss of interaction with Dpb11 (Figure 4.6b).

4.2.2 The Dpb11-Slx4 complex is crucial after replication fork stalling in S-phase

The Dpb11-Slx4 complex mediates cell viability specifically after MMS damage. It is known that MMS alkylates the DNA leading to replication fork stalling in S-phase. To get more insight in how the Dpb11-Slx4 complex contributes to DNA repair, we tested the fate of the *slx4-S486A* mutant cells after a pulse of MMS damage in S-phase. So called recovery experiments were performed as follows. First, cells were synchronized in G1-phase with alpha factor. Then cells were released into S-

RESULTS

phase in a medium supplemented with MMS for 30 minutes. After MMS treatment, cells were released into fresh medium and allowed to recover for 3 hours. During the recovery, samples were taken at different time points and analyzed by various methods. When measuring DNA content by FACS, we observed that the *slx4-S486A* mutant progressed slower in S-phase compared to WT after MMS treatment (Figure 4.7a). Nevertheless, the cell cycle progression was the same in WT and the *slx4-S486A* mutant as observed from the cyclin Clb2 expression profile and PCNA (Pol30) SUMOylation, which are M- and S-phase markers, respectively (Figure 4.7b). These data suggest that the slowed down DNA replication in the *slx4-S486A* mutant is not due to impaired cell cycle progression but rather because of the inability of the *slx4-S486A* mutant to cope with S-phase DNA damage.

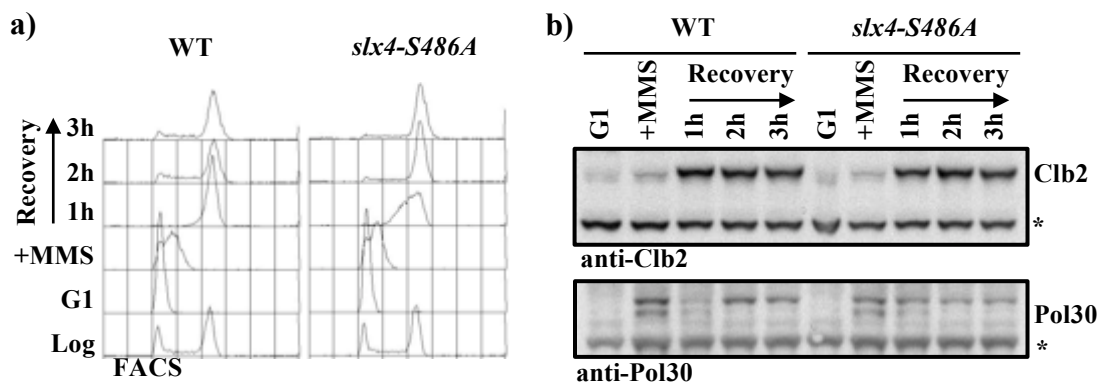


Figure 4.7. DNA repair kinetics but not the cell cycle progression is slowed down in the *slx4-S486A* mutant.

a) Recovery experiment of WT and the *slx4-S486A* mutant showing slowed down S-phase in the *slx4-S486A* mutant. Cells were synchronized in G1, released into S-phase to medium containing MMS. After 30 min cells were released into drug-free medium for 3 hours. The samples were taken at different time points and DNA content was measured by FACS; b) Recovery experiment as in a. Cell cycle progression was evaluated by Western blot using antibodies against Clb2 (upper panel) and Pol30 (lower panel). Asterisk indicates an unspecific band, which was used as a loading control.

The recovery of the *slx4-S486A* mutant after the pulse of DNA damage was also studied using pulsed field gel electrophoresis (PFGE), which enables to visualize chromosomes and allows to follow DNA replication and repair processes. The important feature of the method is that the DNA structures arising from DNA repair and replication intermediates are not able to enter the gel. As expected, from the sample of MMS-damaged cells none of the chromosomes were detected in the PFGE gel. After the pulse of MMS damage most DNA content from WT and the *slx4-S486A* mutant cells stayed in a well and some DNA fragments appeared like a smear on the

RESULTS

gel (Figure 4.8a, lanes 2 and 7). After one hour of recovery yeast chromosomes from WT samples were detected on the gel (Figure 4.8a, lane 3). In contrast, the chromosomes of the *slx4-S486A* mutant entered the gel after two hours of recovery (Figure 4.8a, lane 9). This experiment demonstrates that the DNA replication or repair intermediates persist longer in the *slx4-S486A* mutant compared to WT cells.

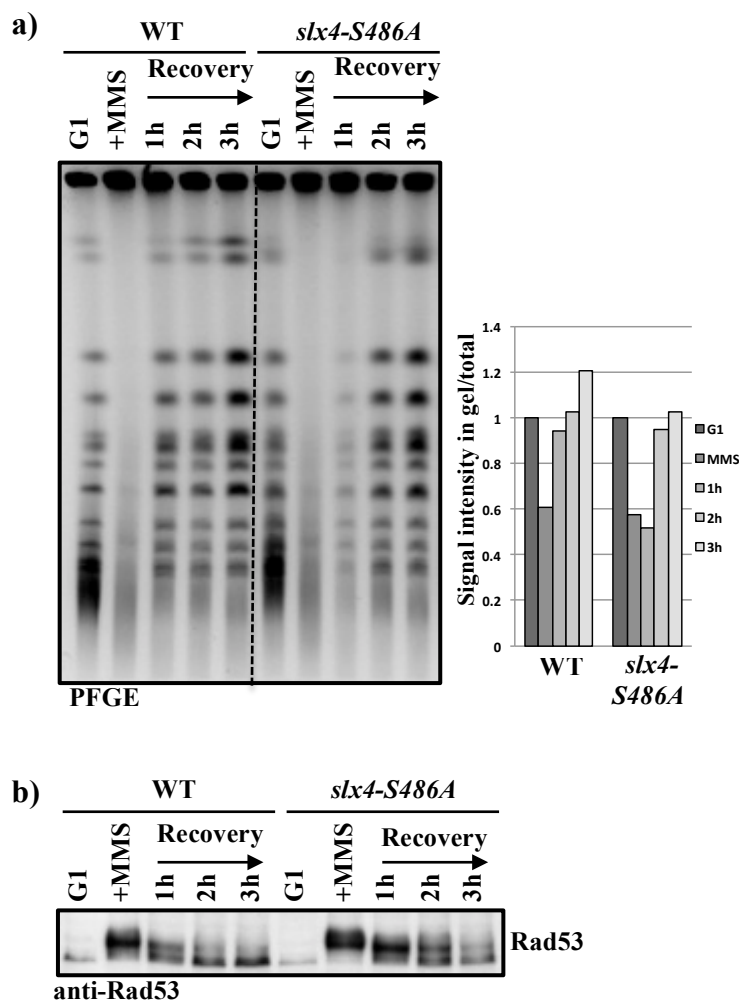


Figure 4.8. DNA replication or repair intermediates, which trigger DNA damage checkpoint activation, persist longer in the *slx4-S486A* mutant.

a) Recovery experiment of WT and the *slx4-S486A* mutant showing slowed down DNA repair kinetics in the *slx4-S486A* mutant. Cells were synchronized in G1, released into S-phase to medium containing MMS. After 30 min cells were released into drug-free medium for 3 hours. The samples were taken at different time points and yeast chromosomes were visualized by PFGE. Quantification of the chromosome signal was performed using ImageJ software. The signal intensity in a lane of the gel was normalized to the whole signal including that in a well; b) Recovery experiment as in a. DNA damage checkpoint activation was evaluated by Western blot using antibodies against Rad53.

DNA repair intermediates containing single stranded DNA structures arising from the DNA replication stalling activate the DNA damage checkpoint. A critical

RESULTS

checkpoint response to DNA damage is the phosphorylation and thereby activation of the effector kinase Rad53 (Sanchez et al., 1999). To determine the DNA damage checkpoint activation kinetics in the *slx4-S486A* mutant during recovery after a pulse of DNA damage using the same experimental setup as described earlier, Rad53 bulk phosphorylation was analyzed. As assumed, a slow migrating band corresponding to the hyperphosphorylated Rad53 in the samples from WT and the *slx4-S486A* mutant cells after treatment with MMS were observed (Figure 4.8b). In WT cells, the phosphorylation of Rad53 gradually disappeared during recovery and after three hours of recovery mainly unphosphorylated Rad53 remained (Figure 4.8b, lane 5). In contrast, in the *slx4-S486A* mutant recovery was slower than in the WT and the hyperphosphorylation of Rad53 remained during the recovery of three hours (Figure 4.8b, lane 10). In conclusion, after a pulse of DNA damage in S-phase the single stranded DNA replication and repair intermediates, which are in turn responsible for activation of the DNA damage checkpoint, persist longer in the *slx4-S486A* mutant than in WT cells.

To prove that the Dpb11-Slx4 complex specifically acts in S-phase, we tested whether the *slx4-S486A* mutant has a phenotype after the pulse of DNA damage outside of S-phase. Since MMS alkylates DNA thereby stalling DNA replication and specifically effecting cells in S-phase but not in G1 and G2/M, the DNA damaging agents, which introduce single and double strand DNA brakes, were chosen. For this purpose the recovery experiment was performed as described previously using cells arrested in G1- or G2/M-phase, which were subsequently treated with single and double strand brakes inducing agents zeocin or phleomycin, respectively. In this experiment DNA replication kinetics were followed by FACS (Figure 4.9a and b) and the DNA damage checkpoint activation was detected by appearance of hyperphosphorylated Rad53 (Figure 4.9c and d). Strikingly, we did not observe any differences between WT and the *slx4-S486A* mutant in recovery after DNA damage in G1 and G2/M (Figure 4.9). Thus, these experiments support the hypothesis that the Dpb11-Slx4 complex has a role after DNA damage particularly in S-phase but not in G1- or G2/M-phases.

RESULTS

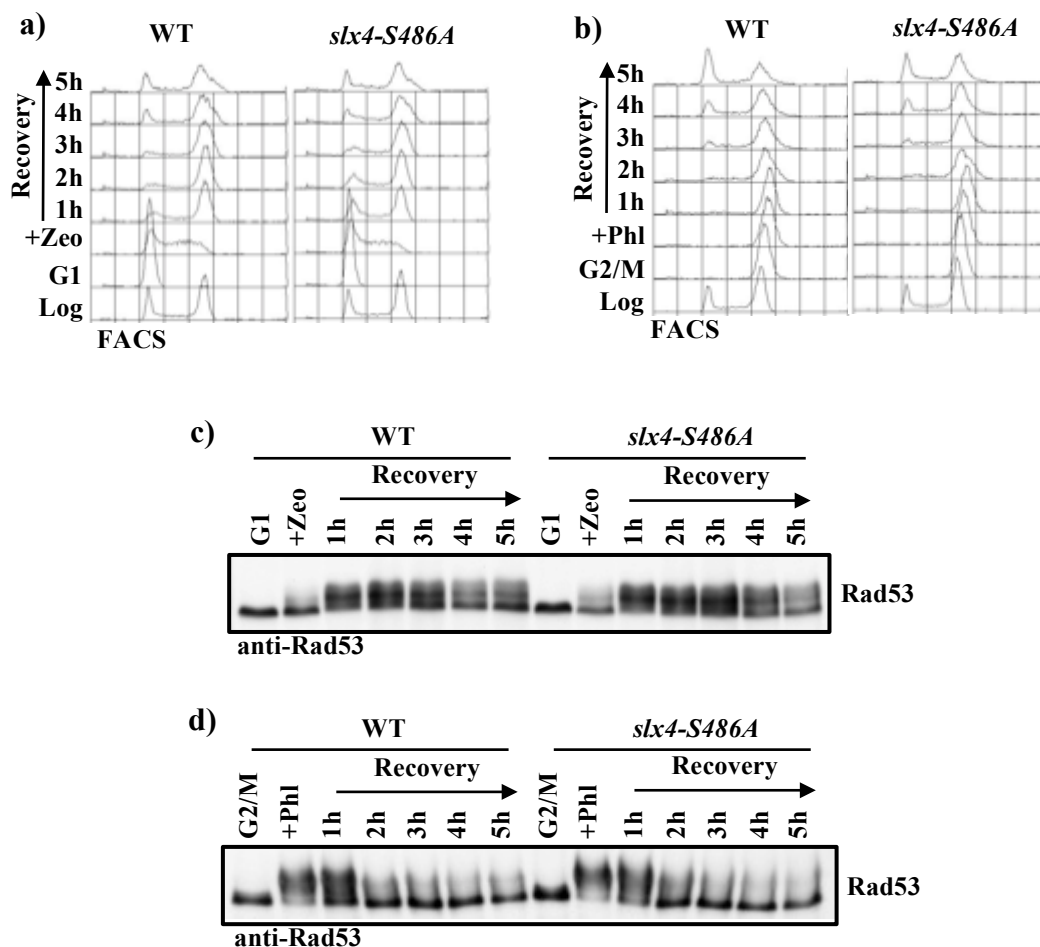


Figure 4.9. The Dpb11-Slx4 complex is not important after DNA damage in G1- and G2/M-phase.

a) Recovery experiment of WT and the *slx4-S486A* mutant showing normal cell cycle progression after DNA damage in G1. Cells were synchronized in G1 and damaged by zeozin (+Zeo). After 30 min cells were released into drug-free medium for 5 hours. The samples were taken at different time points and DNA content was measured by FACS; b) Recovery experiment of WT and the *slx4-S486A* mutant showing normal cell cycle progression after DNA damage in G2. Cells were synchronized in G2 and damaged by phleomycin (+Phl). After 30 min cells were released into drug-free medium for 5 hours. The samples were taken at different time points and DNA content was measured by FACS; c) Recovery experiment as in a. DNA damage checkpoint activation was evaluated by Western blot using antibodies against Rad53; d) Recovery experiment as in b. DNA damage checkpoint activation was evaluated by Western blot using antibodies against Rad53.

4.3 The Dpb11-Slx4 complex promotes Mus81-Mms4-dependent X-shaped DNA structure resolution

DNA lesions in S-phase can be bypassed by post-replication repair (PRR) mechanisms. Error-prone PRR involves the Rev1, Rev3-Rev7 and Rad30 proteins, while error-free PRR requires Rad5 and Ubc13/Mms2 (Ulrich and Jentsch, 2000;

Yang and Woodgate, 2007; Goodman and Woodgate, 2013). In the absence of bypass mechanisms stalled replication forks may collapse, thereby causing the occurrence of DNA double strand breaks (DSBs). In this case homologous recombination (HR) is required to repair the DSB. Since the Dpb11-Slx4 complex is important after DNA damage in S-phase, we questioned whether the complex is exclusively involved in PRR or HR.

4.3.1 The Dpb11-Slx4 complex is not exclusively involved in PRR or HR

The impairment of PRR or HR leads to increased spontaneous recombination and elevated mutation rates. To test the spontaneous recombination rates, we used a yeast strain, which carries a *URA3* gene surrounded by two nonfunctional *leu2* alleles. Both *leu2* alleles have a mutation, namely *leu2-112* and *leu2-k*. After recombination events a cell restores an active *LEU2* gene and keep or lose *URA3*. The spontaneous recombination of WT and the *slx4-S486A* mutant cells was evaluated. For processing the data, the “Maximum-Likelihood” method was used to calculate recombination rates (Rosche and Foster, 2000). Interestingly, the *slx4-S486A* mutant shows minor increase in spontaneous recombination rates, which are similar to WT (Figure 4.10a).

To examine the spontaneous mutation rate, the yeast strains containing the *CAN1* gene were used. The activity of plasma membrane arginine permease Can1 is lethal to the cells exposed to canavanine, a non-proteinogenic amino acid, which when incorporated to proteins may lead to a loss-of-function. Conversely, loss-of-function mutations in the *CAN1* gene allow cells to grow in the presence of canavanine. In this experiment the *rad51* deletion mutant was used as a control, since this mutant shows drastically increased spontaneous mutation rates. After plating WT, the *slx4-S486A* and *rad51* deletion mutant cells on medium containing canavanine, the colonies, which gained a mutation in *CAN1* gene and therefore were able to grow on the selective medium, were counted. The “Maximum-Likelihood” method was used to calculate the mutation rates (Rosche and Foster, 2000). As observed previously, we perceived a high spontaneous mutation rate in the *rad51* deletion cells. However, the spontaneous mutation rate of the *slx4-S486A* mutant was similar to wild type (Figure 4.10b). In conclusion, the Dpb11-Slx4 complex seems not to have a specific role in PRR or HR as observed from the spontaneous recombination and mutagenesis experiments.

RESULTS

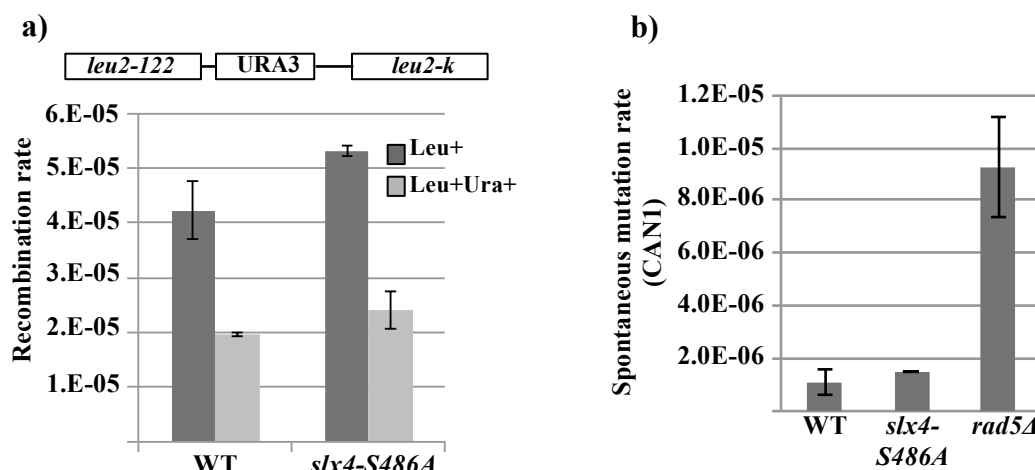


Figure 4.10. Spontaneous recombination and mutation rates are not increased in the *slx4-S486A* mutant.

a) Spontaneous recombination rate of WT and the *slx4-S486A* mutant showing normal spontaneous recombination events in the *slx4-S486A* mutant. Cells were plated on -Leu and -Leu-Ura selective media. Recombinants were counted after 4 days growth at 30°C and the recombination rate was calculated using the “Maximum-Likelihood” method. Dark grey bars present the recombination event when the *URA3* gene was lost. Light grey bars present the recombination event when the *URA3* gene remained. Error bars show the standard deviation from three independent experiments; b) Spontaneous mutation rate of WT, the *slx4-S486A* and *rad5Δ* deletion mutants showing normal spontaneous mutation events in the *slx4-S486A* mutant. Cells were plated on medium supplemented with canavanine. Mutants were counted after 4 days growth at 30°C and the spontaneous mutation rate was calculated using the “Maximum-Likelihood” method. Error bars show the standard deviation from two independent experiments.

To confirm that the Dpb11-Slx4 complex is not exclusively involved in post-replication repair or homologous recombination, we performed genetic interaction analysis. For this purpose, cell growth on MMS was evaluated. To investigate the genetic relationship with the error-prone PRR mechanism, the *REV1*, *REV3* and *RAD30* genes encoding the proteins involved in translesion synthesis were deleted in WT and in the *slx4-S486A* mutant background. Even though the mutants with single deletions of *REV1*, *REV3* and *RAD30* were not sensitive to MMS, these deletions increased the hypersensitivity of the *slx4-S486A* mutant cells (Figure 4.11). This result together with the mutagenesis experiments indicates that the Dpb11-Slx4 complex is not involved in the error-prone post-replication repair mechanism.

RESULTS

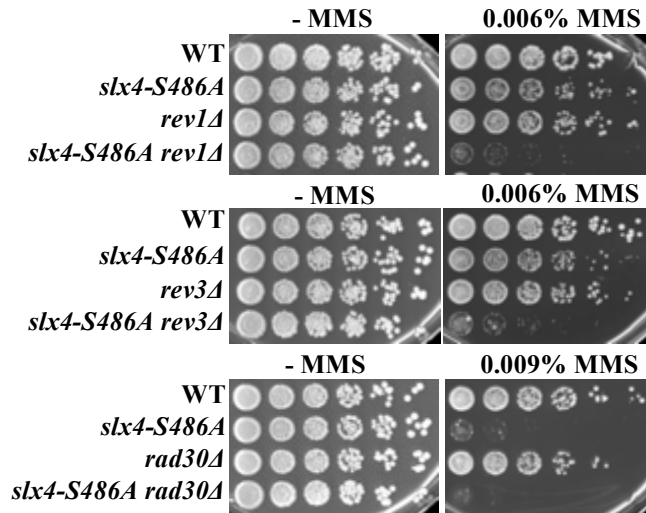


Figure 4.11. The Dpb11-Slx4 complex is not involved in error-prone PRR.

MMS sensitivity of WT, the *slx4-S486A* and *rev1Δ*, *rev3Δ*, *rev30Δ* deletion single mutants and in combination with the *slx4-S486A* mutant. Cells were spotted in serial dilutions on plates containing MMS. The growth was evaluated after incubation for 2 days at 30°C.

Next, we investigated the error-free PRR, in particular the ubiquitin-conjugating enzyme variant Mms2 and the DNA helicase/ubiquitin ligase Rad5, relation to the Dpb11-Slx4 complex. For genetic interaction, cell growth on MMS was tested. The strains with a deletion of *MMS2* and mutations of *RAD5* and the double mutants in combination with *slx4-S486A* were generated. To discriminate between different functional domains of Rad5, which might be involved in the genetic interaction with Dpb11-Slx4, we generated two different *RAD5* point mutants. The KT538,539AA mutations of Rad5 abolishes Rad5 ATPase activity, while Rad5-C914S has a mutation in Rad5 RING finger domain. Using these mutants, we observed that the *mms2Δ* deletion, *rad5-KT438,539AA* and *rad5-C914A* mutants were sensitive to MMS. Importantly, the viability of all these mutants decreased in the background of *slx4-S486A* (Figure 4.12a).

To ascertain that the Dpb11-Slx4 complex is not involved in the error-free PRR, we tested the effect of deletion of *SRS2* and *SIZ1* in the *slx4-S486A* mutant background. Srs2 is a helicase, which disrupts the Rad51 recombinase loading and prevents unscheduled HR events. This activity of Srs2 is very important when the replication stalls and HR is not a preferred way to bypass the lesion. Importantly, the SUMOylation of PCNA by the SUMO ligase Siz1 recruits Srs2 to stalled replication forks. When the error free post-replication repair machinery is impaired, HR is beneficial to a cell. In such a situation absence of Srs2 and Siz1 promotes homologous

RESULTS

recombination and thereby rescues the repair defect of error-free PRR mutants (Pfander et al., 2005). Following this idea, we tested whether the *slx4-S486A* mutant sensitivity to MMS is rescued by deleting *SIZ1* or the C-terminus of *SRS2*. We thus tested the growth on MMS of the *slx4-S486A*, *srs2ΔC* and *siz1Δ* deletion mutants and double mutant combinations. As shown before (Pfander et al., 2005), we did not detect the *srs2ΔC* and *siz1Δ* deletion mutant sensitivity to MMS. Importantly, deleting *SIZ1* or the C-terminus of *SRS2* was not able to rescue the *slx4-S486A* mutant sensitivity (Figure 4.12b). This experiment indicates that the Dpb11-Slx4 complex is not specifically involved in the error-free PRR.

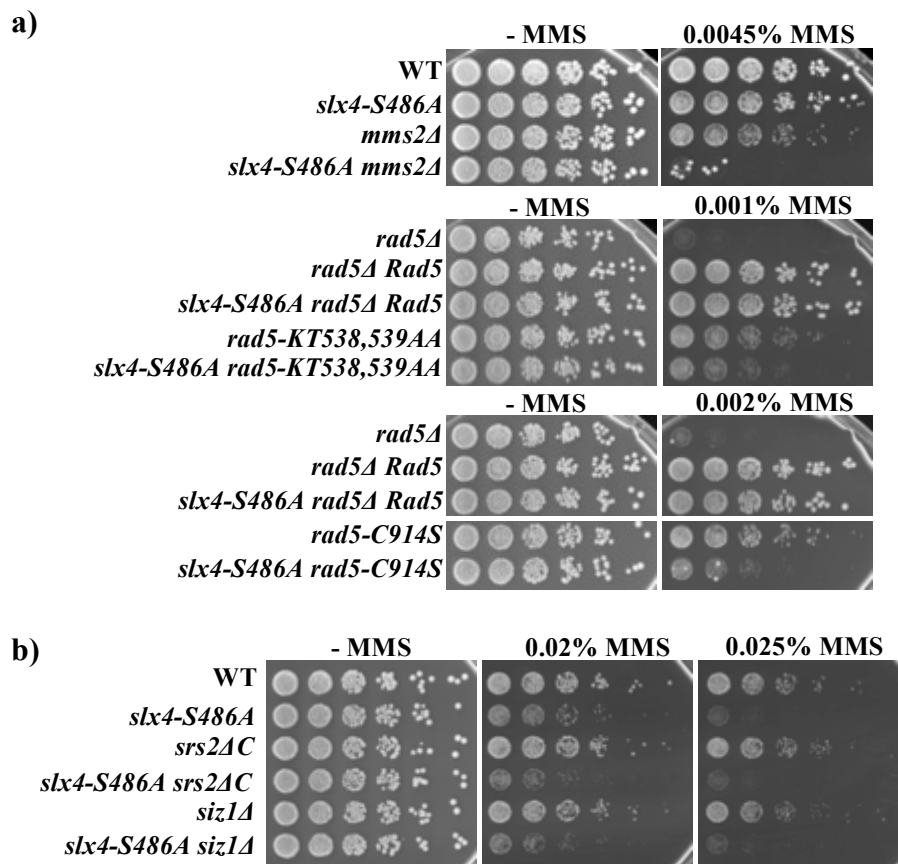


Figure 4.12. The Dpb11-Slx4 complex is not involved in error-free PRR.

a) MMS sensitivity of WT, the *slx4-S486A* and *mms2Δ* deletion, *rad5-KT438,539AA*, *rad5-C914S* single mutants and in combination with *slx4-S486A*. Cells were spotted in serial dilutions on plates containing MMS. The growth was evaluated after incubation for 2 days at 30°C; b) MMS sensitivity of WT, the *slx4-S486A* and *srs2ΔC*, *siz1Δ* deletion single mutants and in combination with *slx4-S486A*. Cells were spotted as in a.

Apart from the PRR, the homologues recombination mechanism is used to repair the stalled replication forks. To test whether the Dpb11-Slx4 complex has a

RESULTS

specific role in HR repair, the epistasis analysis with the *slx4-S486A* mutant and HR-deficient mutants was performed. Interestingly, we found that deletion of the recombinase *RAD51* gene or the strand exchange stimulating protein *RAD55* gene enhanced the *slx4-S486A* mutant sensitivity to MMS. Moreover, an interfering with the resection step of HR by deleting the exonuclease *EXO1* gene had an additive effect on the *slx4-S486A* mutant sensitivity to MMS. Furthermore, the deletion of *RAD1*, the subunit of the nuclease Rad1-Rad10, which is known to process 3' tails after HR, increased the *slx4-S486A* mutant sensitivity to MMS (Figure 4.13a).

A possible involvement of Dpb11-Slx4 in 3' tails processing is better illustrated by the experiment of 3' tail cleavage after HR described previously (Lyndaker et al., 2008). In this experiment we examined how the *slx4-S486A* mutant was able to process one or two non-homologous 3' tails. If the mutant had the problems in processing one or two 3' tails, this would be reflected in reduced cell viability. In this experiment DSBs were induced by activating HO endonuclease, which is expressed after adding galactose to a liquid medium. Next, after plating and incubation of the cells, the survival rate was calculated as the number of colonies arising from induced relative to uninduced cultures. In this assay we did not observe the difference between WT and the *slx4-S486A* mutant cells (Figure 4.13b).

In line with HR experiments, we tested whether Dpb11-Slx4 is involved in HR-like mechanisms as single strand annealing (SSA), which is used to repair DSBs. Analysis of SSA was performed in the background of the yeast strain YMV45, which harbors a *leu2* repeat at each sides of an galactose-inducible DSB (Clerici et al., 2005). To survive after DSB induction, cells have to repair the break by resection followed by annealing of the homologous *leu2* sequences. However, the *slx4-S486A* mutant was not sensitive after the induction of DSB in YMV45 background (Figure 4.13c). In conclusion, the different lines of experiments testing a potential role of the Dpb11-Slx4 complex in HR show that this complex is not specifically involved in any step or kind of homologous recombination.

RESULTS

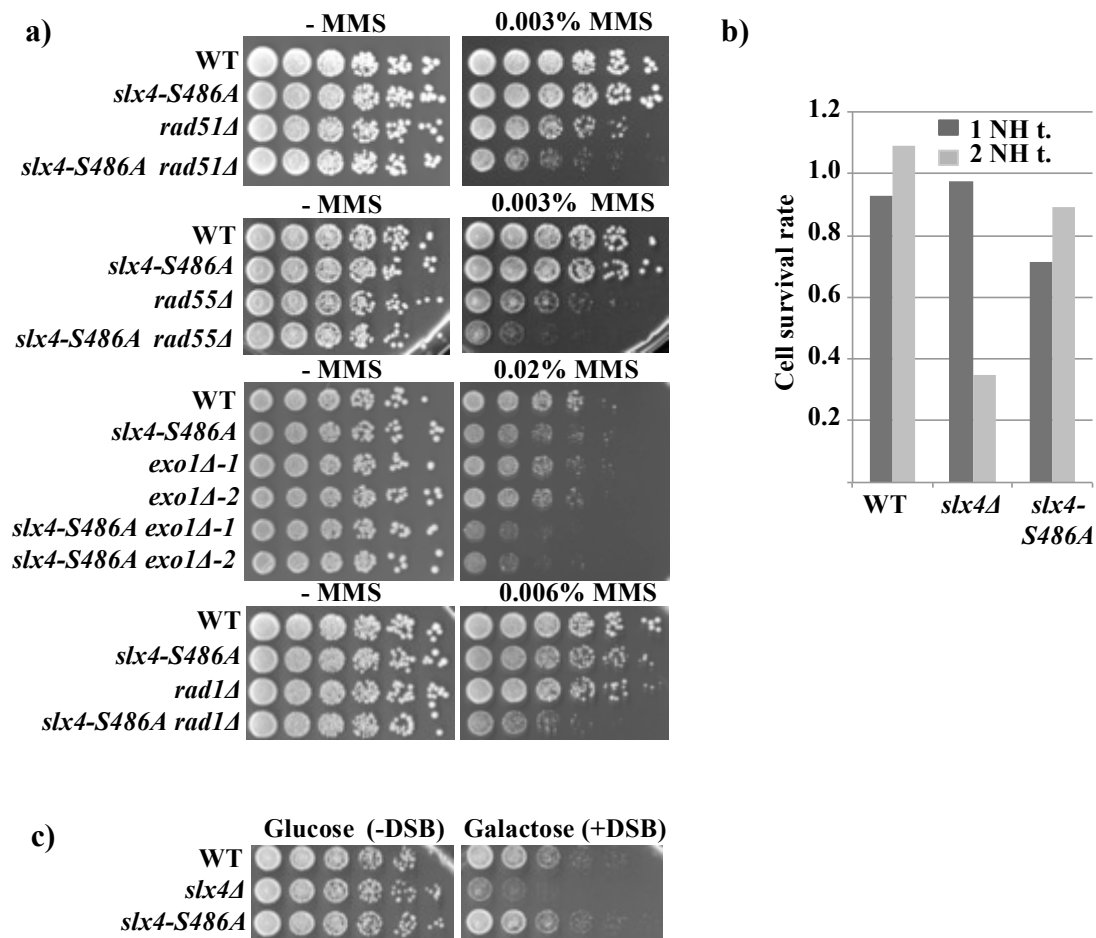


Figure 4.13. The Dpb11-Slx4 complex is not involved in HR.

a) MMS sensitivity of WT, the *slx4-S486A* and *rad51Δ*, *rad55Δ*, *exo1Δ* and *rad1Δ* deletion single mutants and in combination with *slx4-S486A*. Cells were spotted in serial dilutions on plates containing MMS. The growth was evaluated after incubation for 2 days at 30°C; b) Cell survival rate of WT, the *slx4-S486A* and *slx4Δ* deletion mutants after processing one (1 NH t.) or two non-homologous tails (2 NH t.) during DSB repair. Cells were plated on YPD after induction of DSB and colonies were counted after 2 days at 30°C. Cell survival rate was calculated as the number of colonies arising from induced relative to uninduced cultures; c) Sensitivity of WT, the *slx4-S486A* and *slx4Δ* deletion mutants after induction of DSBs. Cells were spotted in serial dilutions on plates containing glucose as a control and galactose for DSB induction. The growth was evaluated after incubation for 2 days at 30°C.

All together, various assays and tests of different mutants demonstrate that the Dpb11-Slx4 complex does neither have a specific/exclusive role in the error-free or error-prone PRR nor in HR. The *slx4-S486A* mutant rather enhances the phenotype of PRR and HR mutants. This suggests that Dpb11-Slx4 might be involved in the common step shared by the post-replication repair and homologous recombination mechanisms. Alternatively, Dpb11-Slx4 might have a role in a pathway that is not

directly related to DNA lesion bypass but rather important at the repair step after DNA lesion is bypassed.

4.3.2 The Dpb11-Slx4 complex functions in the Mus81-Mms4 pathway

A common feature of PRR and HR is resulting DNA repair intermediates which physically link sister chromatids. These DNA molecules are known as joint molecules or X-shaped DNA structures. There are two ways to repair X-shaped DNA structures. The dissolution mechanism enrolls the Sgs1 helicase together with the Top3 topoisomerase and the Rmi1 protein. The resolution is achieved by the action of structure-specific endonucleases like Mus81-Mms4 or Yen1 (Liberi et al., 2005; Mankouri and Hickson, 2006; Mankouri et al., 2007; Rass, 2013).

Having found that the Dpb11-Slx4 complex is not exclusively involved in the post-replication repair or homologous recombination, we asked whether Dpb11-Slx4 is important at a common step to both pathways, in particular in the dissolution or resolution of X-shaped DNA structures.

To visualize X-shaped DNA structures, we took an advantage of the 2D gel electrophoresis in collaboration with B. Szakal and D. Brnzei (Istituto FIRC do Oncologia Molecolare, Milan, Italy). The kinetics of removing of X-shaped DNA structures in the *slx4-S486A* mutant was followed. Since the DNA helicase Sgs1 is able to move X-shaped DNA structures, the experiment was performed in *sgs1Δ* deletion background to stabilize and detect X-shaped DNA structures at the particular DNA region. X-shaped DNA structures look like a “spike” on a gel. Using the *sgs1Δ* deletion and *sgs1Δ slx4-S486A* mutants, the recovery after a pulse of DNA damage experiment was performed. The cells were synchronized in G2-phase and released to medium containing MMS. After a pulse of MMS damage, cells recovered in MMS-free medium. In this experiment a slower disappearance of X-shaped DNA structures in the *sgs1Δ slx4-S486A* mutant compared to the *sgs1Δ* deletion mutant was observed (Figure 4.14). This suggests that the Dpb11-Slx4 complex has a role in the repair of X-shaped DNA structures. Moreover, it appears that Dpb11-Slx4 is not involved in the dissolution mechanism, since the double mutant of *sgs1Δ slx4-S486A* has additive effect in resolution kinetics.

RESULTS

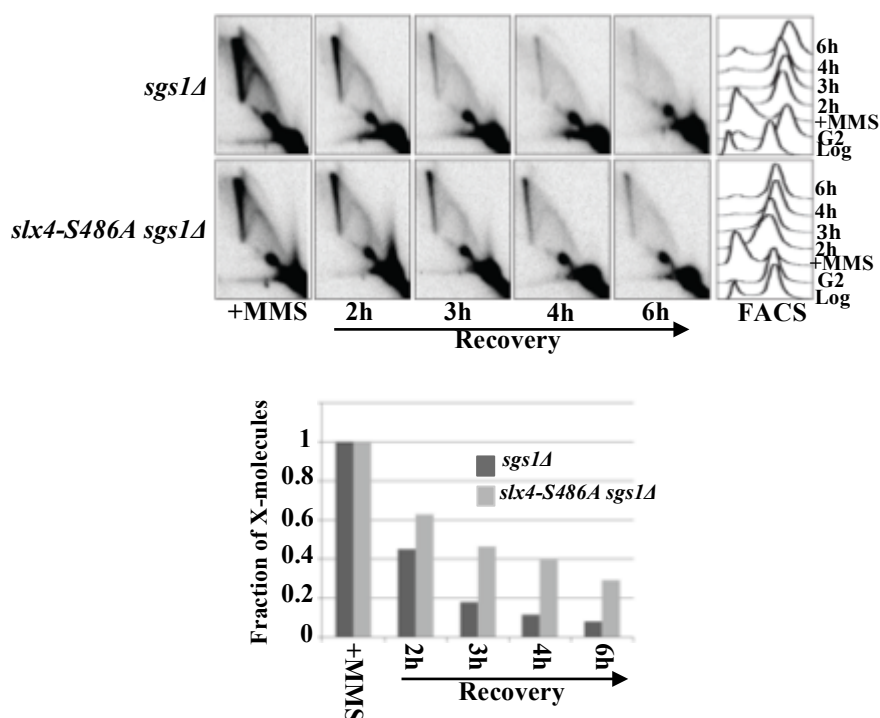


Figure 4.14. The Dpb11-Slx4 complex is involved in repair of X-shaped DNA structures. Recovery experiment of the *sgs1Δ* deletion and *slx4-S486A sgs1Δ* mutants showing slower disappearance of X-shaped DNA structures in the *slx4-S486A* mutant. Cells were synchronized in G2 and release to MMS containing medium. After MMS damage cells were released into drug-free medium for 6 hours. The samples were taken at different time points and analyzed by 2D gel electrophoresis and FACS (upper panel). The fraction of X-shaped DNA structures was quantified (lower panel). For quantification see Szakal and Branzei, 2013. Experiment by B. Szakal and D. Branzei.

Knowing that the Dpb11-Slx4 complex, which consists of two scaffold proteins Dpb11 and Slx4, is important for the repair of X-shaped DNA structures and likely works in the resolution mechanism, we were prompted to find a member, which has an enzymatic activity in the Dpb11-Slx4 complex.

Next, we aimed to investigate the genetic relationship with the resolution enzymes. For this, cells carrying the *slx4-S486A*, *sgs1Δ*, *mus81Δ*, *mms4Δ* and *yen1Δ* deletion mutation were grown in presence of MMS. When the *slx4-S486A* and *sgs1Δ* deletion mutations were combined, the double mutant was more sensitive to MMS compared to the single *slx4-S486A* and *sgs1Δ* deletion mutants (Figure 4.15a). This suggests that Dpb11-Slx4 is not involved in dissolution mechanisms and confirms the results from the figure 4-14. Interestingly, we did find a genetic interaction with Mus81-Mms4. The *mus81Δ* and *mms4Δ* deletion mutants were as sensitive to MMS as the double mutants of *slx4-S486A mus81Δ* and *slx4-S486A mms4Δ* (Figure 4.15b). This indicates that the Dpb11-Slx4 complex functions in the Mus81-Mms4 pathway.

RESULTS

Moreover, this finding indicates the existence of the Dpb11-dependent DNA repair complex in yeast.

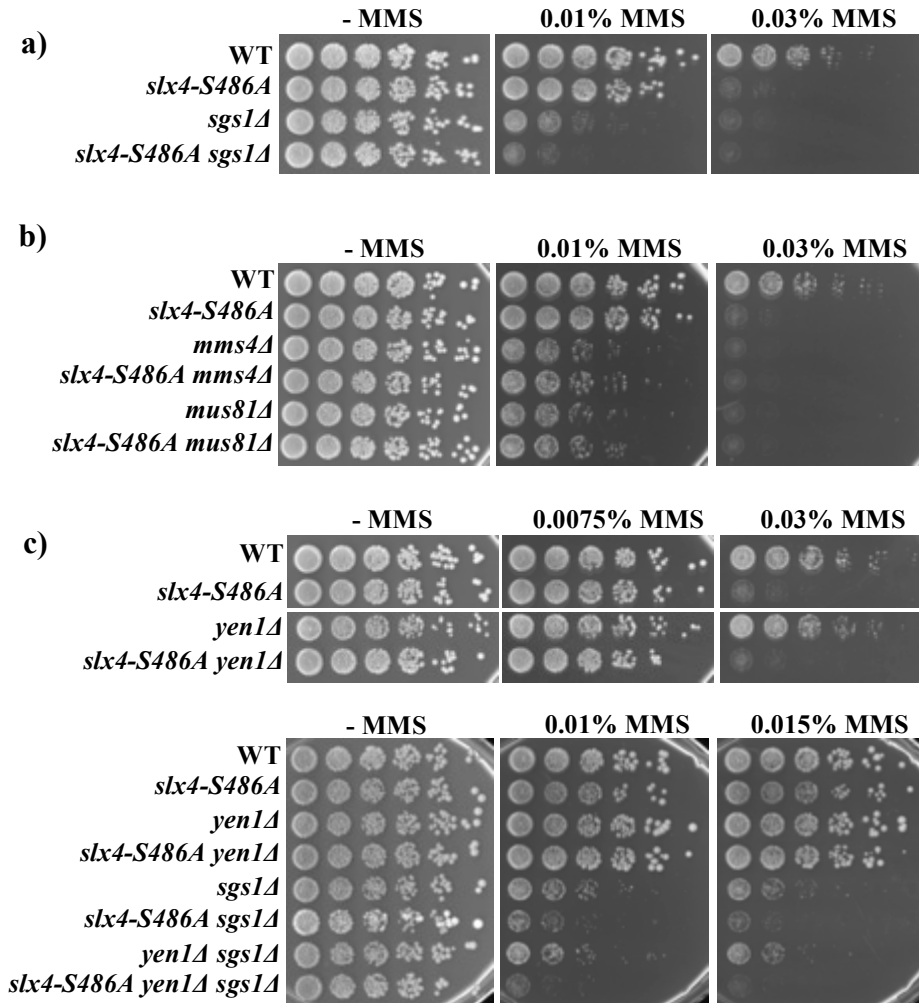


Figure 4.15. The Dpb11-Slx4 complex is not a part of dissolution mechanism but has a role in resolution by Mus81-Mms4 but not Yen1.

a) MMS sensitivity of WT, the *slx4-S486A*, *sgs1Δ* deletion and *slx4-S486A sgs1Δ* mutant. Cells were spotted in serial dilutions on plates containing MMS. The growth was evaluated after incubation for 2 days at 30°C; b) MMS sensitivity of WT, the *slx4-S486A* and *mus81Δ*, *mms4Δ* deletion mutants and in combination with *slx4-S486A*. Cells were spotted as in a; c) MMS sensitivity of WT, the *slx4-S486A* and the *yen1Δ*, *sgs1Δ* deletion single mutants and double and triple mutant combinations. Cells were spotted as in a.

To investigate the Dpb11-Slx4 complex role in Yen1 pathway, the growth on MMS of the *yen1Δ*, *sgs1Δ* deletion, *slx4-S486A* single mutants and double and triple mutant combinations was evaluated. As it was shown before (Tay and Wu, 2010), the *YEN1* deletion did not have any effect to the cell viability in the presence of MMS. Furthermore, the *yen1Δ slx4-S486A* double mutant was as sensitive to MMS as the single *slx4-S486A* mutant. Interestingly, the triple mutant of *slx4-S486A sgs1Δ yen1Δ*

RESULTS

was the most sensitive to MMS of the mutants tested (Figure 4.15c). This indicates that in the *slx4-S486A sgs1Δ yen1Δ* mutant three different pathways of resolution, which involve Mus81-Mms4, Sgs1 and Yen1 to repair X-shaped DNA structures, are disrupted. Furthermore, this result further supports the finding that the Dpb11-Slx4 complex is involved in X-shaped DNA structures resolution by Mus81-Mms4.

Previously in the study it was shown that Mus81-Mms4 influences crossover formation. Moreover, a phosphomimicry mutant of Mms4, which leads to constantly active Mus81-Mms4, displays increased crossover rates (Szakal and Branzei, 2013). Knowing that Dpb11-Slx4 is involved in the same pathway as Mus81-Mms4, we therefore asked how the Dpb11-Slx4 complex influences crossover formation.

To study the crossover rates in the *slx4-S486A* mutant, we took an advantage of the crossover assay described previously (Robert et al., 2006; Szakal and Branzei, 2013). The crossover strain for this assay carries two inactive *ARG* genes on chromosome V and VIII. After homologous recombination between two *arg* alleles of V and VIII chromosomes active *ARG* gene is restored leading to two possible outcomes of a homologous recombination event in the crossover strain. In case of a non-crossover the chromosomes V and VIII remain intact. In case of a crossover a reciprocal translocations between chromosomes V and VIII can be detected by PCR.

For the crossover assay besides WT and the *slx4-S486A* mutant, we used the *mms4Δ* and *slx4Δ* deletion mutants as controls. The cells were plated on -Arg medium to select recombinants. These recombinants were later classified as crossovers or non-crossovers by PCR. Using the “Maximum-Likelihood” method, the recombination and crossover rates were calculated (Rosche and Foster, 2000). We found that, even though the recombination rate was increased in the *slx4-S486A* mutant compared to WT, the crossover rate was lower comparing to the wild type. The *slx4Δ* deletion mutant had identical recombination and crossover rates compared to the *slx4-S486A* mutant, which were lower compared to WT. However, the *mms4Δ* deletion mutant had increased recombination and reduced crossover rates compared to wild type and similar recombination rate but a slightly higher crossover rates compared to the *slx4-S486A* mutant (Figure 4.16). From this experiment we conclude that the Dpb11-Slx4 complex is involved in the crossover formation. Moreover, it seems that in the *slx4-S486A* mutant the balance between dissolution and resolution is shifted. However, with this experiment we cannot distinguish, whether this effect comes from up-regulation of dissolution or down-regulation of resolution in the *slx4-S486A* mutant.

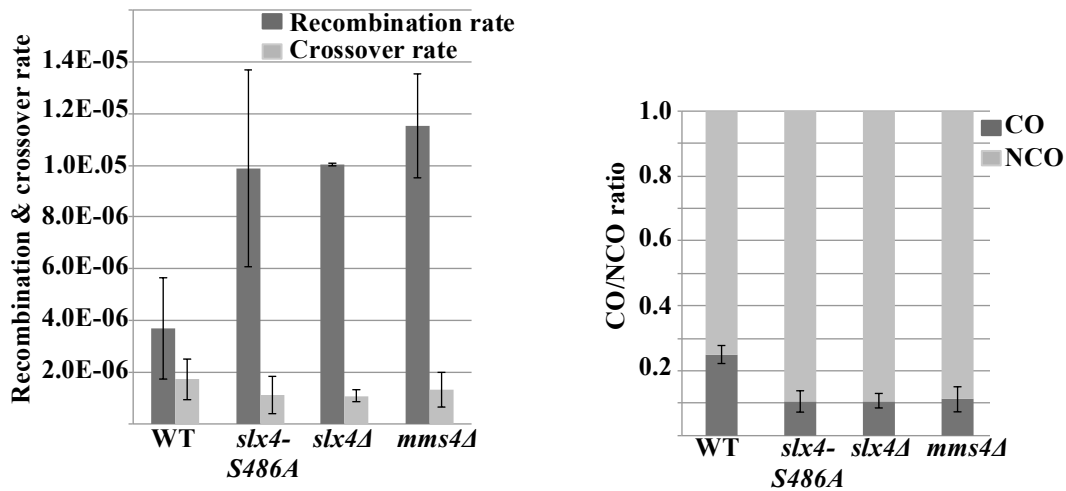


Figure 4.16. The Dpb11-Slx4 complex is involved in crossover formation.

Recombination, crossover rates (left panel) and crossover/non-crossover ratio (right panel) of WT, the *slx4-S486A*, *slx4Δ* and *mms4Δ* deletion mutants. Cells were plated on -Arg medium and recombinants were counted after 4 days growth at 30°C. Crossover and non-crossover outcome was determined by PCR. Recombination and crossover rates were calculated using the “Maximum-Likelihood” method. Error bars represent standard deviation from two independent experiments.

4.3.3 Dpb11-Slx4 physically interacts with Mus81-Mms4

As we found that the Dpb11-Slx4 complex genetically interacts with Mus81-Mms4, we hypothesized that Dpb11-Slx4 might also bind physically to Mus81-Mms4. To test this, first, we performed Y2H experiment using the *DPB11-BD* and *MMS4-AD*. Strikingly, we found that Dpb11 and Mms4 interact physically (Figure 4.17a).

Previous studies showed that Mus81-Mms4 is activated in M-phase after hyperphosphorylation by the Polo-like kinase Cdc5 (Matos et al., 2011; Gallo-Fernandez et al., 2012; Matos et al., 2013; Szakal and Brnzei, 2013; Blanco et al., 2014). Knowing that the Dpb11-Slx4 complex forms already in S-phase and Mus81-Mms4 is active in M-phase, we asked when Dpb11-Slx4 interacts with Mus81-Mms4.

To investigate the cell cycle requirements for the Dpb11-Slx4 binding to Mus81-Mms4, a co-immunoprecipitation experiment was performed. For this, the strain, which expresses FLAG-tagged Mms4, was constructed. To compare the different cell cycle stages, cells were synchronized in G1-, S- and G2/M-phase and immunoprecipitation of Mms4-3FLAG from the arrested cells was carried out. As expected, we detected hypo-phosphorylated Mms4 in G1- and S-phase samples.

RESULTS

Moreover, in G1- and S-phase no Dpb11 and Slx4 binding to FLAG-tagged Mms4 was observed (Figure 4.17b, lanes 2 and 3). In contrast to G1- and S-phase, in G2/M cells almost all Mms4 was hyper-phosphorylated. Importantly, we were able to co-immunopurify Dpb11 and Slx4 only from G2/M cells when Mms4 was hyper-phosphorylated (Figure 4.17b, lane 4). This experiment shows that Dpb11-Slx4 forms a complex with Mus81-Mms4 especially in the G2/M cell cycle stage when Mms4 is phosphorylated.

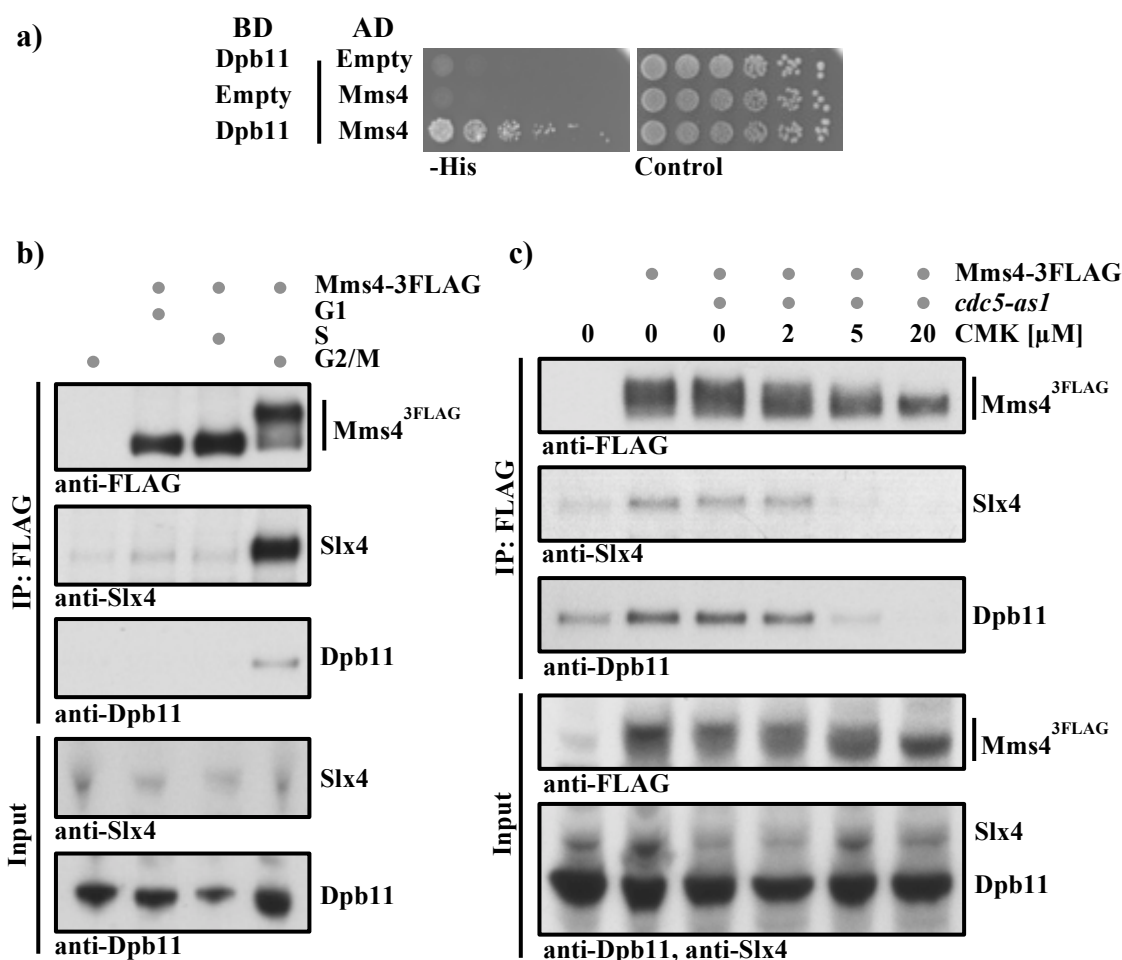


Figure 4.17. The Dpb11-Slx4 complex interaction with Mus81-Mms4 in G2/M depends on Cdc5.

a) Y2H experiment of Mms4 and Dpb11 showing Dpb11-Mms4 interaction. AD-fusion of *MMS4* was co-transformed with BD-fusion of *DPB11*. Cells were spotted on control and selective plates and evaluated after 3 days growth at 30°C; b) CoIP experiment of Dpb11, Slx4 and Mms4 showing Slx4-Dpb11-Mms4 interaction in G2/M. FLAG-tagged Mms4 was used for co-immunopurification from G1, S and G2/M cells. Experiment by L. N. Princz.; c) CoIP experiment of Dpb11, Slx4 and Mms4 showing that Cdc5 mediates the formation of Slx4-Dpb11-Mms4. FLAG-tagged Mms4 was immunopurified from *cdc5-as1* containing cells which were untreated or treated with 2, 5 or 20 μM of CMK. Experiment by L. N. Princz.

RESULTS

To investigate the regulation of Dpb11-Slx4 and Mus81-Mms4 interaction particularly in G2/M-phase, we tested the role of the Polo-like kinase Cdc5. Cdc5 is known to be active in M-phase and required for the phosphorylation and activation of the structure-specific endonuclease Mus81-Mms4 (Matos et al., 2011; Gallo-Fernandez et al., 2012; Matos et al., 2013; Szakal and Branzei, 2013; Blanco et al., 2014). We hypothesized that Cdc5 might promote Mus81-Mms4 binding to Dpb11-Slx4. To reveal the influence of Cdc5, we took an advantage of analog sensitive *cdc5-as1* allele. In the *cdc5-as1* background the activity of Cdc5 is controlled by adding an inhibitor chloromethylketone (CMK). For this study, the experiment was performed using the *cdc5-as1* strain expressing FLAG-tagged Mms4. First, the cells were arrested in G2/M-phase and treated with different amounts of CMK. In the study 2 to 20 μ M of the inhibitor CMK was used. After gradual increase of CMK, a decrease of Mms4 phosphorylation was observed (Figure 4.17c). Importantly, Dpb11-Slx4 interaction with Mms4 after adding 5 and 20 μ M of CMK was not detectable (Figure 4.17c, lanes 5 and 6). These data demonstrate that Dpb11-Slx4 interaction with Mus81-Mms4 is dependent on Mms4 phosphorylation by the Polo-like kinase Cdc5.

Although Slx4-Dpb11 interacts with Mus81-Mms4, not all functions of Mus81-Mms4 depend on the Dpb11-Slx4 complex since the *slx4-S486A* mutant is less sensitive to MMS compared to the *mms4 Δ* or *mus81 Δ* deletion mutants (Figure 4-15b). These findings prompted us to find out whether it is possible to generate a specific Mms4 mutant that is not able to interact with Dpb11 and might lose specifically Dpb11-Slx4-dependent function. To address this question, the *mms4* phosphorylation-site mutants, which have serine or threonine of putative Cdk1 sites replaced by alanine, were created. We chose S/TP sites because Dpb11 often interacts with proteins that are modified by Cdk1 (Tanaka et al., 2007; Zegerman and Diffley, 2007; Pfander and Diffley, 2011). In theory these Cdk1 sites could also prime for Cdc5 phosphorylation of Mms4. Therefore, the *mms4* phosphorylation site mutants were compared in Y2H experiment. We found, that *mms4-S184A* interaction with Dpb11 was reduced comparing to wild type Mms4. Strikingly, *mms4-S201A* almost completely lost the interaction with Dpb11 (Figure 4.18a). These data suggest that S184 and S201 of Mms4 may be important for the interaction with Dpb11.

To further investigate the *mms4* mutants, a strain which expresses *mms4-SS184,201AA* was generated and tested for sensitivity to MMS. Surprisingly, the *mms4-SS184,201AA* mutant was not sensitive to MMS similar to WT (Figure 4.18b).

RESULTS

This might be explained by the existence of the compensatory mechanism, which could take over the task, when the Mus81-Mms4 function is reduced or absent.

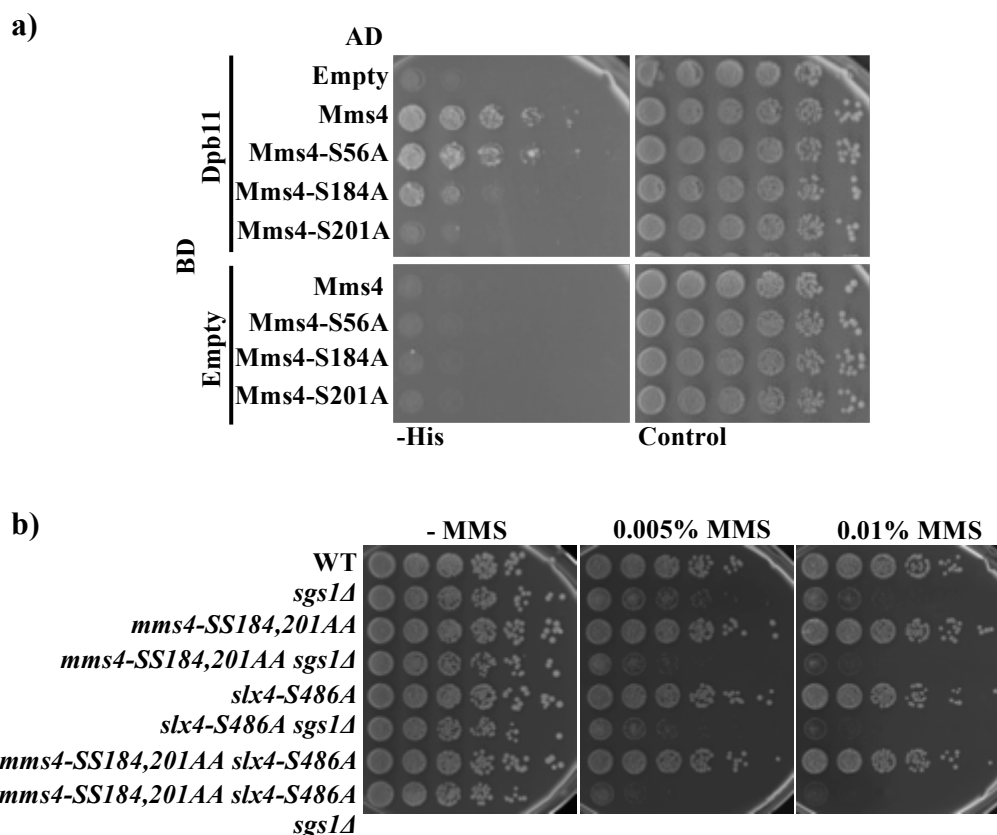


Figure 4.18. S184 and S201 of Mms4 are important for interaction with Dpb11 and after DNA damage.

a) Y2H experiment of Mms4 and Dpb11 showing the reduced Dpb11 interaction with the *mms4* mutants. AD-fusions of *MMS4* and *mms4* mutants were co-transformed with BD-fusion of *DPB11*. Cells were spotted on control and selective plates and evaluated after 3 days at 30°C; b) MMS sensitivity of WT, the *mms4-SS184,201AA*, *sgs1Δ* deletion and *slx4-S486A* mutants and the double and triple mutant combinations. Cells were spotted in serial dilutions on plates containing MMS. The growth was evaluated after incubation for 2 days at 30°C.

Following this idea, we introduced the *SGS1* deletion in the *mms4-SS184,201AA* mutant background and tested the double *mms4-SS184,201AA sgs1Δ* mutant sensitivity to MMS. Strikingly, the *mms4-SS184,201AA sgs1Δ* mutant was more sensitive to MMS compared to the *sgs1Δ* deletion or *mms4-SS184,201AA* single mutants, suggesting, that the double mutation interfered with two pathways of dissolution/resolution (Figure 4.18b). These data indicate that the Mms4 binding to Dpb11 is important after MMS damage especially in the absence of the DNA helicase Sgs1.

RESULTS

In this study, we generated Cdk1-phosphorylation deficient mutants of *slx4* and *mms4*. The S486A mutation of Slx4 and SS184,201AA of Mms4 result in strongly reduced interaction with Dpb11 (Figures 4.3, 4.5a and 4.18a). Moreover, the *slx4-S486A* and *mms4-SS184,201AA sgs1Δ* mutants are sensitive to MMS (Figures 4.6b and 4.18b). For that reasons we hypothesized that this MMS sensitivity of the *slx4* and *mms4* mutants comes from the interfering with the Slx4-Dpb11-Mms4-Mus81 complex formation. To test this hypothesis, the *slx4* and *mms4* mutant sensitivity to MMS was compared. As the *mms4-SS184,201AA* mutant is sensitive to MMS just in the absence of Sgs1, we analyzed the *slx4-S486A* and *mms4-SS184,201AA* mutants in the *SGS1* deletion background. Interestingly, the *slx4-S486A sgs1Δ* mutant was less viable on MMS than the *mms4-SS184,201AA sgs1Δ* mutant. Importantly, the triple mutant of *slx4-S486A mms4-SS184,201AA sgs1Δ* had increased sensitivity to MMS compared to the double mutants (Figure 4.18b). These findings suggest that S486 of Slx4 and SS184,201 of Mms4 are required for different functions. However, it is difficult to rationalize the results given the fact that Mms4 harbors plenty of putative phosphorylation sites and therefore the regulation of Mus81-Mms4 might be very complex. One possible explanation for hypersensitivity of the *slx4-S486A mms4-SS184,201AA sgs1Δ* mutant is as follows. In the *slx4-S486A* or *mms4-SS184,201AA* mutants there might be still a possibility to form Slx4-Dpb11-Mms4-Mus81 complex because of residual Slx4-S486A or Mms4-S184,201AA binding to Dpb11 (Figures 4.5a and 4.18a). However, the potential to form the Slx4-Dpb11-Mms4-Mus81 complex gets lower when Slx4-S486A and Mms4-SS184,201AA are combined in one cell.

Recent studies suggested that S56 and S184 of Mms4 are required for the Mus81-Mms4 endonuclease function. The expression of Mms4-SS56,184ED leads to premature activation of Mus81-Mms4 (Szakal and Branzei, 2013). Therefore we hypothesized that premature activation of Mus81-Mms4 might rescue MMS sensitivity of the *slx4-S486A* mutant by promoting the interaction with the Dpb11-Slx4 complex. To investigate S56, S184 of Mms4 importance in the context of the Dpb11-Slx4 complex, the *slx4-S486A mms4-SS56,184ED* mutant was constructed and tested for sensitivity to MMS. Interestingly, the *slx4-S486A mms4-SS56,184ED* mutant was as sensitive to MMS as the *slx4-S486A* mutant (Figure 4.19). These data suggest that S56 and S184 of Mms4 seem not to be important for the formation of the Slx4-Dpb11-Mms4-Mus81 complex. Alternatively, Mms4-SS56,184ED is not

RESULTS

sufficient to restore the function of the Slx4-Dpb11-Mms4-Mus81 complex. Moreover, premature activation of Mus81-Mms4 might become harmful to cell survival when replication fork stalling occurs in combination with impaired Dpb11-Slx4 interaction in the *slx4-S486A* mutant.

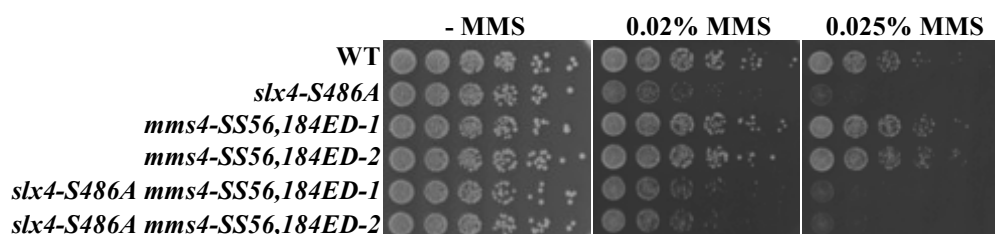


Figure 4.19. Premature activation of Mms4 does not restore the function of the Dpb11-Slx4 complex.

MMS sensitivity of WT, the *slx4-S486A*, *mms4-SS56,184ED* and *slx4-S486A mms4-SS56,184ED* mutants. Cells were spotted in serial dilutions on plates containing MMS. The growth was evaluated after incubation for 2 days at 30°C.

4.4 The DNA damage checkpoint regulates Dpb11-Slx4-dependent Mus81-Mms4 function

The DNA damage checkpoint is crucial for regulating various processes that help to cope with DNA damage in a cell. The DNA damage checkpoint is known to have a particularly important role after DNA damage in S-phase. Checkpoint activation triggers various events leading to induced transcription of DNA repair genes, prevention of late origin firing and stabilization of replication forks (Segurado and Tercero, 2009).

4.4.1 Reduced DNA damage checkpoint activation promotes DNA repair in the absence of Dpb11-Slx4 interaction

Based on the finding that DNA damage checkpoint recovery after treatment with MMS is delayed in the *slx4-S486A* mutant (Figure 4.8b), we asked whether the partial inactivation of the DNA damage checkpoint would suppress the *slx4-S486A* mutant phenotype.

To test the hypothesis, we analyzed three checkpoint mutants that are characterized by partially impaired DNA damage checkpoint activation. First, we made use of a mutant deficient for the methyltransferase Dot1, which lacks the histone-

RESULTS

dependent pathway of DNA damage checkpoint activation. Second, we analyzed the *ddc1-T602A* mutant that is not able to interact with Dpb11 and therefore shows an impaired Dpb11-dependent DNA damage checkpoint activation (Pfander and Diffley, 2011). Third, we took into consideration that tagging of Rad53 with a 3HA epitope also leads to a partially inactive DNA damage checkpoint (Conde et al., 2010). All three DNA damage checkpoint mutants in combination with *slx4-S486A* were tested for growth on plates containing MMS. Strikingly, all three mutants were able to rescue the *slx4-S486A* mutant sensitivity to MMS (Figure 4.20a).

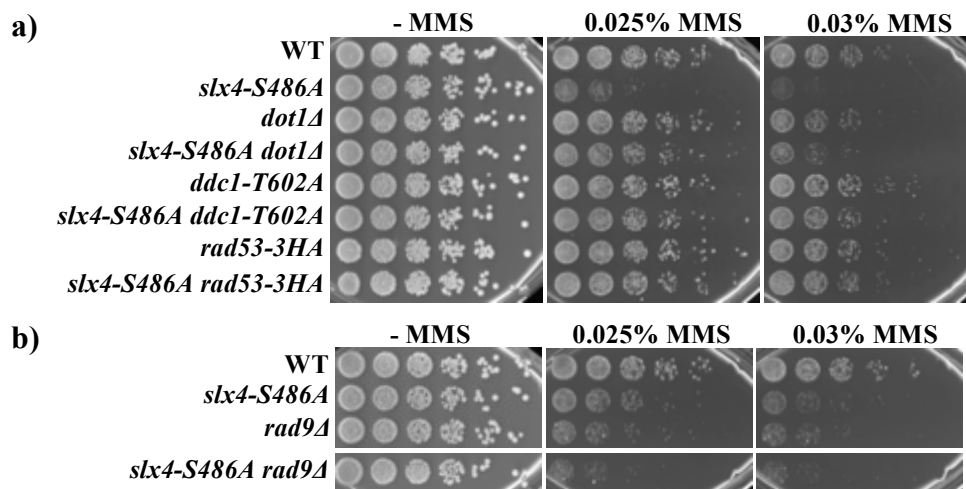


Figure 4.20. DNA damage checkpoint regulates the Dpb11-Slx4 complex.

a) MMS sensitivity of WT, the *slx4-S486A* and *dot1Δ* deletion, *ddc1-T602A*, *rad53-3HA*, *rad9Δ* deletion mutants and in combination with *slx4-S486A*. Cells were spotted in serial dilutions on plates containing MMS. The growth was evaluated after incubation for 2 days at 30°C; b) MMS sensitivity of WT, the *slx4-S486A*, *rad9Δ* deletion and *slx4-S486A rad9Δ* mutants. Cells were spotted as in a).

To better define the role of the DNA damage checkpoint for the regulation of the Slx4-Dpb11-Mms4-Mus81 complex function, we tested the effect of complete DNA damage checkpoint inactivation in the *slx4-S486A* mutant. For this purpose, a strain lacking the DNA damage checkpoint mediator protein Rad9 was constructed. The *rad9Δ* deletion mutant is not able to activate the DNA damage checkpoint (Pfander and Diffley, 2011; Ohouo et al., 2013). In contrast to the mutants characterized by a partial inactivation of the DNA damage checkpoint, the *rad9Δ* deletion mutant was more sensitive to MMS compared to WT cells and the *slx4-S486A* mutant. Consequently, we did not detect the rescue of the *slx4-S486A* mutant sensitivity to MMS by deleting *RAD9* (Figure 4.20b). These data indicate that a

RESULTS

partial but not a complete inactivation of DNA damage checkpoint is beneficial when the Dpb11-Slx4 interaction is impaired.

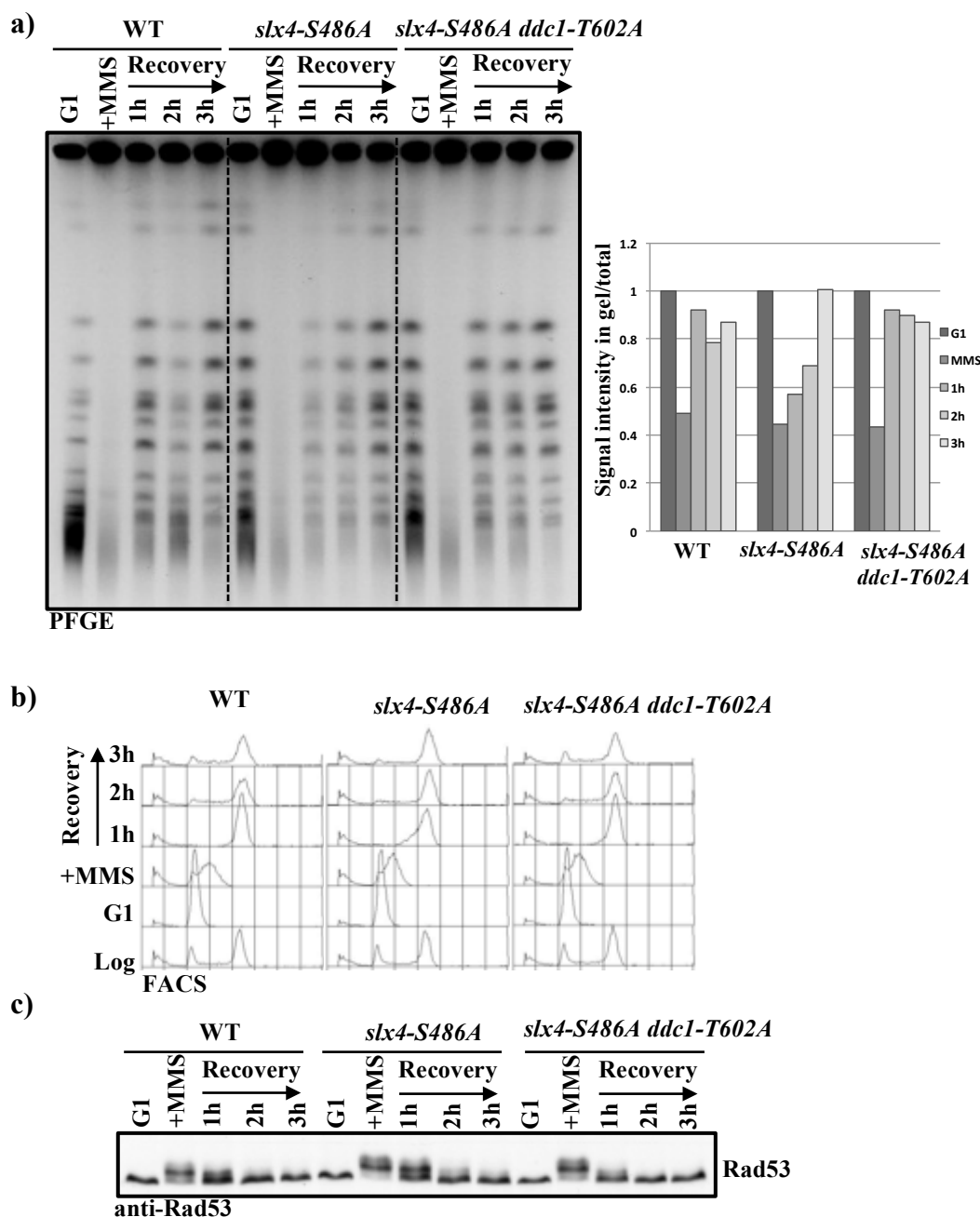


Figure 4.21. Reduced DNA damage checkpoint activation promotes faster DNA repair progression in the *slx4-S486A* mutant.

a) Recovery experiment of WT, the *slx4-S486A* and *slx4-S486A ddc1-T602A* mutants. Cells were synchronized in G1, released to S-phase in the medium with MMS. After 30 min cells were released to drug-free medium for 3 hours. The samples were taken at different time points and yeast chromosomes were visualized by PFGE. Quantification of the chromosome signal was performed using ImageJ software. The signal intensity in a lane of the gel was normalized to the whole signal including that in a well; b) Recovery experiment as in a. DNA content was measured by FACS; c) Recovery experiment as in a. DNA damage checkpoint activation was evaluated by Western blot using antibodies against Rad53.

A possible explanation for the rescue of the *slx4-S486A* mutant sensitivity to MMS by partial DNA damage checkpoint inactivation may be that DNA repair is more efficient under these conditions. To test this hypothesis, we damaged yeast cells with a pulse of MMS and analyzed the chromosomal repair kinetics by pulsed-field gel electrophoresis. Strikingly, we observed that the appearance of chromosomes in the gel was basically identical in the samples of wild type cells and the *slx4-S486A ddc1-T602A* double mutant. After one hour, WT cells and the *slx4-S486A ddc1-T602A* double mutant showed the recovery (Figure 4.21a, lanes 3 and 13). In contrast, the *slx4-S486A* mutant recovered slower, which is in line with data shown previously in figure 4.8a (Figure 4.21a, lanes 6-10). Consistent with the observation obtained by PFGE analysis, DNA replication in the *slx4-S486A ddc1-T602A* mutant had the same kinetics as in WT in contrast to the *slx4-S486A* mutant (Figure 4.21b). Finally, we found that the DNA damage checkpoint during the recovery was deactivated faster in the *slx4-S486A ddc1-T602A* mutant compared to the *slx4-S486A* mutant (4.21c). Together, these results demonstrate that the reduced DNA damage checkpoint activation in the *slx4-S486A* mutant promotes faster repair after treatment with MMS.

4.4.2 Reduced DNA damage checkpoint activation promotes DNA repair by activating Mus81-Mms4

One possible explanation for the rescue of the *slx4-S486A* mutant by the DNA damage checkpoint mutants might be as follows. First, the partially inactive checkpoint might promote the activation of an alternative pathway to resolve X-shaped DNA structures in the *slx4-S486A* mutant. Alternatively, the repair of X-shaped DNA structures may be still dependent on Mus81-Mms4 allowing the Slx4-Dpb11-Mms4-Mus81 complex formation even in the *slx4-S486A* mutant background.

To ascertain whether the rescue of the *slx4-S486A* mutant sensitivity to MMS by the DNA damage checkpoint mutants depends on Mus81-Mms4, we analyzed the *slx4-S486A ddc1-T602A* mutant sensitivity to MMS in the absence of Mms4. Interestingly, we observed that after deleting *MMS4* in the of *slx4-S486A ddc1-T602A* background, the cells became more sensitive to MMS than the *slx4-S486A ddc1-T602A* mutant (Figure 4.22a). Furthermore, after MMS treatment in S-phase, the *mms4Δ* deletion mutant was not able to recover after 3 hours as judged from the Rad53 phosphorylation status in the *mms4Δ* deletion mutant. Even the partial

RESULTS

inactivation of the DNA damage checkpoint did not promote faster recovery of the *mms4Δ* deletion mutant. In the *mms4Δ ddc1-T602A* mutant Rad53 remained phosphorylated during 3 hours of recovery similar to the *mms4Δ* mutant (Figure 4.22b). This confirms the hypothesis that the repair of X-shaped DNA structures in the *slx4-S486A* mutant is dependent on Mus81-Mms4.

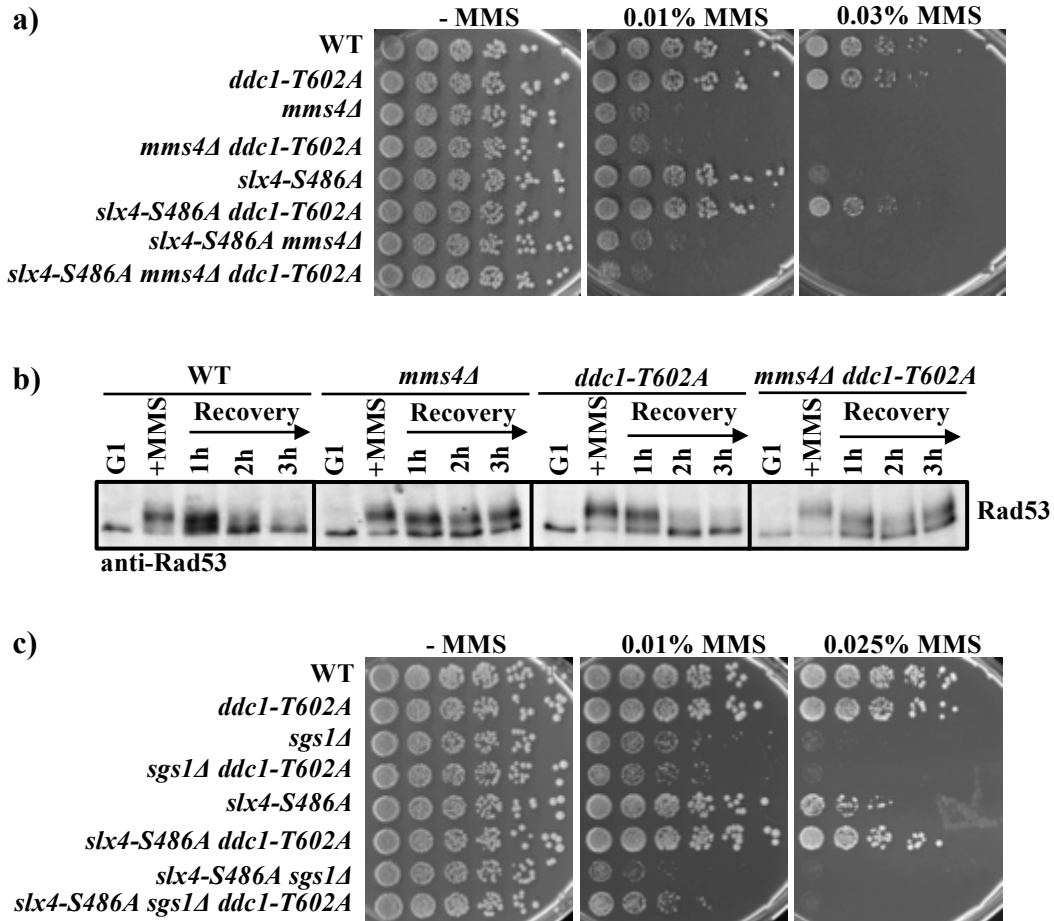


Figure 4.22. The DNA damage checkpoint promotes DNA repair by Mus81-Mms4 but not Sgs1 in the *slx4-S486A* mutant after MMS damage.

a) MMS sensitivity of WT and the *slx4-S486A*, *ddc1-T602A*, *mms4Δ* deletion mutants and double and triple mutant combinations. Cells were spotted in serial dilutions on plates containing MMS. The growth was evaluated after incubation for 2 days at 30°C; b) Recovery experiment of WT, the *mms4Δ* deletion, *ddc1-T602A* and *mms4Δ ddc1-T602A* mutants. Cells were synchronized in G1 and released into S-phase in medium containing MMS. After 30 min cells were released to drug-free medium for 3 hours. The samples were taken at different time points and DNA damage checkpoint activation was evaluated by Western blot using antibodies against Rad53; c) MMS sensitivity of WT and the *slx4-S486A*, *ddc1-T602A*, *sgs1Δ* deletion mutants and double and triple mutant combinations. Cells were spotted as in a.

Next, we also tested whether alternative dissolution pathway is important for the rescue of the *slx4-S486A* mutant when the DNA damage checkpoint is partially

RESULTS

inactive. For this purpose, *SGS1* was deleted in the *slx4-S486A ddc1-T602A* mutant and tested for the growth on MMS. In contrast to previous experiment when *MMS4* was deleted, in the absence of *SGS1* reduced DNA damage checkpoint activation was able to rescue the *slx4-S486A* mutant sensitivity to MMS (Figure 4.22c). Therefore we conclude that an alternative dissolution pathway is not important for the repair of X-shaped DNA structures in the *slx4-S486A ddc1-T602A* mutant.

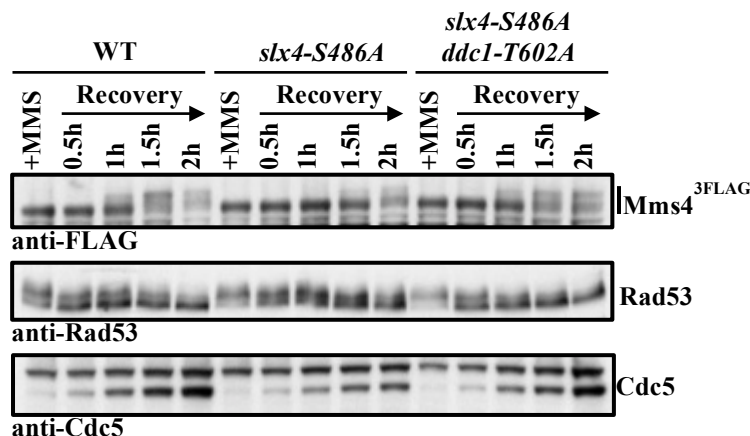


Figure 4.23. The DNA damage checkpoint regulates the formation of the Slx4-Dpb11-Mms4-Mus81 complex.

Recovery experiment of WT, the *slx4-S486A*, *ddc1-T602A* and *slx4-S486A ddc1-T602A* mutants. Cells were synchronized in G1, released into S-phase in medium containing MMS. After 30 min cells were released to drug-free medium for 2 hours. The samples were taken at different time points and evaluated by Western blot using antibodies against Rad53.

A partially inactive DNA damage checkpoint is beneficial in the *slx4-S486A* mutant because it promotes Mus81-Mms4-dependent DNA repair. To investigate how this is achieved mechanistically, we followed the Slx4-Dpb11-Mms4-Mus81 complex formation after a pulse of MMS damage. As we observed in our previous experiments, Mus81-Mms4 interacts with Dpb11-Slx4 after phosphorylation of Mms4 by the Polo-like kinase Cdc5 in mitosis (Figure 4.17). Interestingly, after recovery from MMS damage in S-phase Mms4 phosphorylation in the *slx4-S486A* mutant was delayed for 30 minutes compared with the wild type (Figure 4.23, lanes 3 and 8). Strikingly, partial inactivation of the DNA damage checkpoint allowed Mms4 phosphorylation to occur earlier in the *slx4-S486A* mutant (Figure 4.23, lanes 8 and 13). After one hour of recovery Mms4 was phosphorylated in either WT or the *slx4-S486A ddc1-T602A* mutant (Figure 4.23, lanes 3 and 13). Moreover, Mms4 phosphorylation was consistent with Cdc5 expression. Interestingly, phosphorylation of Mms4 inversely correlated with the activation of DNA damage checkpoint. At the

time point when Rad53 was phosphorylated there was no phosphorylation of Mms4 and vice versa (Figure 4.23). All together, these data suggest that DNA damage checkpoint negatively regulates the formation of the Slx4-Dpb11-Mms4-Mus81 complex.

4.5 Dpb11-Slx4 belongs to a multi-protein complex

In a cell, proteins often form distinct complexes to perform a particular task. Scaffold proteins participate in forming and regulating the action of different protein groups. Since the Slx4-Dpb11-Mms4-Mus81 complex consists of three scaffold proteins, we wondered whether there are more interaction partners particularly enzymes in the complex. Such proteins may be responsible for the recruitment, regulation or activity of the Slx4-Dpb11-Mms4-Mus81 complex.

4.5.1 The Slx4-Dpb11-Mms4-Mus81 complex involves additional proteins

To obtain evidence of proteins interacting with the Slx4-Dpb11-Mms4-Mus81 complex, we analyzed the role of the additional binding surfaces of Dpb11. Within the DNA replication initiation complex BRCT1/2 and BRCT3/4 of Dpb11 binds to Sld3 and Sld2, respectively (Tanaka et al., 2007; Zegerman and Diffley, 2007). For the formation of the Dpb11-dependent DNA damage checkpoint activation complex, Rad9 interacts with BRCT1/2 of Dpb11, the 9-1-1 complex subunit Ddc1 binds to BRCT3/4 and Mec1-Ddc2 is connected to the complex via ATR activating domain (AAD) of the C-terminus of Dpb11 (Pfander and Diffley, 2011).

To determine which domains of Dpb11 are involved in the resolution function, we mutated *DPB11* within the *DPB11-slx4-S486A* fusion. The T12A, T451A and WG700,701AA mutations interfere with the function of BRCT1/2, BRCT3/4 and AAD of Dpb11, respectively. MMS sensitivity of the strains that express the fusions which carry the T12A, T451A and WG700,701AA mutations together with the fusion protein where Dpb11 had the wild type sequence were compared. Interestingly, we found that all strains, which express fusion proteins with the mutation in Dpb11, had increased MMS sensitivity compared to the strain, which expresses Dpb11-slx4-S486A. Particularly, the *dpb11-T451A-slx4-S486A* mutant was the most sensitive to MMS of all mutants tested (Figure 4.24). These data demonstrate that BRCT1/2, C-

RESULTS

terminus with AAD domain and especially BRCT3/4 of Dpb11 appear to have a role in the Slx4-Dpb11-Mms4-Mus81 complex.

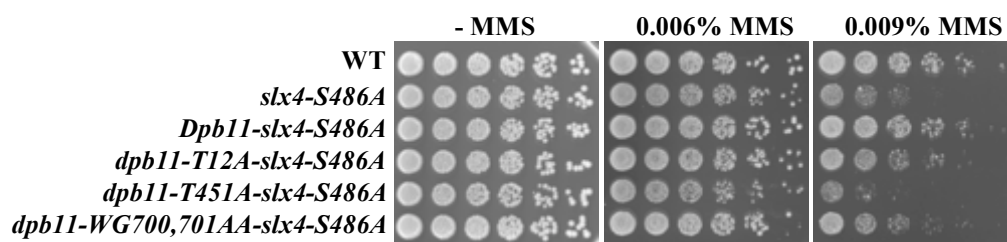


Figure 4.24. BRCT1/2, AAD domain and BRCT3/4 of Dpb11 have a role in the Slx4-Dpb11-Mms4-Mus81 complex.

MMS sensitivity of WT and the *slx4-S486A* and *Dpb11-slx4-S486A* mutants. Yeast strains expressing the Dpb11-slx4-S486A fusions have wild type Dpb11 sequence or T12A, T451A and WG700, 701AA mutations. Cells were spotted in serial dilutions on plates containing MMS. The growth was evaluated after incubation for 2 days at 30°C.

To better define the interaction partners of the Slx4-Dpb11-Mms4-Mus81 complex, we performed SILAC-based MS analysis of Dpb11, Slx4 and Mms4 interactors. When we monitored peptide intensity from co-immunoprecipitation samples of FLAG-tagged Dpb11, we found Dpb11, Slx1, Slx4 and Rtt107 as preferential binders (Figure 4.25a). Interestingly, the highest peptide intensity from FLAG-tagged Slx4 also corresponded to Dpb11, Slx1, Slx4 and Rtt107 (Figure 4.25b). Within the list of the best interactors of FLAG-tagged Mms4 we found Slx1, Rtt107 and Cdc5 (Figure 4.25c). This suggests that the Slx1, Rtt107 and Cdc5 are a part of the Slx4-Dpb11-Mms4-Mus81 complex.

The role of the Polo-like kinase Cdc5 was already evaluated in our previous experiments. Cdc5 phosphorylates Mms4 for the interaction with Dpb11-Slx4 (Figure 4.17c). The Slx1 and Rtt107 proteins are also known to physically interact with Slx4 (Fricke and Brill, 2003; Roberts et al., 2006). To better explain the role of Slx1 and Rtt107 in the Slx4-Dpb11-Mms4-Mus81 complex, we performed epistasis analysis. For this the *SLX1* and *RTT107* genes were deleted in the wild type and the *slx4-S486A* mutant background and the mutants were tested for the growth on MMS. As it was shown before (Flott et al., 2007) the *slx1Δ* deletion mutant was not sensitive to MMS (Figure 4.26a). However, the *rtt107Δ* deletion mutant was sensitive to MMS compared to WT. Interestingly, the *rtt107Δ slx4-S486A* mutant was also sensitive to MMS compared to wild type and as sensitive as the *rtt107Δ* deletion mutant (Figure 4.26b).

RESULTS

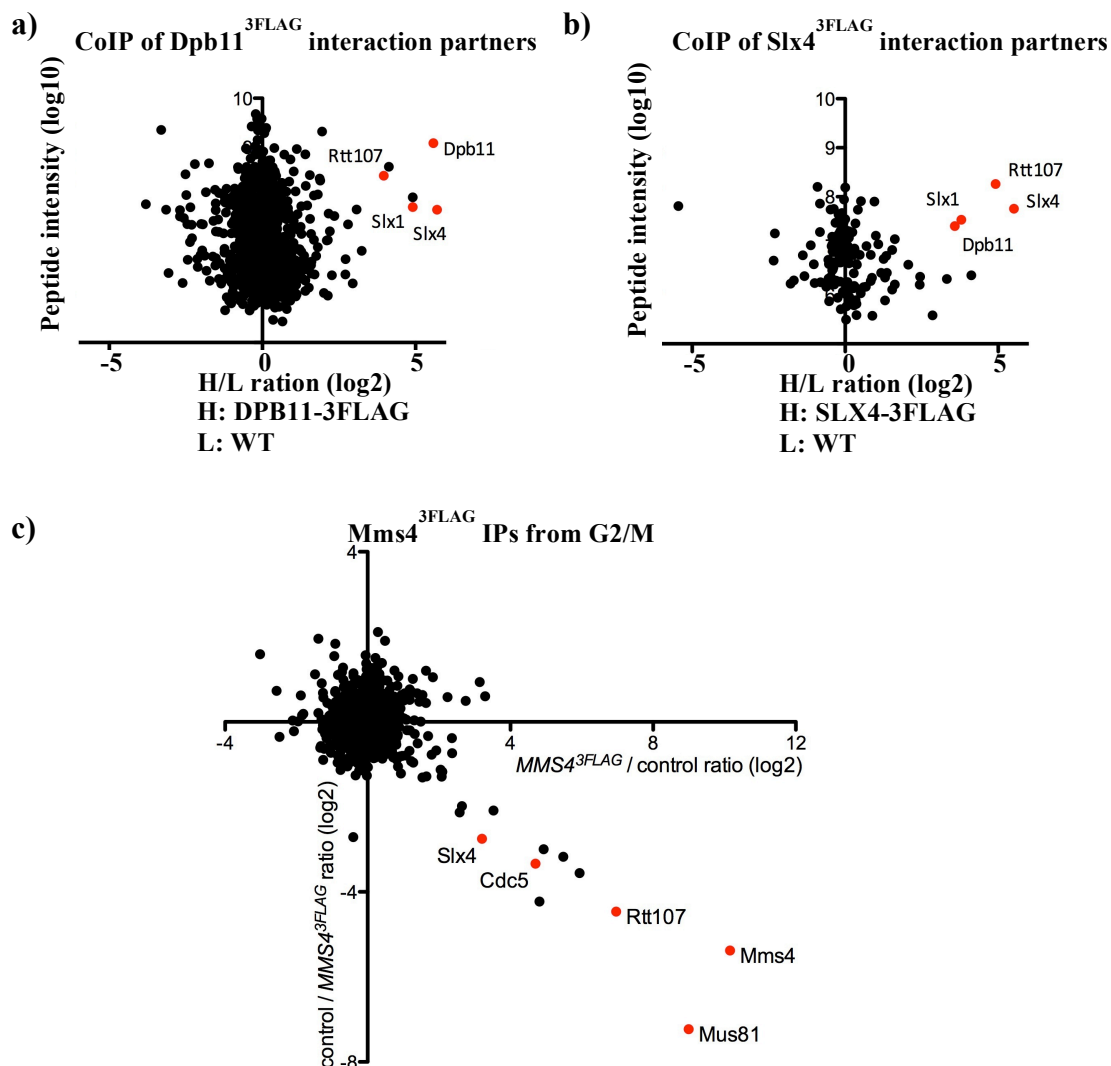


Figure 4.25. The Slx4-Dpb11-Mms4-Mus81 complex has additional interactors.

a) SILAC-based MS experiment of Dpb11 interactors. Co-immunoprecipitation samples from WT and *Dpb11-3FLAG* cells. Dpb11-3FLAG to WT ratio was quantified. Red dots represent the top interactors of Dpb11. Experiment by L. N. Princz; b) SILAC-based MS experiment of Slx4 interactors. Co-immunoprecipitation samples from WT and the *Slx4-3FLAG* cells. Slx4-3FLAG to WT ratio was quantified. Red dots represent the top interactors of Slx4. Experiment by L. N. Princz; c) SILAC-based MS experiment of Mms4 interactors. Co-immunoprecipitation samples from G2/M arrested cells of WT and strain expressing FLAG-tagged Mms4. WT to Mms4-3FLAG ratio was quantified. Red dots represent the top interactors of Mms4. Experiment by L. N. Princz.

As we showed that partially inactive DNA damage checkpoint rescues the *slx4-S486A* mutant phenotype (Figures 4.20a and 4.21), we tested whether the *DOT1* deletion and *ddc1-T602A* mutation similarly affect the *rtt107Δ* deletion mutant. Strikingly, a partial rescue of the *rtt107Δ* deletion mutant sensitivity to MMS by the *DOT1* deletion and *ddc1-T602A* mutation was observed (Figure 4.26c). These findings imply that the scaffold protein Rtt107 is a part of the Slx4-Dpb11-Mms4-

RESULTS

Mus81 complex. Moreover, DNA damage checkpoint regulation of the Slx4-Dpb11-Mms4-Mus81 complex might depend also on Rtt107.

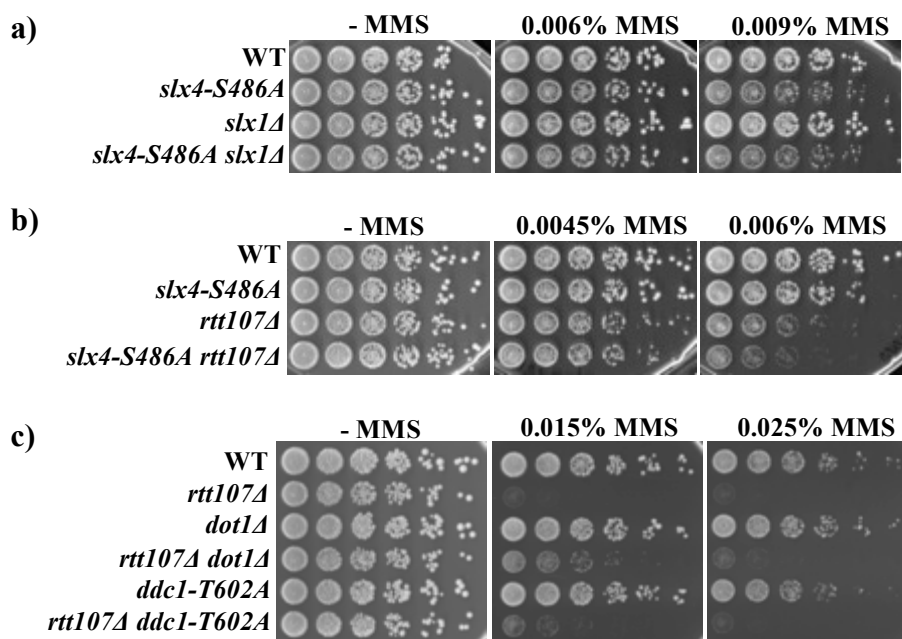


Figure 4.26. Slx1 and Rtt107 are potential interactors of Slx4-Dpb11-Mms4-Mus81.

a) MMS sensitivity of WT, the *slx4-S486A*, *slx1Δ* deletion and *slx4-S486A slx1Δ* mutants. Cells were spotted in serial dilutions on the plates containing MMS. The growth was evaluated after incubation for 2 days at 30°C; b) MMS sensitivity of WT, the *slx4-S486A*, *rtt107Δ* deletion and *slx4-S486A rtt107Δ* mutants. Cells were spotted as in a; c) MMS sensitivity of WT, the *rtt107Δ*, *dot1Δ* deletion, *ddc1-T602A*, *rtt107Δ dot1Δ* deletion and *rtt107Δ ddc1-T602A* mutants. Cells were spotted as in a.

4.5.2 Rtt proteins have a role in the recruitment of Slx4-Dpb11-Mms4-Mus81

Having found that Rtt107 is involved in the Slx4-Dpb11-Mms4-Mus81 complex, we asked whether the Slx4-Dpb11-Mms4-Mus81 complex is recruited on damage sites via Rtt107.

Rtt107 is a scaffold protein containing six BRCT repeats which often serve as binding modules for phosphorylated proteins (Zappulla et al., 2006). Rtt107 is similar to Dpb11, which also harbors BRCT repeats that are known to bind mainly CDK phosphorylated proteins bringing them into complexes (Tanaka et al., 2007; Zegerman and Diffley, 2007; Pfander and Diffley, 2011). Rtt107 interacts with Slx4, Rad55, H2A, the Smc5/6 complex and Rtt101 (Chin et al., 2006; Roberts et al., 2006; Roberts et al., 2008; Leung et al., 2011; Li et al., 2012). It was shown that N-terminus of Rtt107, which has four BRCT repeats, is important for the interaction with Slx4

RESULTS

and the Smc5/6 complex (Leung et al., 2011). The C-terminal domain of Rtt107 with two BRCT repeats binds the phosphorylated histone H2A (Li et al., 2012). Here, we aimed to test which part of Rtt107 thereby which interactors of Rtt107 function together with the Slx4-Dpb11-Mms4-Mus81 complex.

At first, to narrow down the list of candidates, we examined whether C-terminus of Rtt107 with BRCT5/6 is important for the function of the Slx4-Dpb11-Mms4-Mus81 complex. For this, the strains that express Rtt107 without C-terminal part containing BRCT5/6 in the wild type and the *slx4-S486A* mutant background were generated and tested for the growth on MMS. Importantly, the *rtt107ΔC* mutant was more sensitive to MMS compared to WT. Moreover, the *rtt107ΔC* mutant was as sensitive to MMS as the *slx4-S486A rtt107ΔC* mutant (Figure 4.27a). This suggests that the C-terminus of Rtt107 is important for the Slx4-Dpb11-Mms4-Mus81 function. However, this experiment does not completely rule out the requirement of the N-terminus of Rtt107 with BRCT1/2/3/4, which might still have a role in the Slx4-Dpb11-Mms4-Mus81 complex.

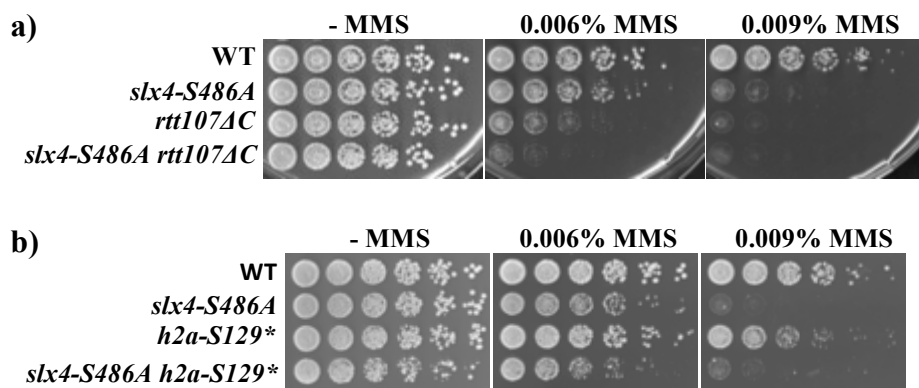


Figure 4.27. The C-terminus of Rtt107 is important for the Dpb11-Slx4 complex.

a) MMS sensitivity of WT, the *slx4-S486A*, *rtt107ΔC* and *slx4-S486A rtt107ΔC* mutants. Cells were spotted in serial dilutions on plates containing MMS. The growth was evaluated after incubation for 2 days at 30°C; b) MMS sensitivity of WT, the *slx4-S486A*, *hta-S129** and *slx4-S486A hta-S129** mutants. Cells were spotted as in a.

After DNA damage the DNA damage checkpoint kinase Mec1/Tel1 phosphorylates the histone H2A on S129. This chromatin modification mediates the recruitment of the DNA repair proteins to damage sites (Downs et al., 2000). The C-terminus of Rtt107 with BRCT5/6 was shown to interact with phosphorylated H2A (Li et al., 2012). To find out whether the H2A branch of recruitment is important for the Slx4-Dpb11-Mms4-Mus81 complex, the *hta* mutant, which cannot be

RESULTS

phosphorylated on S129 was generated. The *h2a-S129** mutation was also introduced in the *slx4-S486A* mutant background. Interestingly, the *h2a-S129** mutant did not show any sensitivity to MMS. Moreover, the *slx4-S486A h2a-S129** mutant was as sensitive to MMS as the *slx4-S486A* mutant (Figure 4.27b). Since the absence of phosphorylated H2A does not affect cell viability on MMS, we are not able to conclude neither that phosphorylated H2A is involved in the complex nor that it does not play any role in function of the Slx4-Dpb11-Mms4-Mus81 complex.

To understand the influence of the N-terminus of Rtt107 on the Slx4-Dpb11-Mms4-Mus81 complex function, we tested the best-characterized interactor of the N-terminus of Rtt107 - the Smc5/6 complex. Since the deletion of any Smc5/6 complex subunit is lethal, the experiments were carried out using the *smc6-9* temperature sensitive mutant. This particular mutant is viable at the permissive temperature of 30°C and is sensitive to MMS. Interestingly, the *slx4-S486A smc6-9* mutant was as sensitive to MMS as the *smc6-9* mutant suggesting the epistatic relationship (Figure 4.28a). These data suggest that the Smc5/6 complex is a part of the Slx4-Dpb11-Mms4-Mus81 complex.

Previously the cullin Rtt101, which assembles into a multi-subunit ubiquitin ligase, and the acetyltransferase Rtt109, which modifies histone H3, were shown to be involved in the accumulation of Rtt107 at the DNA damage sites in response to stalled replication forks (Roberts et al., 2008). Therefore, we next focused on Rtt101 and Rtt109. To ascertain that Rtt101 and Rtt109 are required for the recruitment of the Slx4-Dpb11-Mms4-Mus81 complex, we conducted epistasis analysis by testing MMS sensitivity of the *rrt101Δ*, *rrt109Δ* deletion, *slx4-S486A* mutants and the double mutant combinations. Strikingly, the *rrt101Δ slx4-S486A* and *rrt109Δ slx4-S486A* mutants were as sensitive to MMS as the *rrt101Δ* and *rrt109Δ* deletion mutants, respectively (Figure 4.28 b and c). These findings suggest that Rtt101 and Rtt109 are important for the function of the Slx4-Dpb11-Mms4-Mus81 complex.

All together, although these experiments do not completely rule out the requirements for the recruitment of the Slx4-Dpb11-Mms4-Mus81 complex, it provides the first evidence of what members might be involved in this process.

RESULTS

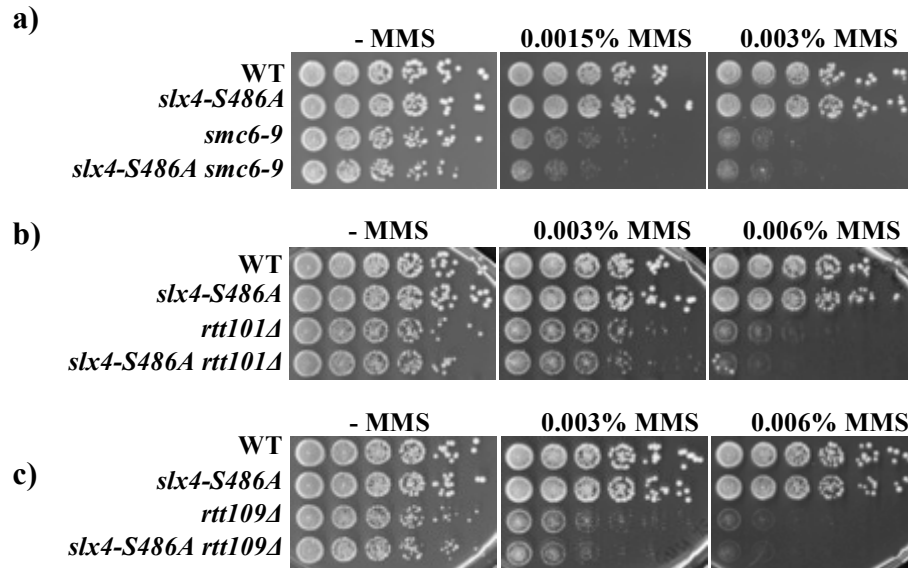


Figure 4.28. Smc5/6, Rtt101 and Rtt109 genetically interact with Dpb11-Slx4.

a) MMS sensitivity of WT, the *slx4-S486A*, *smc6-9* and *slx4-S486A smc6-9* mutants. Cells were spotted in serial dilutions on plates containing MMS. The growth was evaluated after incubation for 2 days at 30°C; b) MMS sensitivity of WT, the *slx4-S486A*, *rtt101Δ* deletion and *slx4-S486A rtt101Δ* mutants. Cells were spotted as in a; c) MMS sensitivity of WT, the *slx4-S486A*, *rtt109Δ* deletion and *slx4-S486A rtt109Δ* mutants. Cells were spotted as in a.

5 DISCUSSION

In this study the role of the Dpb11-Slx4 complex in DNA repair was investigated. Our results demonstrate that the interaction of Dpb11 and Slx4 is mediated by Cdk1-dependent phosphorylation at S486 of Slx4 and that this interaction is important for cell survival after MMS damage. The interaction-deficient *slx4-S486A* mutant showed slower repair of X-shaped DNA structures, an epistatic relationship with the structure-specific endonuclease Mus81-Mms4 and higher crossover rates suggesting, that the complex is involved in X-shaped DNA structure resolution by Mus81-Mms4. Interestingly, Dpb11-Slx4 binds Mus81-Mms4 in G2/M after Mms4 phosphorylation by Cdc5, thus forming the Slx4-Dpb11-Mms4-Mus81 complex. Moreover, in cells expressing Slx4-S486A the DNA damage checkpoint stays active longer after MMS damage. Partial inactivation of the checkpoint alleviates the *slx4-S486A* mutant phenotype due to increased Dpb11-Slx4 interaction with Mus81-Mms4. Thus, our research presented in this thesis uncovers a novel mechanism how Dpb11-Slx4 promotes X-shaped DNA structure resolution.

5.1 Dpb11 forms a complex with Slx4 and Mus81-Mms4

Molecular scaffolds, including Dpb11, are of great significance in regulating different processes in a cell. A feature of such molecular bridges is to bring particular proteins together and mediate the formation of functional complexes. To date, three individual Dpb11 complexes were described (Tanaka et al., 2007; Zegerman and Diffley, 2007; Pfander and Diffley, 2011; Ohouo et al., 2013). Here, we discovered a novel Dpb11 complex, which is composed of the scaffold protein Slx4 and the structure-specific endonuclease Mms4-Mus81.

Although Dpb11 binding to Slx4 was detected previously (Ohouo et al., 2010; Ohouo et al., 2013), here we present the first report that Dpb11 interacts with Mms4 and bridges Mus81-Mms4 with Slx4. This may be seen as apparent contradiction to other studies where Mus81-Mms4 was shown not to form a complex with Slx4 (Schwartz et al., 2012), but could be explained by a different experimental procedure,

as we detected the Slx4-Dpb11-Mms4-Mus81 complex formation exclusively in G2/M arrested cells.

Interestingly, the full Slx4-Dpb11-Mms4-Mus81 complex formation occurs in two steps. First, Dpb11 interaction with Slx4 is needed already in S-phase since we observed the remarkable increase of Dpb11 binding to Slx4 after MMS treatment when most of the cells are in S-phase. Second, Dpb11-Slx4 physically interacts with Mus81-Mms4 in G2/M phase and forms the entire Slx4-Dpb11-Mms4-Mus81 complex.

While Slx4 interaction with Dpb11 occurs in S-phase and G2/M, the Mms4 binds to Dpb11 only in G2/M. The different cell cycle stage requirements for a full Slx4-Dpb11-Mms4-Mus81 complex formation might increase the complexity of Slx4-Dpb11-Mms4-Mus81 regulation. Alternatively, the Dpb11-Slx4 pool detected earlier during the cell cycle may have additional physical interactions unrelated to Mus81-Mms4.

Importantly, the Dpb11-Slx4 interaction depends not only on the cell cycle stage but also on the absence or presence of DNA damage. After DNA damage more Dpb11 binds Slx4 suggesting a particular regulation of the Slx4-Dpb11-Mms4-Mus81 complex. This regulation can be achieved via the three molecular scaffolds Slx4, Dpb11 and Mms4 in the complex.

5.2 The Slx4-Dpb11-Mms4-Mus81 complex is regulated by the cell cycle

In general, scaffold proteins may work as readers of posttranslational modifications (PTMs) such as CDK phosphorylation. This example applies to Dpb11 which was previously shown to interact mainly with Cdk1 phosphorylated proteins (Tanaka et al., 2007; Zegerman and Diffley, 2007; Pfander and Diffley, 2011). On the other hand, scaffold proteins may themselves be targets of PTMs as it was shown for Slx4 and Mms4 (Toh et al., 2010; Matos et al., 2011; Gallo-Fernandez et al., 2012; Matos et al., 2013; Szakal and Branzei, 2013).

The Slx4-Dpb11-Mms4-Mus81 complex is regulated during cell cycle based on several evidences. First, Dpb11 binding to Slx4 is far stronger in G2/M compared to G1-phase. Second, Dpb11-Slx4 interaction with Mus81-Mms4 can only be observed

DISCUSSION

in G2/M-phase. Third, for Dpb11-Slx4 binding to Mms4 Cdk1 and Polo-like kinase Cdc5 are required.

Moreover, we identified specific sites in Slx4 and Mms4 required for the Slx4-Dpb11-Mms4-Mus81 complex formation and regulation. These sites are S486 of Slx4 and S184 and S201 of Mms4. Importantly, S486 of Slx4 and S184 and S201 of Mms4 match the CDK consensus motif. Analysis of Slx4 phosphorylation by quantitative mass spectrometry consistently demonstrates that S486 of Slx4 is in fact a Cdk1-phosphorylation site.

Phosphorylation of S486 stimulates Slx4 binding to Dpb11 but Slx4-S486A shows some residual binding to Dpb11. The same may be true for Mms4-SS184,201AA which may also have a residual binding to Dpb11 since the Mms4-S184A and Mms4-S201A interaction with Dpb11 in our Y2H experiment is not completely abolished.

Currently, it is unclear whether SS184,201 of Mms4 constitute the direct binding site for Dpb11, given the requirement for Polo-like kinase Cdc5. One possibility is that SS184,201 of Mms4 could prime Mms4 for the phosphorylation by Cdc5 since Cdk1 is thought to pre-phosphorylate Cdc5 targets (Golan et al., 2002; Yamaguchi et al., 2005). Therefore, it would be interesting to map the Cdc5 phosphorylation site(s) of Mms4, which are required for Dpb11 binding.

An important concept that emerges from our studies is that the regulation of the Slx4-Dpb11-Mms4-Mus81 complex is achieved in two steps. The interaction of Dpb11-Slx4 requires Cdk1, whereas Dpb11-Slx4 binding to Mus81-Mms4 additionally requires Cdc5. An intriguing possibility is that Slx4 may be an upstream regulator of the Slx4-Dpb11-Mms4-Mus81 complex, as Slx4 might bring Polo-like kinase Cdc5 into the complex, similarly as it was observed in mammalian cells (Svendsen et al., 2009). Slx4 might thus enable phosphorylation of Mms4 by Cdc5 and facilitate the second step of Slx4-Dpb11-Mms4-Mus81 regulation. This hypothesis could explain why Mms4 phosphorylation is delayed in the *slx4-S486A* mutant during recovery after MMS damage. However, in the absence of DNA damage in the *slx4-S486A* mutant background Mms4 is phosphorylated and binds to Dpb11 (Gritenaite et al., 2014).

So the Slx4-Dpb11-Mms4-Mus81 complex incorporates different kinase regulation signals at different cell cycle stage. Why is such a complex regulation

required? The most straightforward answer is to temporally regulate X-shaped DNA structure resolution by Mus81-Mms4.

To repair X-shaped DNA structures, cells evolved two different mechanisms: dissolution and resolution. Dissolution by Sgs1-Top3-Rmi1 is known to be the major pathway, whereas resolution by Mus81-Mms4 and Yen1 is restricted to M-phase and thereby will only face the remaining pool of X-shaped DNA structures (Liberi et al., 2005; Karras and Jentsch, 2010; Matos et al., 2011; Gallo-Fernandez et al., 2012; Matos et al., 2013; Szakal and Brnzei, 2013; Blanco et al., 2014). It is possible that this temporal restriction of structure-specific nucleases represents a pathway to protect replication forks from cleavage since structure-specific endonucleases are able to cut replication forks structures (Osman and Whitby, 2007). Consequently, by regulating the Dpb11-Slx4 complex the cell cycle regulates the repair of X-shaped DNA structures.

5.3 The Dpb11-Slx4 complex is important for X-shaped DNA structure resolution

To date, yeast Dpb11 was shown to be involved in DNA replication initiation and DNA damage checkpoint activation (Tanaka et al., 2007; Zegerman and Diffley, 2007; Mordes et al., 2008; Navadgi-Patil and Burgers, 2008; Pfander and Diffley, 2011). The mammalian orthologous protein of Dpb11 TopBP1 functions not only in DNA replication initiation and the DNA damage checkpoint but also in DNA repair and transcription. Here, we identified a novel Dpb11 complex in yeast, which is involved in DNA repair, particularly in the resolution of X-shaped DNA structures.

For functional studies we generated the *slx4-S486A* mutant. Importantly, Slx4-S486A is not able to interact with Dpb11, but shows normal binding to other Slx4 interactors like Rtt107 and Slx1. Therefore, *slx4-S486A* is a separation of function mutant. However, it seems that S486 of Slx4 is also important for the regulation of the DNA damage checkpoint (Ohouo et al., 2013) suggesting that the S486A mutation in Slx4 influences two different functions of Dpb11-Slx4.

Interestingly, the experiment presented in figure 4.14 using the *slx4-S486A* mutant shows the involvement of Dpb11-Slx4 in the resolution of X-shaped DNA structure resolution. Notably, the *slx4-S486A* mutant is hypersensitive to MMS but

not to other types of DNA damaging agents. These results led to the conclusions that the Dpb11-Slx4 complex is involved in the repair of stalled replication forks. Indeed, slower recovery of the *slx4-S486A* mutant after MMS damage and slowed down S-phase progression highlight the *slx4-S486A* problems in S-phase. Importantly, the cell cycle progression is the same as in wild type suggesting that problems might result from the repair defect of the *slx4-S486A* mutant.

Stalled replication forks can be repaired by post-replication repair (PRR) or homologous recombination (HR). Surprisingly, testing an extensive array of HR or PRR mutants, we did not find an epistatic relationship of the *slx4-S486A* mutant with either pathway. This suggests that the complex is not exclusively involved in PRR or HR. One possible interpretation is that Dpb11-Slx4 functions in a common step subsequent to HR or error-free PRR, in particular, the resolution of X-shaped DNA molecules.

X-shaped DNA structures form bridges which keep sister chromatids together, therefore disturbing proper segregation of chromosomes. These DNA structures originate from DNA replication and repair processes and, importantly, must be resolved before anaphase. Unresolved X-shaped DNA structures lead to chromatin bridges, consequently, to insertions, deletions and translocations and thereby threaten genome stability.

Our analysis of the *slx4-S486A* mutant suggests a role of the Dpb11-Slx4 complex in the resolution of X-shaped DNA structures based on following observations. First, using 2D gel electrophoresis we found that in the *slx4-S486A sgs1Δ* mutant X-shaped DNA structures are resolved with slower kinetics. Consistently, the same result was obtained by using a *slx4Δ* deletion mutant and conditionally inactivated Sgs1 in form of the *Tc-sgs1* allele. Second, RPA foci persist in the *slx4-S486A* mutant after MMS damage suggesting that ssDNA repair intermediates are present in the *slx4-S486A* mutant background. Third, Dpb11-chromatin bridges are increased in the *slx4-S486A* mutant, especially, in combination with *SGS1* deletion (Gritenaite et al., 2014). Importantly, since the *sgs1Δ* deletion mutant shows a stronger phenotype in the absence of the Dpb11-Slx4 interaction, this excludes Dpb11-Slx4 from the Sgs1-dependent dissolution pathway of X-shaped DNA structures and conversely suggests a role for Dpb11-Slx4 in the resolution pathway.

Interestingly, three structure-specific nucleases – Slx1-Slx4, Mus81-Mms4 and Yen1 - were reported to have roles in X-shaped DNA structure resolution mechanisms (Rass, 2013). Although Slx1 was observed to bind to Dpb11 and Slx4, suggesting that Slx1 could be a part of the Dpb11-Slx4 complex, we found that the *slx1Δ* deletion mutant is not sensitive to MMS. This suggests that the endonuclease Slx1 is not participating with Dpb11 and Slx4 in the resolution of X-shaped DNA structures, or, alternatively Slx1 is involved in Dpb11-Slx4 complex function but acts redundantly with another protein. Consequently, there is the possibility that other protein compensates for Slx1 in the respective deletion background, which should be confirmed experimentally.

Intriguingly, while our data show that Mus81-Mms4 genetically and physically interacts with Dpb11-Slx4, not all Mus81-Mms4 functions depend on Dpb11-Slx4. This is highlighted by the finding that the *MUS81* or *MMS4* deletion mutants show a higher sensitivity to MMS than the *slx4-S486A* mutant. This suggests that Mus81-Mms4 might function in a Dpb11-dependent as well as Dpb11-independent manner.

Importantly, in contrast to dissolution, which always generates non-crossover products, the outcomes of resolution are crossover or non-crossover products. Previous work suggests that Mus81-Mms4 is involved in crossover formation (Szakal and Branzei, 2013). Notably, constantly active Mms4 leads to increased crossover rates. Strikingly, we observed a role of Dpb11-Slx4 in crossover formation as well, since crossover rates are reduced in the *slx4-S486A* mutant.

Recently it was observed that Dpb11 is important for the processing of anaphase bridges (Germann et al., 2014). Anaphase bridges form when DNA replication and repair intermediates such as X-shaped DNA structures are not resolved before mitosis. In line with this study, we observed a co-localization of Dpb11 and Slx4 as well as Mus81 on anaphase bridges. Moreover, we observed that the number of the Dpb11-positive anaphase bridges is increased in the *slx4-S486A* mutant and that this phenotype is even more pronounced in the *sgs1Δ* deletion background. This is in line with the 2D gel electrophoresis experiment, which demonstrated that X-shaped DNA structures are resolved slower in the *slx4-S486A* mutant and in particular in the *sgs1Δ* deletion background. Our finding that there are more Dpb11-positive anaphase bridges in the *slx4-S486A* mutant therefore further supports the model that Dpb11-Slx4 is involved in the repair of X-shaped DNA structures.

Our analysis of the *mms4-SS184,201AA* mutant showed that S184 and S201 of Mms4 are not only important for the interaction with Dpb11 but also the function of Mus81-Mms4. In the absence of *SGS1* the *mms4-SS184,201AA* mutant is hypersensitive to MMS indicating that these particular sites, which are possibly required for Mms4 binding to Dpb11, are important for the Mus81-Mms4 function. Interestingly, *mms4-SS184,201AA* in combination with *slx4-S486A* increases the sensitivity to MMS compared to the single mutants. This lack of epistasis could be explained by the assumption that the *slx4-S486A* and *mms4-SS184,201AA* mutants only partially abrogate the interaction with Dpb11 (see above). In this situation a combination of both would further reduce the number of functional Slx4-Dpb11-Mms4-Mus81 complexes and hence increase the sensitivity to MMS.

Importantly, we tested not only phosphorylation deficient Mms4 mutant but also the phosphomimicry mutant of Mms4 to get more functional insights of the Slx4-Dpb11-Mms4-Mus81 complex. The *mms4-SS56,184ED* mutant of Mms4 was shown to lead to premature activation of Mus81-Mms4 and to increase the crossover formation in yeast (Szakal and Branzei, 2013). However, the *mms4-SS56,184ED* mutant does not rescue the MMS sensitivity of the *slx4-S486A* mutant. We suggest two possible explanations. First, the SS56,184ED mutations introduced to Mms4 by Szakal and Branzei only partially overlap with those sites we found to be important for the Mms4 interaction with Dpb11. Second, the stimulation of Mus81-Mms4 activity might depend on Dpb11-dependent and Dpb11-independent mechanisms, thus these two scenarios might require different sites for Mus81-Mms4 regulation. This hypothesis is in line with our observation that the deletion of MUS81 or MMS4 results in higher sensitivity of the mutants to MMS than the *slx4-S486A* mutant. Moreover, it is currently not clear if the SS56,184ED mutations in Mms4 actually enhance the binding to Dpb11.

In conclusion, our study shows that besides DNA replication initiation and DNA damage checkpoint activation complexes, Dpb11 forms at least one DNA repair complex in yeast, which functions in the resolution of X-shaped DNA structures by Mus81-Mms4.

5.4 The DNA damage checkpoint has a role in the resolution of X-shaped DNA structures

The DNA damage checkpoint is known to have an important role after DNA damage in S-phase. Checkpoint activation triggers various events leading to induced transcription of DNA repair genes, prevention of late origin firing and stabilization of replication forks. Our results provide novel insights into the regulation of the repair of stalled replication forks by the DNA damage checkpoint.

In this study we observed that a defect in Dpb11-Slx4 complex formation can be overcome by the partial inactivation of the DNA damage checkpoint. We evaluated three different scenarios of checkpoint activity: normal, partially active and inactive. Interestingly, when the formation of the Dpb11-Slx4 complex is impaired, partial inactivation of DNA damage checkpoint is beneficial to cell survival after DNA damage. In this scenario, partial DNA damage checkpoint inactivation leads to an earlier activation of the structure-specific endonuclease Mus81-Mms4 and thereby to DNA repair by resolution. However, when the checkpoint is completely inactivated, cells are not able to cope with MMS damage, probably due to the collapse of replication forks (Lopes et al., 2001). This observation suggests that DNA damage checkpoint activation needs to be balanced in *slx4-S486A* mutant cells in order to ensure survival after MMS damage.

Why may a fully active checkpoint be harmful in *slx4-S486A* mutant cells? A fully active DNA damage checkpoint in the Dpb11-Slx4 interaction deficient mutant might lead to a disturbed balance between dissolution and resolution pathways. We speculate that delayed phosphorylation of Mms4 and activation of Mus81-Mms4 might reduce the time to repair X-shaped DNA structures by resolution thereby entering anaphase with a pool of unresolved X-shaped DNA structures. This could result in more severe defects like breakage of chromosomes, thus decreasing the ability of the *slx4-S486A* mutant to maintain genome stability leading to cell death.

Consistently, when the DNA damage checkpoint is partially inactive, Mms4 phosphorylation occurs earlier in the *slx4-S486A* mutant after MMS damage. We suggest two possible explanations. First, the DNA damage checkpoint inhibits Cdc5, thus delaying Mms4 phosphorylation and Mus81-Mms4 activation. Second, the DNA damage checkpoint could regulate Mus81-Mms4 function directly via Mms4.

It has been observed in fission yeast that the active DNA damage checkpoint kinase Rad3 phosphorylates Eme1, the Mms4 orthologous protein in fission yeast. However, inconsistent with the idea of checkpoint inhibition, Eme1 phosphorylation activates Mus81-Eme1 in contrast to our studies where the DNA damage checkpoint inhibits the activity of Mus81-Mms4 (Dehe et al., 2013).

The DNA damage checkpoint might influence DNA repair by resolution also indirectly via regulation of Polo-like kinases. It has previously been observed that the Polo-like kinase PLK1 is inhibited by the DNA damage checkpoint in mammalian cells (Smits et al., 2000; Taylor and Stark, 2001). Initially it was suggested that the activity of Cdc5 is high in DNA damage-arrested cells of budding yeast (Hu et al., 2001). In contrast, another study showed that in the presence of DNA damage Cdc5 activity is partially reduced and dependent on Rad53 (Zhang et al., 2009). Since Mms4 is a target of the Polo-like kinase Cdc5 and we found that after MMS treatment of the *slx4-S486A* mutant Cdc5 expression and Mms4 phosphorylation are delayed, we conclude that the active DNA damage checkpoint inhibits Cdc5 thus delaying Mus81-Mms4 activation.

Yet another model that potentially could explain the relationship of Dpb11, Slx4 and the checkpoint has been suggested recently (Ohouo et al., 2013). The authors suggested Dpb11-Slx4 as a regulator of the checkpoint and therefore explained the MMS hypersensitivity of the *slx4-S486A* mutant by an impaired Slx4-Rtt107 function in DNA damage checkpoint regulation. It is known that Dpb11 is involved in checkpoint activation by forming a complex with Rad9, the 9-1-1 complex and Mec1-Ddc2 (Mordes et al., 2008; Navadgi-Patil and Burgers, 2008; Pfander and Diffley, 2011). In the Ohouo et al. model Slx4 competes with Rad9 for Dpb11 binding, thus inhibiting the DNA damage checkpoint. However, this does not seem to be the case in our hands, as we find that Slx4 binds to a different domain of Dpb11 than Rad9. Furthermore, we obtained results that suggest a Dpb11-Slx4 function in DNA repair by resolution, but it is difficult to rule out an involvement of the checkpoint in those experiments. Furthermore, the experiment with the linear fusion of Dpb11-Slx4 is in contrast to the checkpoint dampening model suggested by Ohouo et al. In the *Dpb11-slx4-S486A* strain the Dpb11-slx4-S486A fusion protein is expressed as a second copy of Dpb11, therefore the possibility for Rad9 to form a checkpoint complex with Dpb11 is even higher in this background. If the function of Slx4 was to reduce the

number of Dpb11 checkpoint complexes, we would expect to see an increased rather than decreased MMS sensitivity.

In summary, our experiments suggest an intricate relationship of the DNA damage checkpoint and the resolution of X-shaped DNA structures. As it is almost impossible to manipulate DNA repair without influencing the checkpoint and vice versa, we currently cannot rule out a function of Dpb11-Slx4 as checkpoint regulator.

5.5 Dpb11-Slx4 is a part of a multi-protein complex

Various processes in a cell are carried out by multi-protein complexes. This allows the distribution of tasks within the complex. In such complexes scaffold proteins often work as platforms allowing the higher organization or transient interactions of proteins acting in the same pathway.

In our study we evaluated the Slx4-Dpb11-Mms4-Mus81 complex, which consist of three scaffold proteins and the structure-specific endonuclease Mus81. Importantly, we found that besides these four components there are more interactors within the complex, suggesting a perhaps even more complex architecture.

First, Dpb11 could bind at least one or two additional proteins via the BRCT1/2 and the C-terminal AAD domains, similarly as in DNA replication initiation and DNA damage checkpoint activation complexes (Tanaka et al., 2007; Zegerman and Diffley, 2007; Mordes et al., 2008; Navadgi-Patil and Burgers, 2008; Pfander and Diffley, 2011). In contrast to well described Dpb11 complexes, where one domain of Dpb11 binds one interaction partner, it seems that not only BRCT1/2 and the C-terminus of Dpb11 are important for proper function of the Dpb11-slx4-S486A fusion but also BRCT3/4. Therefore, BRCT3/4 of Dpb11 in Slx4-Dpb11-Mms4-Mus81 function serves not only for the binding of Slx4 but also for binding of additional partners like Mms4. Indeed our initial data suggest a Mms4 interaction with BRCT3/4 of Dpb11 (unpublished data). How can two proteins bind one pair of BRCT repeats? This is possibly achieved via Dpb11 oligomerization which might also involve BRCT3/4. Dpb11 oligomerization is very likely as it was observed in mammalian cells (Liu et al., 2006; Liu et al., 2013), but it needs to be confirmed in yeast.

Another important part of the complex is Rtt107. Previously it was found that Rtt107 interacts with Slx4 and it is important after MMS induced DNA damage

(Roberts et al., 2006). Our data are in line with this study since we found similar and epistatic phenotypes for the *rtt107Δ* deletion and *slx4-S486A* mutants. Moreover, the physical interaction of Rtt107 with Slx4 and Dpb11 is robust. Therefore, Rtt107 is a part of Dpb11-Slx4 complex and we hypothesize that it functions to recruit the Slx4-Dpb11-Mms4-Mus81 complex to DNA damage sites.

Rtt107 is a scaffold protein and besides Slx4 it has several interaction partners, which are important for genome integrity processes. Li and colleagues proposed that the Rtt107 protein is recruited to sites of MMS induced damage by interacting with phosphorylated histone H2A (Li et al., 2012). Moreover, it was found that the recruitment of Rtt107 depends on the presence of the acetyltransferase Rtt109 and the Rtt101-containing ubiquitin ligase complex, which is also known to physically interact with Rtt107 (Roberts et al., 2008). Furthermore, Rtt107 binds to Nse6 which is a subunit of the Smc5/6 complex (Leung et al., 2011).

The different interactors - phosphorylated H2A, Rtt101 and Smc5/6 proteins - may all be part of one mechanism of Rtt107 recruitment or alternatively different proteins might recruit Rtt107 under different conditions or to different DNA damage sites. We therefore asked, which Rtt107 interactors may function together with the Slx4-Dpb11-Mms4-Mus81 complex. We found a genetic interaction between the *slx4-S486A* and *rtt101Δ* and *rtt109Δ* deletion mutants. These results lend further credence to an earlier suggestion that chromatin modification by Rtt101 and Rtt109 is required after the damaged or stalled replication forks (Roberts et al., 2008).

Chromatin modifications are required for the regulation of different processes on genomic DNA. The acetyltransferase Rtt109 targets H3K9, H3K23 and H3K27 and H3K56 (Schneider et al., 2006; Recht et al., 2006; Berndsen et al., 2008; Fillingham et al., 2008; Burgess et al., 2010). Interestingly, the acetylation of H3K56 was shown to have a role after DNA damage in S-phase, but it seems not to be required for the recruitment of Rtt107 (Masumoto et al., 2005; Ozdemir et al., 2005). Therefore, the nature of chromatin for the recruitment of the Slx4-Dpb11-Mms4-Mus81 complex remain to be elucidated.

Further evaluation of the Rtt107 interactors, however, could not rule out an involvement of phosphorylated H2A and the Smc5/6 complex. In the case of phosphorylated H2A the limitation was that the *h2a-S129** mutant is not sensitive to MMS, perhaps due to a functional overlap with the phosphorylated H2B. Importantly, we provide evidence that Smc5/6 may be a part of the Slx4-Dpb11-Mms4-Mus81

complex since the *slx4-S486A* mutant is epistatic with the *smc6-9* mutant. However, closer inspection of the Smc5/6 complex, for example investigation of a physical interaction with Slx4-Dpb11-Mms4-Mus81, is required to confirm this finding.

In summary, here, we provide the first evidence for the protein and chromatin modification requirements of the Slx4-Dpb11-Mms4-Mus81 complex function and perhaps recruitment. This is achieved by the presence of the ubiquitine ligase subunit Rtt101 and the acetyltransferase Rtt109. Phosphorylated H2A and the Smc5/6 complex might also be important. However, further studies are required to address the question of the recruitment of the Slx4-Dpb11-Mms4-Mus81 complex more in detail.

5.6 The Dpb11-Slx4 complex exists in mammalian cells

Recent efforts have shown that a complex similar to Dpb11-Slx4 also exists in human cells and is formed by the orthologous proteins TopBP1 and SLX4 (Gritenaite et al., 2014). The TopBP1-SLX4 interaction is CDK-dependent similar as in yeast, but further details, for example the complex architecture, remain to be investigated.

Additionally, it has been shown that in mammalian cells CDK- and PLK1-mediated phosphorylation brings SLX1-SLX4 and MUS81-EME1 to one SLX-MUS complex where MUS81 binds SLX4 directly in G2/M phase. The complex formation increases the endonuclease activity (Wyatt et al., 2013). As our data show formation of a similar complex in yeast, the difference is that in *S. cerevisiae* Dpb11 is required as a bridge, while in humans SLX4 directly binds to MUS81. Since there is no evidence about a direct Slx4-Mms4 interaction in yeast (Gritenaite et al.), closer inspection of bridged SLX4 and EME1 interaction by TopBP1 in mammalian system is interesting as it could uncover an additional layer of MUS81-EME1 regulation in human cells.

In mammalian systems the SLX-MUS interaction increases resolvase activity. However, our studies did not show any influence of the Dpb11-Slx4 complex on Mus81-Mms4 activity *in vitro* (Gritenaite et al., 2014). One possible explanation to this is that the experimental design is not optimal to visualize the Dpb11-Slx4 influence on X-shaped DNA structure resolution. Another explanation is that Dpb11-Slx4 does not directly affect the activity of Mus81-Mms4, but rather works as a recruitment mode for the resolvase.

DISCUSSION

One more open question comparing the mammalian and yeast Dpb11-Slx4 complexes is the role of Slx1. We find that Slx1 is a part of the Dpb11-Slx4 complex, however, the deletion of *SLX1* does not lead to MMS sensitivity. In contrast, human SLX1 contributes to activity of the SLX-MUS complex. One explanation is that Slx1 function in the yeast Dpb11-Slx4 complex can be replaced by another protein, which could be recruited via Dpb11. This hypothesis may also explain why in yeast Slx4 and Mus81-Mms4 are bridged by Dpb11.

Taken together, the Dpb11-Slx4 complex is conserved as TopBP1-SLX4 also exists in human cells. Despite the similarities and differences of these complexes, the overall function of Dpb11-Slx4 and TopBP1-SLX4 might be the same. Since mutations of TopBP1 are related to human disease (Forma et al., 2013; Forma et al., 2014), future studies should be conducted in order to further elucidate the mechanism and function of Dpb11-Slx4 and TopBP1-SLX4 complexes.

6 MATERIALS AND METHODS

Chemicals and reagents were provided by Amersham-Pharmacia, Applied Biosystems, Biomol, Biorad, Difco, Fluka, Invitrogen, Merck, New England Biolabs, Promega, Roth, Roche, Riedel de Haen, Serva, Sigma and Thermo Scientific. Standard techniques were used for microbiological, molecular biological and biochemical methods or the instructions of the manufacturer were followed. De-ionized sterile water, sterile solutions and sterile flasks were used for the described methods.

6.1 Computational analyses

For DNA and protein sequence search and comparison, protein physical and genetic interactions, mutant phenotypes, scientific literature search electronic services were applied using *Saccharomyces Genome Database* (<http://www.yeastgenome.org/>) and Information of *National Center for Biotechnology* (<http://www.ncbi.nlm.nih.gov/>). DNA Star software (EditSeq, SeqBuilder, SeqMan) was used for the DNA restriction enzyme maps, DNA sequencing analysis and primer design.

Quantification of the PFGE signal was performed using ImageJ software (<http://rsb.info.nih.gov/ij/>). Microsoft Office package 2008 (Microsoft Corp.) and Adobe Photoshop (Adobe Systems Inc.) were used for the presentation of text, tables, graphs and figures.

6.2 Microbiological and genetic techniques

6.2.1 *E. coli* techniques

<i>E. coli</i> strain	Genotype	Source
BL21-Gold	<i>B F ompT hsdS (r_B⁻ m_B⁻) dcm⁺ Tet^r gal endA Hte</i>	Agilent Technologies
Stellar	<i>F⁻, endA1, supE44, thi-1, recA1, relA1, gyrA96, phoA, Φ80d lacZΔ M15, Δ (lacZYA - argF) U169, Δ (mrr - hsdRMS - mcrBC), ΔmcrA, λ-</i>	Clontech

E. coli media:

LB medium/(plates): 1% Tryptone (Difco)
 0.5% Yeast extract (Difco)
 1% NaCl
 (1.5% Agar)
 sterilized by autoclaving

SOC medium: 2% Tryptone
 0.5% Yeast extract
 10 mM NaCl
 2.5 mM KCl
 10 mM MgCl₂
 20 mM Glucose
 sterilized by autoclaving

Cultivation and storage of *E. coli* cells

LB media was used to grow liquid cultures at 37°C with constant shaking. Cultures on solid media were incubated at 37°C. Ampicillin concentration of 50 µg/ml in the media was used for selection of transformed *E. coli*. Cultures on solid media were stored at 4°C for no longer than 5 days.

Transformation of plasmid DNA into competent *E. coli* cells

Competent *E. coli* cells were thawed on ice shortly before transformation. For transformation of DL21-Gold cells 50 µl of competent cells were mixed with 0.5-2 µl of ligation sample or 10 ng of plasmid DNA and incubated on ice for 15 min. Next, the heat-shock was performed for 45 s and the transformation mixture was placed for 2 min on ice. Then, the cells were resuspended in 1ml LB media without antibiotics and recovered at 37°C on a shaker for 1 h. After incubation, cells were plated on the solid media containing ampicillin and incubated overnight at 37°C.

For transformation of Stella cells, 50 µl of competent cells were mixed with 5 ng of DNA and incubated for 30 min on ice. Heat-shock was performed for 45 s at 42°C. Then, cells were kept for 5 min on ice. Prewarmed SOC medium was added to final volume of 500 µl and cells were incubated by shaking at 37°C for 1 h. Next, cells were plated on selective media and incubated overnight at 37°C.

6.2.2 *S. cerevisiae* techniques

<i>S. cerevisiae</i> vectors	Purpose	Reference
pYIplac128, pYIplac211	INT plasmids	(Gietz and Sugino, 1988)
pRS303, pRS304, pRS306	INT plasmids	(Sikorski and Hieter, 1989)
pGAD-C1-3, pGBD-C1-3	Two-hybrid	(James et al., 1996)

S. cerevisiae plasmids

In this study all generated yeast two-hybrid constructs were based on pGAD-C1-3 vectors for the AD N-terminal fusions and pGBD-C1-3 vectors for the BD N-terminal fusions. The particular ORFs (full-length or fragments) were amplified by PCR from genomic DNA of W303 yeast extracts using specific primers and compatible restriction enzyme sites. Site-directed mutagenesis with specific primers was used to introduce mutations. For all PCR reactions Phusion and Pfu Turbo high-fidelity polymerases were used, and restriction enzymes were provided by NEB.

Integrative plasmids were based on Yiplac and pRS vectors. In order to express proteins at their endogenous levels, the full-length ORFs surrounded by the upstream promoter and downstream terminator were amplified and cloned into integrative plasmids. All *slx4*, *dpb11*, *mms4* mutant plasmids were constructed by site-directed mutagenesis using specific primer pairs.

***S. cerevisiae* strains**

All yeast strains are based on W303 (Thomas and Rothstein, 1989). Two-hybrid analyses were performed in the strain PJ69-7A (James et al., 1996). Chromosomally tagged yeast strains and mutants used in this study were constructed by PCR-based, genetic crossing and standard techniques (Knop et al., 1999; Janke et al., 2004).

Strain	Relevant genotype	Reference
1093-5A	<i>ADE2+ RAD5+ CAN1+ ura3-1 his3-11,15 trp1-1 leu2-3,112</i>	Klein, 2001
CCG1908	<i>smc6-9</i>	Torres-Rosell et al., 2005
FY1485	<i>arg4deltaBglII CAN1 URA3::arg4deltaEcoRV::ura3-1 (au locus)</i>	Szakai and Branzei, 2013
HY2295	<i>arg4deltaBglII CAN1 URA3::arg4deltaEcoRV::ura3-1 (au locus) mms4::hphMX4</i>	Szakai and Branzei, 2013
Y2050	<i>ade2-1 trp1-1 his3-11 his3-15 can1-100 leu2-112::URA3::leu2-k</i>	Aguilera and Klein, 1988
YDG5	<i>pMBV13 hml::ADE1 mata::hisG hmr::ADE1 leu2-cs ade3::GAL::HO slx4::kanMx4</i>	This study
YDG32	<i>pMBV13 hml::ADE1 mata::hisG hmr::ADE1 leu2-cs ade3::GAL::HO slx4::kanMx4 trp1-1::slx4-S486A::TRP1</i>	This study
YDG40	<i>slx4::kanMx4 trp1-1::slx4-S486A::TRP1</i>	This study
YDG66	<i>rad51::natNT2</i>	This study
YDG71	<i>ho HML@ hmr::ADE1 ade3::GAL::HO slx4Δ::natNT2</i>	This study
YDG74	<i>ho HML@ hmr::ADE1 ade3::GAL::HO MATa- kanMx4 slx4::natNT2</i>	This study
YDG77	<i>ho HML@ hmr::ADE1 ade3::GAL::HO slx4::natNT2 trp1-1::slx4-S486A::TRP1</i>	This study
YDG79	<i>ho HML@ hmr::ADE1 ade3::GAL::HO MATa- kanMx4 slx4::natNT2 trp1-1::slx4-S486A::TRP1</i>	This study
YDG82	<i>ho HML@ hmr::ADE1 ade1-100 leu2-3,112 lys5 trp1::hisG' ura3-52 ade3::GAL::HO MATa- kanMx4</i>	This study
YDG96	<i>leu2-112::URA3::leu2-k slx4::kanMx slx4- S486A::TRP1</i>	This study
YDG126	<i>rad1::hphNTI</i>	This study
YDG127	<i>rtt107::hphNTI</i>	This study
YDG134	<i>slx1::hphNTI</i>	This study

MATERIALS AND METHODS

YDG135	<i>slx4::kanMx trp1-1::slx4-S486A::TRP1 slx1::hphNTI</i>	This study
YDG136	<i>rtt101::hphNTI</i>	This study
YDG137	<i>slx4::kanMx trp1-1::slx4-S486A::TRP1 rtt101::hphNTI</i>	This study
YDG138	<i>rtt109::hphNTI</i>	This study
YDG139	<i>slx4::kanMx trp1-1::slx4-S486A::TRP1 rtt109::hphNTI</i>	This study
YDG140	<i>rad55::hphNTI</i>	This study
YDG141	<i>slx4::kanMx4 trp1-1::slx4-S486A::TRP1 rad55::hphNTI</i>	This study
YDG142	<i>rtt107dC::hphNTI</i>	This study
YDG143	<i>slx4::kanMx trp1-1::slx4-S486A::TRP1 rtt107dC::hphNTI</i>	This study
YDG150	<i>mms2::hphNTI</i>	This study
YDG151	<i>slx4::kanMx trp1-1::slx4-S486A::TRP1 mms2::hphNTI</i>	This study
YDG153	<i>slx4::kanMx trp1-1::slx4-S486A::TRP1 rtt107::hphNTI</i>	This study
YDG167	<i>slx4::kanMx trp1-1::dpb11-T12A-slx4- S486A::TRP1</i>	This study
YDG168	<i>slx4::kanMx trp1-1::dpb11-T451A-slx4- S486A::TRP1</i>	This study
YDG169	<i>slx4::kanMx trp1-1::dpb11-WG700,701AA- slx4-S486A::TRP1</i>	This study
YDG175	<i>rad5::hphNTI</i>	This study
YDG180	<i>hta1S129*::hphNTI hta2S129*::natNT2</i>	This study
YDG181	<i>slx4::kanMx trp1-1::slx4-S486A::TRP1 hta1S129*::hphNTI hta2S129*::natNT2</i>	This study
YDG182	<i>slx4::kanMx trp1-1::slx4-S486A::TRP1 rad51::hphNTI</i>	This study
YDG183	<i>rev1::hphNTI</i>	This study
YDG184	<i>slx4::kanMx trp1-1::slx4-S486A::TRP1 rev1::hphNTI</i>	This study
YDG185	<i>rev3::hphNTI</i>	This study
YDG186	<i>slx4::kanMx trp1-1::slx4-S486A::TRP1 rev3::hphNTI</i>	This study
YDG187	<i>rad30::hphNTI</i>	This study
YDG188	<i>slx4::kanMx trp1-1::slx4-S486A::TRP1 rad30Δ::hphNTI</i>	This study
YDG189	<i>slx4::kanMx trp1-1::slx4-S486A::TRP1 his3- 11,15::sgs1::HIS3</i>	This study
YDG190	<i>slx4::kanMx trp1-1::slx4-S486A::TRP1</i>	This study

MATERIALS AND METHODS

YDG206	<i>slx4::kanMx4 trp1-1::slx4-S486A::TRP1</i>	This study
YDG207	<i>CAN1+ ADE2+ ura3-1 his3-11,15 trp1-1 leu2-3,112 rad5::hphNT1</i>	This study
YDG209	<i>rad5::hphNT1 ura3-1::RAD5+::URA3</i>	This study
YDG211	<i>rad5::hphNT1 ura3-1::rad5+-C914S::URA3</i>	This study
YDG212	<i>slx4::kanMx4 trp1-1::slx4-S486A::TRP1 rad5::hphNT1 ura3-1::RAD5+::URA3</i>	This study
YDG214	<i>slx4::kanMx4 trp1-1::slx4-S486A::TRP1 rad5::hphNT1 ura3-1::rad5+-C914S::URA3</i>	This study
YDG215	<i>slx4::kanMx4 trp1-1::slx4-S486A::TRP1 smc6-9</i>	This study
YDG217	<i>srs2ΔC::hphNT1</i>	This study
YDG218	<i>slx4::kanMx4 trp1-1::slx4-S486A::TRP1 srs2ΔC::hphNT1</i>	This study
YDG219	<i>siz1::hphNT1</i>	This study
YDG220	<i>slx4::kanMx4 trp1-1::slx4-S486A::TRP1 siz1::hphNT1</i>	This study
YDG240	<i>rad5::hphNT1 ura3-1::rad5+- KT538,539AA::URA3</i>	This study
YDG241	<i>rad5::hphNT1 ura3-1::rad5+- KT538,539AA::URA3 slx4::kanMx4 trp1- 1::slx4-S486A::TRP1</i>	This study
YDG251	<i>his3-11,15::rad53-3HA::HIS3</i>	This study
YDG252	<i>slx4Δ::kanMx4 trp1-1::slx4-S486A::TRP1 his3- 11,15::rad53-3HA::HIS3</i>	This study
YDG278	<i>exo1::hphNT1</i>	This study
YDG279	<i>slx4Δ::kanMx4 trp1-1::slx4-S486A::TRP1 exo1::hphNT1</i>	This study
YDG287	<i>slx4::kanMx4 trp1-1::slx4-S486A::TRP1 dot1::natNT2</i>	This study
YDG288	<i>slx4::kanMx4 trp1-1::slx4-S486A::TRP1 ddc1- T602A::natNT2</i>	This study
YDG289	<i>mms4::hphNT1</i>	This study
YDG290	<i>slx4::kanMx4 trp1-1::slx4-S486A::TRP1 mms4::hphNT1</i>	This study
YDG291	<i>yen1::hphNT1</i>	This study
YDG292	<i>slx4::kanMx4 trp1-1::slx4-S486A::TRP1 yen1::hphNT1</i>	This study
YDG293	<i>slx4::kanMx trp1-1::DPB11-slx4-S486A::TRP1</i>	This study
YDG305	<i>dot1::natNT2 rtt107::hphNT1</i>	This study
YDG306	<i>ddc1-T602A::natNT2 rtt107::hphNT1</i>	This study
YDG329	<i>sgs1::hphNT1</i>	This study
YDG303	<i>ddc1-T602A::natNT2</i>	This study
YDG304	<i>dot1::natNT2</i>	This study

MATERIALS AND METHODS

YDG309	<i>slx4::kanMx4 trp1-1::slx4-S486A::TRP1 ddc1-T602A::natNT2 mms4::hphNT1</i>	This study
YDG310	<i>ddc1-T602A::natNT2 mms4::hphNT1</i>	This study
YDG313	<i>slx4::kanMx4 trp1-1::slx4-S486A::TRP1 ddc1-T602A::natNT2 sgs1::hphNT1</i>	This study
YDG314	<i>ddc1-T602A::natNT2 sgs1::hphNT1</i>	This study
YDG335	<i>mus81Δ::hphNT1</i>	This study
YDG336	<i>slx4::kanMx4 trp1-1::slx4-S486A::TRP1 mus81::hphNT1</i>	This study
YDG339	<i>MMS4-3FLAG::hphNTI</i>	This study
YDG340	<i>slx4::kanMx trp1-1::slx4-S486A::TRP1 MMS4-3FLAG::hphNTI</i>	This study
YDG355	<i>mms4::hphNTI leu2 3,112::mms4SS184,201AA::LEU2</i>	This study
YDG356	<i>mms4::hphNTI leu2-3,112::mms4SS184,201AA::LEU2 his3-11,15::sgs1::HIS3</i>	This study
YDG357	<i>slx4::kanMx trp1-1::slx4-S486A::TRP1 mms4::hphNTI leu2-3,112::mms4SS184,201AA::LEU2</i>	This study
YDG358	<i>slx4::kanMx trp1-1::slx4-S486A::TRP1 mms4::hphNTI leu2-3,112::mms4SS184,201AA::LEU2 his3-11,15::sgs1::HIS3</i>	This study
YDG363	<i>rad9::hphNTI</i>	This study
YDG364	<i>slx4::kanMx trp1-1::slx4-S486A::TRP1 rad9::hphNTI</i>	This study
YDG366	<i>slx4::kanMx trp1-1::slx4-S486A::TRP1 ddc1-T602A::natNT2 MMS4-3FLAG::hphNTI</i>	This study
YDG367	<i>mms4::hphNTI leu2-3,112::mms4SS56,184ED::LEU2</i>	This study
YDG368	<i>slx4::kanMx trp1-1::slx4-S486A::TRP1 mms4::hphNTI leu2-3,112::mms4SS56,184ED::LEU2</i>	This study
YDG376	<i>yen1::hphNTI sgs1::natNT2</i>	This study
YDG377	<i>slx4::kanMx trp1-1::slx4-S486A::TRP1 yen1Δ::hphNT1 sgs1::natNT2</i>	This study
YLW1	<i>arg4deltaBglII CAN1 URA3::arg4deltaEcoRV::ura3-1 (au locus) slx4::kanMx</i>	This study
YLW4	<i>arg4deltaBglII CAN1 URA3::arg4deltaEcoRV::ura3-1 (au locus) slx4::kanMx trp1-1::slx4-S486A::TRP1</i>	This study

MATERIALS AND METHODS

YMS540	<i>ho HML@ hmr::ADE1 ade1-100 leu2-3,112 lys5 trp1::hisG' ura3-52 ade3::GAL::HO</i>	Sugawara et al., 2003
YMV45	<i>pMBV13 hml::ADE1 mata::hisG hmr::ADE1 leu2-cs ade3::GAL::HO ade1 lys5 ura3-52</i>	Vaze et al., 2002

***S. cerevisiae* media and solutions**

YPD/YPGal (plates): 1% Yeast extract (Difco)
 2% Bacto-peptone (Difco)
 2% D-(+)-Glucose or Galactose
 (2% Agar)
 sterilized by autoclaving

YPD G148/NAT/Hph/CAN plates: YPD medium containing 2% agar was autoclaved and cooled to 50°C prior to addition of G418 (geneticine disulfate; Sigma), NAT (noursethricin, HKI Jena) or Hph (hygromycin B, PAA Laboratories) to 200 mg/l, 100 mg/l, 500 mg/l and 600 mg/l final concentration, respectively.

SC-media (plates): 0.67% Yeast nitrogen base (Difco)
 0.2% Drop out amino acid mix
 (according to the requirements)
 2% Glucose
 (2% Agar)
 sterilized by autoclaving

Drop out amino acid mix: 30 mg Arg, Tyr, Leu, Lys
 50 mg Phe
 100 mg Glu, Asp
 150 mg Val
 200 mg Thr
 400 mg Ser

MATERIALS AND METHODS

Rich sporulation plates:	0.5% Yeast extract 3% Potassium acetate 0.2% Glucose 4% Agar sterilize by autoclaving, then add filter sterilized amino acid solution
Zymolase 100T solution:	0.9 M Sorbitol 0.1 M Tris-HCl, pH 8.0 0.2 M EDTA, pH 8.0 50 mM DTT 0.5 mg/ml Zymolase 100T (Seikagaku Corp., Japan)
SORB:	100 mM LiOAc 10 mM Tris-HCl, pH 8.0 1 mM EDTA, pH 8.0 1 M Sorbitol sterilized by filtration
PEG:	100 mM LiOAc 10 mM Tris-HCl, pH 8.0 1 mM EDTA, pH 8.0 40 % PEG-3350 sterilized by filtration

Cultivation and storage of *S. cerevisiae*

A single yeast colony from freshly streaked plates was inoculated as a liquid culture and incubated ON at 30°C with constant shaking. From this preculture the main culture was inoculated to an OD₆₀₀ of 0.1-0.2 and incubated in baffled-flasks (size \geq 5x liquid culture volume) on a shaking platform (150-220 rpm) at 30°C until mid-log growth phase had been reached (equals to OD₆₀₀ of 0.6-0.9). Photometer was used to determine the density of the culture (OD₆₀₀ of 1 is equal to 1.5×10^7 cells/ml).

Cultures on agar plates were stored at 4°C up to 1-2 months. For long-term storage, stationary cultures were frozen in 15% (v/v) glycerol solutions at -80°C.

Preparation of competent yeast cells

For preparation of competent cells, a mid-log phase growing culture was used. Yeast cells from 50 ml at OD₆₀₀ of 0.5-0.7 were harvested by centrifugation (500g, 3 min, room temperature), washed with 1/2 volume sterile water, then with 1/10 volume SORB solution, pelleted and suspended in 360µl SORB solution. Next, 40µl of carrier DNA (heat denatured salmon sperm DNA, 10 mg/ml) was added and competent cells were resuspended and stored in 50µl aliquots at -80°C.

Transformation of competent yeast cells

For transformation, 200ng of circular or 2µg of linearized plasmid DNA/PCR product were mixed with 10µl or 50µl competent yeast cells, respectively. Then, six volumes of PEG solution were added and the cell suspension was incubated for 30 min at 30°C. Subsequently, DMSO (10% final concentration) was added and a heat-shock was performed at 42°C for 15 min. Cells were centrifuged (500g, 3 min, room temperature), resuspended in 100µl sterile water and plated on the selective media plates. If antibiotics were used for selection, the transformed cells were incubated for 3 h in 5 ml liquid YPD medium prior to plating. The transformants were selected after 2-3 days growth at 30°C. If necessary, the transformants were replica-plated on selective media plates to remove the background of false-positive colonies.

Genomic integration by homologous recombination

The YIplac and pRS vector series were used for stable integration of DNA into the yeast genome. Only stably integrated vectors are propagated in yeast since YIplac and pRS plasmids do not contain autonomous replication elements. The ORFs of the respective genes were cloned into YIplac and pRS vectors including the endogenous promoter and terminator. A restriction enzyme that specifically cuts within the auxotrophy marker gene was used to linearize vectors before transformation. These linearized plasmids were then integrated into the genome by homologous recombination with the endogenous locus of the marker gene.

In order to delete, truncate, C-terminally tag endogenous genes with epitopes a similar approach was used. For this method, PCR products were used to transform

competent yeast cells. To allow homologous recombination with the endogenous locus of a particular gene, PCR products were generated using the primers that contain nucleotide sequences for amplification of special cassettes or regions of interest in the genome (including the marker gene for selection) as well as sequences complementary to the gene of interest required for proper integration. For gene deletions, the forward primer contains 55 bp of the promoter sequence 5' of the start codon of the respective gene, while the reverse primer includes 55 bp of the terminator sequence 3' of the stop codon. A forward primer containing 55 bp 5' of the stop codon were used instead for C-terminal epitope tagging of a gene. In a similar fashion, gene truncations and point mutations were introduced through homologous recombination. In general, after amplification PCR products were purified and concentrated using ethanol precipitation, and competent yeast cells were transformed and plated on selective media plates. The correct recombination was confirmed by yeast colony PCR, Western blot analysis (if possible) and sequencing of the modified genomic loci.

PCR screening of genomic recombination events

For the verification of chromosomal gene disruptions, correct recombination events, "yeast colony-PCR" was used. The screening strategy is based on oligonucleotide probes, which anneal upstream/downstream of altered chromosomal locus (primer I) and within the introduced selection marker gene (primer II). To prepare for PCR, a single yeast colony from a selective media plate was resuspended in 50µl of 0.02M NaOH and incubated at 95°C for 5min with rigorous shaking (1400 rpm). Then, the solution was briefly centrifuged (13000 rpm, room temperature) and 2µl of supernatant was directly used as a template for PCR. For PCR DNA oligonucleotides were custom-made by Eurofins MWG Operon.

PCR reaction mix:	2µl template DNA
	2.5µl 10x ThermoPol buffer
	0.9µl dNTPs (10mM)
	1.6µl primer I (10 µM)
	1.6µl primer II (10 µM)
	0.25µl <i>Taq</i> DNA polymerase
	16.15µl dH ₂ O

MATERIALS AND METHODS

Cycling parameters (30 amplification cycles):

PCR step	Temperature (°C)	Time	30 cycles
Initial denaturation	94	5 min	
Denaturation	94	30 s	
Annealing	50	30 s	
Elongation	72	1 min/kb	
Final elongation	72	10 min	
Cooling	4	∞	

Mating type analysis of haploid yeast strains

For the identification of yeast mating types, the tester strains RH448a and RC757alpha were used. These strains are hypersensitive to the pheromone secreted by yeast strains of the opposite mating type. A dense suspension of 1ml of a tester strain in sterile water was mixed with 50ml of molten agar (1% w/v water, pre-cooled to 40°C) and 5ml mixture was poured over YPD plate. Plates containing cultures to be analyzed were either replica-plated on the a- and alpha-tester plates, or single colonies of unknown mating type were streaked on each tester plate. A so-called “halo” of a clear agar is generated since the tester strains cannot grow in proximity to colonies of different mating type. Therefore, after 1-2 days of incubation at 30°C, a “halo” appears around a haploid colony, if the mating type of the strain is different. Since the diploid cells do not secrete any mating type pheromones, they do not give “halo” on both mating type tester plates.

Mating of haploid yeast strains

Freshly streaked haploid strains of opposite mating types were mixed and spotted together on YPD plates allowing the mating at 30°C. Cells were then either streaked on respective selection plates to identify diploids or mating type analysis was performed for individual colonies.

Sporulation and tetrad analysis of diploid yeast strains

Diploid yeast cells were streaked on rich sporulation media plates and incubated for 3 days at 30°C. After incubation, yeast cells were mixed with water and 10 µl of this mixture was added to 10 µl Zymolase 100T solution and incubated at room

temperature for 10 min. The spores were dissected in tetrads with a micromanipulator (Singer MSM System) and grown on YPD plates at 30°C for 2-3 days. Tetrads were analyzed genotypically by replica-plating on selective media plates or by their phenotypes when applicable.

Analysis of protein-protein interactions using the two-hybrid system

The full-length ORFs, fragments and mutant variants of proteins used for yeast two-hybrid assays in this study were fused to the C-terminus of the DNA-binding domain (BD) or activation domain (AD) of the Gal4 transcription factor by cloning them into pGBD-C1 or pGAD-C1 vectors, respectively. PJ69-7A cells were used to transform the expression constructs (James et al., 1996). Physical interaction between BD- and AD-fusion proteins leads to reconstitution of the Gal4 transcription factor, which induces expression of *HIS3* and *ADE2* reporter genes and allows cell growth in the respective selection plates. Cells and interactions were evaluated after growth for 3 days at 30°C.

Synchronization by alpha-factor and nocodazole

Treatment of a mating type cells with the alpha-factor pheromone or nocodazole results in cell cycle arrest at G1- or G2/M-phase, respectively. For such cell cycle synchronization, mid-log phase cell cultures were supplemented with 5-10 µg/ml alpha-factor (stock solution in water) or 5 µg/ml nocodazole (stock solution in DMSO). After 1.5 h incubation at 30°C, the arrest efficiency was determined microscopically (typically >90%) or by FACS analysis. The release from synchronization was performed by washing once in YPD, and suspending cells in YPD with 0.033% or 0.04% MMS. For recovery experiments, cells were washed after 30' of damage treatment, and suspended in drug free YPD media with or without nocodazole.

Phenotypic analysis of yeast mutants, growth and cell survival assays

Nonessential gene knockout strains and mutants were tested for growth impairments and DNA damage sensitivity by spotting equal amounts of cells in serial dilutions onto solid YPD media containing DNA damage inducing agents such as MMS, phleomycin, HU, CPT or 4-NQO. For UV treatment, cells were spotted on YPD before treatment by UV light in the irradiation chamber BS-03 (Dr. Groebel

UV-Elektronik GmbH) and incubated in the dark. For all growth and cell survival analysis, overnight cultures were harvested and resuspended in sterile water to $OD_{600}=0.5$. Five-fold serial dilutions were prepared and spotted onto the respective plates. Cells were evaluated after 2-3 days growth at 30°C.

Liquid cultures were incubated for 30-45 min at 30°C in the presence of MMS (0.033%), zeocin (0.2 mg/ml) or phleomycin (0.2 mg/ml).

Mutation and recombination assays

Mutation rates were determined using a *CANI* forward mutation assay (Klein, 2001). Interchromosomal recombination rates were determined using a direct-repeat system using *leu2* heteroalleles (Aquilera and Klein, 1988) and crossover rates were determined using a system harbouring two *arg4* alleles on chromosome V and VIII (Robert et al. 2006, Szakal and Branzei, 2013). In all cases mutation/recombination rates were determined using fluctuation analysis and a maximum-likelihood approach. Therefore, for each strain ten independent cultures originated from the single cell were analyzed. To get single colonies 100 cells were plated or streaked for single colonies on YPD media plates and incubated for 2 days at 30 °C. The frequency of mutants/recombinants in all cultures was determined by plating on selective media. The total cell number was determined by plating an appropriate dilution on non-selective media. For determination of CO rates, for each culture ten *ARG+* colonies were picked, analyzed by PCR for CO or NCO events (Szakal and Branzei 2013) and the overall number of crossover recombinants was extrapolated. From the number of mutants/recombinants/crossover recombinants the number of mutational/recombinational/crossover events was determined using a maximum-likelihood approach and rates were determined by dividing by the number of cell divisions (Pfander et al., 2005). For each strain 2-3 independent experiments were performed to determine mean and standard deviation.

Mating type switching assay (HO-sensitivity)

To determine the cell survival after processing 1 or 2 non-homologues tails after homologues recombination, cell were grown in YPRaff to $OD_{600}=0.5$. The liquid culture then was split in half and to one half 2% galactose was added to induce double strand brake. The other half was supplemented with 2% glucose and used as a control. After 30 min particular amount of cells were plated on YPD plates and colonies were

counted after 2-3 days growth at 30°C. The cell survival was calculated by dividing the colonies number after galactose treatment from the number of colonies after glucose treatment.

FACS analysis

1×10^7 - 2×10^7 cells were harvested by centrifugation and resuspended in 70% ethanol + 50 mM Tris pH 7.8. After centrifugation cells were washed with 1 ml 50 mM Tris pH 7.8 (Tris buffer) followed by resuspending in 520 μ l RNase solution (500 μ l 50 mM Tris pH 7.8 + 20 μ l RNase A (10 mg/ml in 10 mM Tris pH 7.5, 10 mM $MgCl_2$) and incubation for 4 h at 37 °C. Next, cells were treated with proteinase K (200 μ l Tris buffer + 20 μ l proteinase K (10 mg/ml in 50% glycerol, 10 mM Tris pH 7.5, 25 mM $CaCl_2$) and incubated for 30' at 50 °C. After centrifugation cells were resuspended in 500 μ l Tris buffer. Before measuring the DNA content, samples were sonified (5"; 50% CYCLE) and stained by SYTOX solution (999 μ l Tris buffer + 1 μ l SYTOX). Measurement was performed using FL1 channel 520 for SYTOX-DNA on a BD FACSCalibur system operated via the CELLQuest software (Becton Dickinson).

6.3 Molecular biology techniques

General molecular biology and cloning techniques including DNA amplification/site-directed mutagenesis by PCR, restriction digest, ligation or analysis of DNA by agarose gel electrophoresis were performed according to standard (Sambrook and Russell, 2001) or manufacturer's protocols.

General buffers and solutions

TE buffer:	10 mM Tris-HCl, pH 8.0
	1 mM EDTA
	sterilized by autoclaving

MATERIALS AND METHODS

TBE buffer 5x:	90 mM Tris 90 mM Boric acid 2.5 mM EDTA, pH 8.0 sterilized by autoclaving
DNA loading buffer 6x:	0.5% SDS 0.25% (w/v) Bromophenol blue 0.25% Glycerol 25 mM EDTA, pH 8.0

6.3.1 Isolation of DNA

Isolation of plasmid DNA from *E. coli*

A single *E. coli* colony carrying the DNA plasmid of interest was inoculated to 5 ml LB medium containing ampicillin and incubated overnight at 37°C. Plasmids were isolated using the AccuPrep plasmid extraction kit (Bioneer Corp.) according to the manufacturer's instructions. NanoDrop spectrophotometer was used to determine the yield of isolated DNA.

Isolation of chromosomal DNA from *S. cerevisiae*

Breaking buffer:	2% Triton X-100 1% SDS 100 mM NaCl 10 mM Tris-HCl, pH 8.0 1 mM EDTA, pH 8.0
------------------	---

Yeast genomic DNA was isolated for further use as a template for amplification of genes via PCR. A stationary culture cells from 10 ml were centrifuged (1500g, 5 min), washed in 0.5 ml water and resuspended in 200 µl breaking buffer. Next, 200 µl phenol/chloroform/isoamyl alcohol (24:24:1 v/v/v) and 300 mg acid-washed glass beads (425-600 µm; Sigma) were added and the mixture was vortexed for 5 min. The lysate was mixed with 200 µl TE buffer, centrifuged (14000 rpm, 5 min, room temperature) and the supernatant was transferred to a new microcentrifuge tube.

Precipitation of DNA was carried by adding 1 ml ethanol (absolute) and centrifugation (14000 rpm, 3 min, room temperature). The pellet was resuspended in 0.4 ml TE buffer and RNA contaminants were destroyed by treatment with 30 µl of DNase-free RNase A (1 mg/ml) for 5 min at 37°C. Then, 10 µl ammonium acetate (3 M) and 1 ml ethanol (absolute) were added to precipitate DNA. After brief centrifugation (14000 rpm, room temperature), the pellet was resuspended in 100 µl TE buffer.

Precipitation of DNA

For ethanol precipitation, 1/10 volume sodium acetate (3 M, pH 4.8) and 2.5 volumes ethanol (absolute) were added to the DNA solution and incubated at -20°C for 30 min. Then, the mixture was centrifuged (13000 rpm, 15 min, room temperature) and the pellet was washed with 0.5 ml ethanol (70%). The DNA pellet was air-dried and resuspended in sterile water.

Determination of DNA concentration

The DNA concentration was photometrically determined by measuring the absorbance at a wavelength of 260 nm (OD₂₆₀) using the NanoDrop ND-1000 spectrophotometer (PeqLab). An OD₂₆₀ of 1 equals to a concentration of 50 µg/ml double-stranded DNA.

6.3.2 Molecular cloning

Digestion of DNA with restriction enzymes

Standard protocols (Sambrook and Russell, 2001) and the instructions of the manufacturer (NEB) were used to perform the sequence-specific cleavage of DNA with restriction enzymes. In general, 5 to 10 units of the respective restriction enzyme were used for digestion of 1 µg DNA. Normally, the restriction reaction samples were incubated for 2 h in the recommended buffers (NEB) and at the permissive temperature. To avoid re-ligation of linearized vectors, the 5' end of the vector was dephosphorylated by adding 1 µl of Calf Intestinal Phosphatase (CIP; NEB) and incubating at 37°C for 1 h.

Separation of DNA by agarose gel electrophoresis

To isolate DNA fragments, DNA samples were mixed with 6x DNA loading buffer and subjected to electrophoresis using 1% agarose gels containing 0.5 µg/ml ethidium bromide at 120V in TBE buffer. Since ethidium bromide intercalates to DNA, an UV transilluminator (324 nm) was used to visualize separated DNA fragments. The size of the fragments was estimated according to standard size DNA markers (1 kb DNA ladder; Invitrogen).

Isolation of DNA fragments from agarose gels

After separation by gel electrophoresis, DNA fragments were excised from the agarose gel using a sterile razor blade. Then, QIAquick Gel Extraction Kit (Qiagen) according to manufacturer's instructions was used to extract DNA from the agarose block. DNA was eluted with an appropriate volume of sterile water.

Ligation of DNA fragments

The amounts of the linearized vector and insert required for the ligation reaction were measured by NanoDrop ND-1000 spectrophotometer (PeqLab). For the ligation reaction, a ratio of 1:3 to 1:10 of vector to insert was used. The 10 µl ligation reaction sample contained 100 ng of vector DNA and 10 units of T4 DNA ligase (NEB). The ligation reaction was performed at 16°C for 4 to 12 h.

Sequence- and ligation-independent (SLIC) cloning

For the SLIC reaction, 10-200 ng (<0.5 kb: 10-50 ng, 0.5 to 10 kb: 50-100 ng, >10 kb: 50-200 ng) purified PCR fragment and 50-200 ng (<10 kb: 50-100 ng, >10 kb: 50-200 ng) linearized vector were used. The 10 µl SLIC reaction sample contained 1 µl 5x In-Fusion HD Enzyme Premix (Clontech). The total reaction volume was adjusted to 10 µl using dH₂O and the reaction was mixed. After incubation for 15 min at 50°C, then the sample was placed on ice and used for the transformation procedure. For long-term storage SLIC reaction sample can be stored at -20°C.

DNA sequencing

The Core Facility of the Max Planck Institute of Biochemistry carried out the DNA sequencing reactions using the ABI-Prism 3730 DNA sequencer (Applied

Biosystems Inc.). The 7.5 µl sequencing samples contained 300 ng DNA and 2 µl primer (10 µM). The sequencing reactions and the subsequent sample preparation steps were done with the DYEnamic ET terminator cycle sequencing kit (GE Healthcare), according to the manufacturer's instructions.

6.3.3 Polymerase chain reaction

To specifically amplify DNA fragments from small amounts of DNA templates the polymerase chain reaction (PCR) technique was used. For amplification of DNA fragments for subsequent cloning, amplification of yeast targeting cassettes (e.g., for chromosomal gene disruption), screening/sequencing of genomic recombination events and site-directed mutagenesis, PCR was applied.

Amplification of genomic DNA fragments

For the generation of genomic DNA fragments for subsequent cloning, direct yeast transformation and sequencing, full-length ORFs or selected sequences were amplified from genomic DNA using the *Phusion* High-Fidelity DNA polymerase (NEB). PCR reactions in a volume of 50 µl were prepared in 0.2 ml tubes (Biozym) on ice. A PCR Mastercycler (Eppendorf) was used for the reaction.

PCR reaction mix:	200 ng Genomic DNA
	10 µl 5x GC buffer
	1.75 µl dNTP-Mix (10 mM each; NEB)
	3.2 µl Forward primer (10 µM)
	3.2 µl Reverse primer (10 µM)
	1 µl DMSO
	1 µl MgCl ₂ (50 mM)
	0.5 µl <i>Phusion</i> DNA polymerase
	adjust to 50 µl with dH ₂ O

MATERIALS AND METHODS

Cycling parameters (30 amplification cycles):

PCR step	Temperature (°C)	Time	30 cycles
Initial denaturation	98	4 min	
Denaturation	98	30 s	
Annealing	50	30 s	
Elongation	72	1 min/kb	
Final elongation	72	10 min	
Cooling	4	∞	

Amplification of chromosomal targeting cassettes

A PCR strategy based on the targeted introduction of heterologous DNA sequences into genomic locations via homologous recombination was used to perform chromosomal gene deletions, epitope tagging and other alterations of the yeast genome (Knop et al., 1999; Janke et al., 2004). Targeting cassettes were amplified by PCR using primers containing homology to the genomic target locus. The 50 μ l PCR reactions were prepared and cycling conditions were used as described above (Amplification of genomic DNA fragments). After amplification, PCR products were concentrated by ethanol precipitation, dissolved in 10 μ l sterile water and used directly for the transformation of competent yeast cells or stored at -20°C.

PCR reaction mix:	100 ng plasmid DNA
	10 μ l HF buffer
	1.75 μ l dNTP-Mix (10 mM each; NEB)
	3.2 μ l Forward primer (10 μ M)
	3.2 μ l Reverse primer (10 μ M)
	0.5 μ l <i>Phusion</i> DNA polymerase
	adjust to 50 μ l with dH ₂ O

Site-directed mutagenesis

To introduce specific point mutations in plasmid DNA sequences, a PCR-base strategy according to the Quick-change protocol (Stratagene) was used. This method is based on two complementary oligonucleotide primers with the codon to be mutated in the middle of the sequence flanked by at least 15-20 additional nucleotides, each

MATERIALS AND METHODS

corresponding to the target sequence. The *Pfu Turbo* DNA polymerase (Stratagene) has proven to be the enzyme of choice for this technique. DNA oligonucleotides for PCR were custom-made by Eurofins MWG Operon.

PCR reaction mix:	50-100 ng plasmid DNA
	2.5 µl 10x Pfu buffer
	0.63 µl Forward primer (10 µM)
	0.63 µl Reverse primer (10 µM)
	0.63 µl dNTPs (10mM)
	0.5 µl <i>Pfu Turbo</i> DNA polymerase
	adjust to 25 µl with dH ₂ O

Cycling parameters (20 amplification cycles):

PCR step	Temperature (°C)	Time	20 cycles
Initial denaturation	95	3 min	
Denaturation	95	30 s	
Annealing	55	60 s	
Elongation	68	2 min/kb	
Final elongation	72	10 min	
Cooling	4	∞	

To eliminate template plasmid DNA that does not contain the mutation, 25 µl of the PCR reaction were treated with 1 µl of DpnI endonuclease for 1-2 hours at 37°C. DpnI endonuclease is specific for methylated and hemimethylated DNA. Since most plasmid DNA from *E. coli* is methylated, DpnI treatment of the PCR product leads to the selective digestion of the parental DNA template. After digestion, the PCR product was directly used for *E. coli* transformation. DNA sequencing was performed to identify mutated plasmids.

6.3.4 Separation and visualization of yeast chromosomes

Solutions

Zymolyase solution: 50 mM EDTA
 10 mM Tris, pH 8.0
 20 mM NaCl
 1 mg/ml Zymolyase (T100)

Proteinase K solution: 0.5 M EDTA, pH 8.0
 1 mg/ml Proteinase K
 10 mg/ml Sodium lauryl sarcosine

Pulsed-field gel electrophoresis (PFGE)

In the recovery experiments 8×10^7 of cells were taken for every time point and centrifuged at $5000 \times g$ 10 min at 4 °C. Cells were resuspended in 1 ml cold 0.1% sodium azide and centrifuged at 3000 rpm for 3 min. Remaining pellets were resuspended in 50 µl zymolyase buffer and mixed with equal amount of 2% agarose. The samples were transferred to the plug mold. The plugs were incubated in zymolyase buffer at 37 °C for 1 h, followed by treatment with proteinase K at 50 °C for 24-48 h. Next, the plugs were washed 3 times with 50 mM EDTA and loaded. Electrophoresis was performed using the CHEF-DRIII pulsed-field electrophoresis system (Bio-Rad) according to the manufacturer's instructions. The gel was stained with 1 µg/ml ethidium bromide and scanned under UV light. Quantification of PFGE signals was performed using ImageJ. For every time point the signal from the bands that have entered the gel was normalized to the total signal in the lane including that from the well, and the values from every time point were normalized relative to the G1 signal.

6.4 Biochemistry techniques

General buffers and solutions

HU sample buffer:	8 M Urea
	5% SDS
	1 mM EDTA
	1.5% DTT
	1% Bromphenol blue
MOPS running buffer:	50 mM MOPS
	50 mM Tris base
	3.5 mM SDS
	1 mM EDTA
SDS-PAGE running buffer:	25 mM Tris base
	192 mM Glycine
	0.1% SDS
Transfer buffer:	250 mM Tris base
	192 mM Glycine
	0.1% SDS
	20% Methanol
TBST:	25 mM Tris-HCl, pH 7.5
	137 mM NaCl
	2.6 mM KCl
	0.1% Tween 20

6.4.1 Preparation of yeast protein extracts

Preparation of denatured protein extracts (TCA-precipitation)

In most cases yeast cells were lysed under denaturing conditions to preserve post-translational modifications. For preparation of denatured protein extracts for

every time point, 2×10^7 cells were harvested and frozen in liquid nitrogen. Cells were suspended in 1 ml water and 150 μ l 1.85 M NaOH/7.5% β -mercaptoethanol was added. After 15 min incubation on ice, 150 μ l 55% TCA was added and incubated for 10 min. Proteins were pelleted by centrifugation (13000 rpm, 4°C, 2 min) and suspended in 50 μ l HU-buffer. The samples were boiled at 65 °C for 10 min and used for analysis by Western blot or stored at -20°C.

6.4.2 Gel electrophoresis and immunoblot techniques

SDS-polyacrylamide gel electrophoresis (SDS-PAGE)

For separation of proteins, SDS-PAGE was performed using self-poured (see recipe below) or pre-cast 4-12% gradient NuPAGE Bis-Tris polyacrylamide gels (Invitrogen). These gels allow resolution of proteins over a large range of different molecular weight (from 10 to 200 kDa) and do not require stacking gels. Samples for electrophoresis were prepared by TCA-precipitation, desolved in HU sample buffer and heated for 5 min at 95°C. Electrophoresis was carried out at a constant voltage of 140V using MOPS running buffer and pre-cast gels or at 200V using SDS-PAGE running buffer and self-poured gels. The Novex Sharp pre-stained protein standard (Invitrogen) was used as a molecular weight marker. The gels were subsequently subjected to immunoblotting.

Solution for pouring 10% SDS-PAGE gels:

Separating gel (4 mini gels):	5 ml 40% Acrylamide
	1.32 ml 2% Bis-Acrylamide
	5 ml 1.5 M Tris-HCl, pH 8.8
	200 μ l 10% SDS
	8.7 ml dH ₂ O
	25 μ l TEMED
	100 μ l 10% APS

MATERIALS AND METHODS

Stacking gel (4 mini gels):	640 µl 40% Acrylamide
	350 µl 2% Bis-Acrylamide
	625 µl 1M Tris-HCl, pH 6.8
	50 µl 10% SDS
	3.32 ml dH ₂ O
	20 µl TEMED
	40 µl 10% APS

Western blot analysis

For western blot analysis, proteins separated by PAGE were transferred to polyvinylidene fluoride (PVDF) membranes (Immobilon-P, 0.45 µm pore size; Millipore) using a wet tank blot system (Hoefer). Fresh transfer buffer and a constant voltage of 90V for 90 min at 4°C were used for the blotting procedure. Subsequently, membranes were blocked for 30 min in 5% skim milk powder (Fluka) dissolved in TBST and further incubated overnight with primary antibody at 4°C with constant shaking. Then, membranes were washed three times with TBST (5 min incubation) and incubated with the respective horseradish peroxidase HRP-coupled secondary antibody (1:5000 dilution; Dianova) for 1-3 h in TBST at room temperature. After five further washes with TBST (5 min incubation), the protein signals were obtained by chemiluminescence using ECL kit (Amersham) according to the manufacturer's instructions. Signal detection was performed taking qualitative exposures with a film.

Primary antibodies

Proteins were detected using specific antibodies: rabbit-anti-Rad53 (JD147, J. Diffley), rabbit-anti-Slx4 (2057, Pfander lab), goat-anti-Cdc5 (sc-6733, Santa Cruz), rabbit-anti-Clb2 (sc-9071, Santa Cruz), rabbit-anti-FLAG (Sigma), rabbit-anti-Pol30 PCNA (a0031, Pfander lab).

7 REFERENCES

- Agarwal R, Tang Z, Yu H, Cohen-Fix O. Two distinct pathways for inhibiting pds1 ubiquitination in response to DNA damage. *J Biol Chem* 278, 45027-45033 (2003).
- Alberghina L, Rossi RL, Querin L, Wanke V, Vanoni M. A cell sizer network involving Cln3 and Far1 controls entrance into S phase in the mitotic cycle of budding yeast. *J Cell Biol* 167, 433-443 (2004).
- Alcasabas AA, Osborn AJ, Bachant J, Hu F, Werler PJ, Bousset K, Furuya K, Diffley JF, Carr AM, Elledge SJ. Mrc1 transduces signals of DNA replication stress to activate Rad53. *Nat Cell Biol* 3, 958-965 (2001).
- Allen JB, Zhou Z, Siede W, Friedberg EC, Elledge SJ. The SAD1/RAD53 protein kinase controls multiple checkpoints and DNA damage-induced transcription in yeast. *Genes Dev* 8, 2401-2415 (1994).
- Andersen PL, Xu F, Xiao W. Eukaryotic DNA damage tolerance and translesion synthesis through covalent modifications of PCNA. *Cell Res* 18, 162-173 (2008).
- Aguilera A, Klein HL. Genetic control of intrachromosomal recombination in *Saccharomyces cerevisiae*. I. Isolation and genetic characterization of hyper-recombination mutations. *Genetics* 119, 779-790 (1988).
- Araki H. Cyclin-dependent kinase-dependent initiation of chromosomal DNA replication. *Curr Opin Cell Biol* 22, 766-771 (2010).
- Araki H, Leem SH, Phongdara A, Sugino A. Dpb11, which interacts with DNA polymerase II(epsilon) in *Saccharomyces cerevisiae*, has a dual role in S-phase progression and at a cell cycle checkpoint. *Proc Natl Acad Sci U S A* 92, 11791-11795 (1995).
- Ashton TM, Hickson ID. Yeast as a model system to study RecQ helicase function. *DNA Repair (Amst)* 9, 303-134 (2010).
- Aylon Y, Liefshitz B, Kupiec M. The CDK regulates repair of double-strand breaks by homologous recombination during the cell cycle. *EMBO J* 23, 4868-4875 (2004).
- Bachrati CZ, Hickson ID. RecQ helicases: suppressors of tumorigenesis and premature aging. *Biochem J* 374, 577-606 (2003).
- Bailly V, Lamb J, Sung P, Prakash S, Prakash L. Specific complex formation between yeast RAD6 and RAD18 proteins: a potential mechanism for targeting RAD6 ubiquitin-conjugating activity to DNA damage sites. *Genes Dev* 8, 811-820 (1994).
- Ball HL, Ehrhardt MR, Mordes DA, Glick GG, Chazin WJ, Cortez D. Function of a conserved checkpoint recruitment domain in ATRIP proteins. *Mol Cell Biol* 27, 3367-3377 (2007).
- Ball HL, Myers JS, Cortez D. ATRIP binding to replication protein A-single-stranded DNA promotes ATR-ATRIP localization but is dispensable for Chk1 phosphorylation. *Mol Biol Cell* 16, 2372-2381 (2005).
- Baroni E, Viscardi V, Cartagena-Lirola H, Lucchini G, Longhese MP. The functions of budding yeast Sae2 in the DNA damage response require Mec1- and Tel1-dependent phosphorylation. *Mol Cell Biol* 24, 4151-4165 (2004).
- Barr FA, Silljé HH, Nigg EA. Polo-like kinases and the orchestration of cell division. *Nat Rev Mol Cell Biol* 5, 429-440 (2004).
- Belle JJ, Casey A, Courcelle CT, Courcelle J. Inactivation of the DnaB helicase leads to the collapse and degradation of the replication fork: a comparison to UV-induced arrest. *J Bacteriol* 189, 5452-5462 (2007).
- Bennett RJ, Noirot-Gros MF, Wang JC. Interaction between yeast sgs1 helicase and DNA topoisomerase III. *J Biol Chem* 275, 26898-26905 (2000).

REFERENCES

- Berndsen CE, Tsubota T, Lindner SE, Lee S, Holton JM, Kaufman PD, Keck JL, Denu JM. Molecular functions of the histone acetyltransferase chaperone complex Rtt109-Vps75. *Nat Struct Mol Biol* 15, 948-956 (2008).
- Bernstein KA, Shor E, Sunjevaric I, Fumasoni M, Burgess RC, Foiani M, Branzei D, Rothstein R. Sgs1 function in the repair of DNA replication intermediates is separable from its role in homologous recombinational repair. *EMBO J* 28, 915-925 (2009).
- Binz SK, Sheehan AM, Wold MS. Replication protein A phosphorylation and the cellular response to DNA damage. *DNA Repair (Amst)* 3, 1015-1024 (2004).
- Blanco MG, Matos J, West SC. Dual control of Yen1 nuclease activity and cellular localization by Cdk and Cdc14 prevents genome instability. *Mol Cell* 54, 94-106 (2014).
- Boddy MN, Lopez-Girona A, Shanahan P, Interthal H, Heyer WD, Russell P. Damage tolerance protein Mus81 associates with the FHA1 domain of checkpoint kinase Cds1. *Mol Cell Biol* 20, 8758-8766 (2000).
- Botuyan MV, Nominé Y, Yu X, Juranic N, Macura S, Chen J, Mer G. Structural basis of BACH1 phosphopeptide recognition by BRCA1 tandem BRCT domains. *Structure* 12, 1137-1146 (2004).
- Branzei D, Foiani M. Maintaining genome stability at the replication fork. *Nat Rev Mol Cell Biol* 11, 208-219 (2010).
- Branzei D, Vanoli F, Foiani M. SUMOylation regulates Rad18-mediated template switch. *Nature* 456, 915-920 (2008).
- Broomfield S, Chow BL, Xiao W. MMS2, encoding a ubiquitin-conjugating-enzyme-like protein, is a member of the yeast error-free postreplication repair pathway. *Proc Natl Acad Sci U S A* 95, 5678-5683 (1998).
- Broomfield S, Hryciw T, Xiao W. DNA postreplication repair and mutagenesis in *Saccharomyces cerevisiae*. *Mutat Res* 486, 167-184 (2001).
- Brush GS, Morrow DM, Hieter P, Kelly TJ. The ATM homologue MEC1 is required for phosphorylation of replication protein A in yeast. *Proc Natl Acad Sci U S A* 93, 15075-15080 (1996).
- Brusky J, Zhu Y, Xiao W. UBC13, a DNA-damage-inducible gene, is a member of the error-free postreplication repair pathway in *Saccharomyces cerevisiae*. *Curr Genet* 37, 168-174 (2000).
- Budd ME, Campbell JL. DNA polymerases required for repair of UV-induced damage in *Saccharomyces cerevisiae*. *Mol Cell Biol* 15, 2173-2179 (1995).
- Burgess RJ, Zhou H, Han J, Zhang Z. A role for Gcn5 in replication-coupled nucleosome assembly. *Mol Cell* 37, 469-480 (2010).
- Byun TS, Pacek M, Yee MC, Walter JC, Cimprich KA. Functional uncoupling of MCM helicase and DNA polymerase activities activates the ATR-dependent checkpoint. *Genes Dev* 19, 1040-1052 (2005).
- Cejka P, Plank JL, Bachrati CZ, Hickson ID, Kowalczykowski SC. Rmi1 stimulates decatenation of double Holliday junctions during dissolution by Sgs1-Top3. *Nat Struct Mol Biol* 17, 1377-1382 (2010).
- Cerritelli SM, Crouch RJ. Ribonuclease H: the enzymes in eukaryotes. *FEBS J* 276, 1494-1505 (2009).
- Chang M, Bellaoui M, Boone C, Brown GW. A genome-wide screen for methyl methanesulfonate-sensitive mutants reveals genes required for S phase progression in the presence of DNA damage. *Proc Natl Acad Sci U S A* 99, 16934-16939 (2002).
- Chen CC, Carson JJ, Feser J, Tamburini B, Zabaronick S, Linger J, Tyler JK. Acetylated lysine 56 on histone H3 drives chromatin assembly after repair and signals for the completion of repair. *Cell* 134, 231-243 (2008).
- Chen CF, Brill SJ. Binding and activation of DNA topoisomerase III by the Rmi1 subunit. *J Biol Chem* 282, 28971-28979 (2007).
- Chen XB, Melchionna R, Denis CM, Gaillard PH, Blasina A, Van de Weyer I, Boddy MN, Russell P, Vialard J, McGowan CH. Human Mus81-associated endonuclease cleaves Holliday junctions in vitro. *Mol Cell* 8, 1117-1127 (2001).

REFERENCES

- Chin JK, Bashkirov VI, Heyer WD, Romesberg FE. Esc4/Rtt107 and the control of recombination during replication. *DNA Repair (Amst)* 5, 618-628 (2006).
- Ciccina A, Constantinou A, West SC. Identification and characterization of the human mus81-eme1 endonuclease. *J Biol Chem* 278, 25172-25178 (2003).
- Ciccina A, McDonald N, West SC. Structural and functional relationships of the XPF/MUS81 family of proteins. *Annu Rev Biochem* 77, 259-287 (2008).
- Clerici M, Mantiero D, Lucchini G, Longhese MP. The *Saccharomyces cerevisiae* Sae2 protein promotes resection and bridging of double strand break ends. *J Biol Chem* 280, 38631-38638 (2005).
- Cobb JA, Schleker T, Rojas V, Bjergbaek L, Tercero JA, Gasser SM. Replisome instability, fork collapse, and gross chromosomal rearrangements arise synergistically from Mec1 kinase and RecQ helicase mutations. *Genes Dev* 19, 3055-3069 (2005).
- Conde F, Ontoso D, Acosta I, Gallego-Sánchez A, Bueno A, San-Segundo PA. Regulation of tolerance to DNA alkylating damage by Dot1 and Rad53 in *Saccharomyces cerevisiae*. *DNA Repair (Amst)* 9, 1038-1049 (2010).
- Constantinou A, Chen XB, McGowan CH, West SC. Holliday junction resolution in human cells: two junction endonucleases with distinct substrate specificities. *EMBO J* 21, 5577-5585 (2002).
- Cortez D, Glick G, Elledge SJ. Minichromosome maintenance proteins are direct targets of the ATM and ATR checkpoint kinases. *Proc Natl Acad Sci U S A* 101, 10078-10083 (2004).
- Cotta-Ramusino C, Fachinetti D, Lucca C, Doksan Y, Lopes M, Sogo J, Foiani M. Exo1 processes stalled replication forks and counteracts fork reversal in checkpoint-defective cells. *Mol Cell* 17, 153-159 (2005).
- Courcelle CT, Belle JJ, Courcelle J. Nucleotide excision repair or polymerase V-mediated lesion bypass can act to restore UV-arrested replication forks in *Escherichia coli*. *J Bacteriol* 187, 6953-6961 (2005).
- Clapperton JA, Manke IA, Lowery DM, Ho T, Haire LF, Yaffe MB, Smerdon SJ. Structure and mechanism of BRCA1 BRCT domain recognition of phosphorylated BACH1 with implications for cancer. *Nat Struct Mol Biol* 11, 512-518 (2004).
- Connolly B, Parsons CA, Benson FE, Dunderdale HJ, Sharples GJ, Lloyd RG, West SC. Resolution of Holliday junctions in vitro requires the *Escherichia coli* ruvC gene product. *Proc Natl Acad Sci U S A* 88, 6063-6067 (1991).
- Cox MM, Goodman MF, Kreuzer KN, Sherratt DJ, Sandler SJ, Mariani KJ. The importance of repairing stalled replication forks. *Nature* 404, 37-41 (2000).
- Dehé PM, Coulon S, Scaglione S, Shanahan P, Takedachi A, Wohlschlegel JA, Yates JR 3rd, Llorente B, Russell P, Gaillard PH. Regulation of Mus81-Eme1 Holliday junction resolvase in response to DNA damage. *Nat Struct Mol Biol* 20, 598-603 (2013).
- Delacroix S, Wagner JM, Kobayashi M, Yamamoto K, Karnitz LM. The Rad9-Hus1-Rad1 (9-1-1) clamp activates checkpoint signaling via TopBP1. *Genes Dev* 21, 1472-1477 (2007).
- DePamphilis ML, Wassarman PM. Replication of eukaryotic chromosomes: a close-up of the replication fork. *Annu Rev Biochem* 49, 627-666 (1980).
- Desany BA, Alcasabas AA, Bachant JB, Elledge SJ. Recovery from DNA replicational stress is the essential function of the S-phase checkpoint pathway. *Genes Dev* 12, 2956-2970 (1998).
- Di Caprio L, Cox BS. DNA synthesis in UV-irradiated yeast. *Mutat Res* 82, 69-85 (1981).
- Doe CL, Ahn JS, Dixon J, Whitby MC. Mus81-Eme1 and Rqh1 involvement in processing stalled and collapsed replication forks. *J Biol Chem* 277, 32753-32759 (2002).
- Donnianni RA, Ferrari M, Lazzaro F, Clerici M, Tamilselvan Nachimuthu B, Plevani P, Muzi-Falconi M, Pelliccioli A. Elevated levels of the polo kinase Cdc5 override the Mec1/ATR checkpoint in budding yeast by acting at different steps of the signaling pathway. *PLoS Genet* 6, e1000763 (2010).
- Downs JA, Lowndes NF, Jackson SP. A role for *Saccharomyces cerevisiae* histone H2A in DNA repair. *Nature* 408, 1001-1004 (2000).

REFERENCES

- Driscoll R, Hudson A, Jackson SP. Yeast Rtt109 promotes genome stability by acetylating histone H3 on lysine 56. *Science* 315, 649-652 (2007).
- D'Souza S, Walker GC. Novel role for the C terminus of *Saccharomyces cerevisiae* Rev1 in mediating protein-protein interactions. *Mol Cell Biol* 26, 8173-8182 (2006).
- Dunin-Horkawicz S, Feder M, Bujnicki JM. Phylogenomic analysis of the GIY-YIG nuclease superfamily. *BMC Genomics* 7, 98 (2006).
- Dutertre S, Ababou M, Onclercq R, Delic J, Chatton B, Jaulin C, Amor-Gu  ret M. Cell cycle regulation of the endogenous wild type Bloom's syndrome DNA helicase. *Oncogene* 19, 2731-2738 (2000).
- Ehmsen KT, Heyer WD. *Saccharomyces cerevisiae* Mus81-Mms4 is a catalytic, DNA structure-selective endonuclease. *Nucleic Acids Res* 36, 2182-2195 (2008).
- Ehmsen KT, Heyer WD. A junction branch point adjacent to a DNA backbone nick directs substrate cleavage by *Saccharomyces cerevisiae* Mus81-Mms4. *Nucleic Acids Res* 37, 2026-2036 (2009).
- Elia AE, Cantley LC, Yaffe MB. Proteomic screen finds pSer/pThr-binding domain localizing Plk1 to mitotic substrates. *Science* 299, 1228-1231 (2003).
- Enserink JM, Kolodner RD. An overview of Cdk1-controlled targets and processes. *Cell Div* 13, 5-11 (2010).
- Fekairi S, Scaglione S, Chahwan C, Taylor ER, Tissier A, Coulon S, Dong MQ, Ruse C, Yates JR 3rd, Russell P, Fuchs RP, McGowan CH, Gaillard PH. Human SLX4 is a Holliday junction resolvase subunit that binds multiple DNA repair/recombination endonucleases. *Cell* 138, 78-89 (2009).
- Fillingham J, Recht J, Silva AC, Suter B, Emili A, Stagljar I, Krogan NJ, Allis CD, Keogh MC, Greenblatt JF. Chaperone control of the activity and specificity of the histone H3 acetyltransferase Rtt109. *Mol Cell Biol* 28, 4342-4353 (2008).
- Flott S, Alabert C, Toh GW, Toth R, Sugawara N, Campbell DG, Haber JE, Pasero P, Rouse J. Phosphorylation of Slx4 by Mec1 and Tel1 regulates the single-strand annealing mode of DNA repair in budding yeast. *Mol Cell Biol* 27, 6433-6445 (2007).
- Flott S, Rouse J. Slx4 becomes phosphorylated after DNA damage in a Mec1/Tel1-dependent manner and is required for repair of DNA alkylation damage. *Biochem J* 391, 325-333 (2005).
- Forma E, Brzeziańska E, Krze  lak A, Chwatko G, J  zwiak P, Szymczyk A, Smolarz B, Romanowicz-Makowska H, R   ański W, Bry  s M. Association between the c.*229C>T polymorphism of the topoisomerase II   binding protein 1 (TopBP1) gene and breast cancer. *Mol Biol Rep* 40, 3493-3502 (2013).
- Forma E, W  jcik-Krowiranda K, J  zwiak P, Szymczyk A, Bie  kiewicz A, Bry  s M, Krze  lak A. Topoisomerase II   binding protein 1 c.*229C>T (rs115160714) gene polymorphism and endometrial cancer risk. *Pathol Oncol Res* 20, 597-602 (2014).
- Frei C, Gasser SM. The yeast Sgs1p helicase acts upstream of Rad53p in the DNA replication checkpoint and colocalizes with Rad53p in S-phase-specific foci. *Genes Dev* 14, 81-96 (2000).
- Fricke WM, Bastin-Shanower SA, Brill SJ. Substrate specificity of the *Saccharomyces cerevisiae* Mus81-Mms4 endonuclease. *DNA Repair (Amst)* 4, 243-251 (2005).
- Fricke WM, Brill SJ. Slx1-Slx4 is a second structure-specific endonuclease functionally redundant with Sgs1-Top3. *Genes Dev* 17, 1768-1778 (2003).
- Fukunaga K, Kwon Y, Sung P, Sugimoto K. Activation of protein kinase Tel1 through recognition of protein-bound DNA ends. *Mol Cell Biol* 31, 1959-1971 (2011).
- Gallo-Fern  ndez M, Saugar I, Ortiz-Baz  n M  , V  zquez MV, Tercero JA. Cell cycle-dependent regulation of the nuclease activity of Mus81-Eme1/Mms4. *Nucleic Acids Res* 40, 8325-8335 (2012).
- Garcia V, Furuya K, Carr AM. Identification and functional analysis of TopBP1 and its homologs. *DNA Repair (Amst)* 4, 1227-1239 (2005).

REFERENCES

- Germann SM, Schramke V, Pedersen RT, Gallina I, Eckert-Boulet N, Oestergaard VH, Lisby M. TopBP1/Dpb11 binds DNA anaphase bridges to prevent genome instability. *J Cell Biol* 204, 45-59 (2014).
- Gietz RD, Sugino A. New yeast-Escherichia coli shuttle vectors constructed with in vitro mutagenized yeast genes lacking six-base pair restriction sites. *Gene* 74, 527-534 (1988).
- Gilbert CS, Green CM, Lowndes NF. Budding yeast Rad9 is an ATP-dependent Rad53 activating machine. *Mol Cell* 8, 129-136 (2001).
- Glover DM, Hagan IM, Tavares AA. Polo-like kinases: a team that plays throughout mitosis. *Genes Dev* 12, 3777-3787 (1998).
- Golan A, Yudkovsky Y, Hershko A. The cyclin-ubiquitin ligase activity of cyclosome/APC is jointly activated by protein kinases Cdk1-cyclin B and Plk. *J Biol Chem* 277, 15552-15557 (2002).
- Goodman MF, Woodgate R. Translesion DNA polymerases. *Cold Spring Harb Perspect Biol* 5, a010363 (2013).
- Gritenaite D, Princz LN, Szakal B, Bantele SC, Wendeler L, Schilbach S, Habermann BH, Matos J, Lisby M, Branzei D, Pfander B. A cell cycle-regulated Slx4-Dpb11 complex promotes the resolution of DNA repair intermediates linked to stalled replication. *Genes Dev* 28, 1604-1619 (2014).
- Guzder SN, Habraken Y, Sung P, Prakash L, Prakash S. Reconstitution of yeast nucleotide excision repair with purified Rad proteins, replication protein A, and transcription factor TFIIH. *J Biol Chem* 270, 12973-12976 (1995).
- Han J, Li Q, McCullough L, Kettelkamp C, Formosa T, Zhang Z. Ubiquitylation of FACT by the cullin-E3 ligase Rtt101 connects FACT to DNA replication. *Genes Dev* 24, 1485-1490 (2010).
- Han J, Zhang H, Zhang H, Wang Z, Zhou H, Zhang Z. A Cul4 E3 ubiquitin ligase regulates histone hand-off during nucleosome assembly. *Cell* 155, 817-829 (2013).
- Han J, Zhou H, Horazdovsky B, Zhang K, Xu RM, Zhang Z. Rtt109 acetylates histone H3 lysine 56 and functions in DNA replication. *Science* 315, 653-655 (2007).
- Hanway D, Chin JK, Xia G, Oshiro G, Winzeler EA, Romesberg FE. Previously uncharacterized genes in the UV- and MMS-induced DNA damage response in yeast. *Proc Natl Acad Sci U S A* 99, 10605-10610 (2002).
- Harfe BD, Jinks-Robertson S. DNA mismatch repair and genetic instability. *Annu Rev Genet* 34, 359-399 (2000).
- Heller RC, Marians KJ. Replisome assembly and the direct restart of stalled replication forks. *Nat Rev Mol Cell Biol* 7, 932-943 (2006).
- Higgins NP, Kato K, Strauss B. A model for replication repair in mammalian cells. *J Mol Biol* 101, 417-425 (1976).
- Hoege C, Pfander B, Moldovan GL, Pyrowolakis G, Jentsch S. RAD6-dependent DNA repair is linked to modification of PCNA by ubiquitin and SUMO. *Nature* 419, 135-141 (2002).
- Hoeijmakers JH. Genome maintenance mechanisms for preventing cancer. *Nature* 411, 366-374 (2001).
- Hofmann RM, Pickart CM. Noncanonical MMS2-encoded ubiquitin-conjugating enzyme functions in assembly of novel polyubiquitin chains for DNA repair. *Cell* 96, 645-653 (1999).
- Holt LJ, Tuch BB, Villén J, Johnson AD, Gygi SP, Morgan DO. Global analysis of Cdk1 substrate phosphorylation sites provides insights into evolution. *Science* 325, 1682-1686 (2009).
- Hsieh P, Yamane K. DNA mismatch repair: molecular mechanism, cancer, and ageing. *Mech Ageing Dev* 129, 391-407 (2008).
- Hu F, Wang Y, Liu D, Li Y, Qin J, Elledge SJ. Regulation of the Bub2/Bfa1 GAP complex by Cdc5 and cell cycle checkpoints. *Cell* 107, 655-665 (2001).
- Huertas P, Cortés-Ledesma F, Sartori AA, Aguilera A, Jackson SP. CDK targets Sae2 to control DNA-end resection and homologous recombination. *Nature* 455, 689-692 (2008).
- Ip SC, Rass U, Blanco MG, Flynn HR, Skehel JM, West SC. Identification of Holliday junction resolvases from humans and yeast. *Nature* 456, 357-361 (2008).

REFERENCES

- Ira G, Malkova A, Liberi G, Foiani M, Haber JE. Srs2 and Sgs1-Top3 suppress crossovers during double-strand break repair in yeast. *Cell* 115, 401-411 (2003).
- Ira G, Pelliccioli A, Balijja A, Wang X, Fiorani S, Carotenuto W, Liberi G, Bressan D, Wan L, Hollingsworth NM, Haber JE, Foiani M. DNA end resection, homologous recombination and DNA damage checkpoint activation require CDK1. *Nature* 431, 1011-1017 (2004).
- Ishimi Y, Komamura-Kohno Y, Kwon HJ, Yamada K, Nakanishi M. Identification of MCM4 as a target of the DNA replication block checkpoint system. *J Biol Chem* 278, 24644-24650 (2003).
- Iwasaki H, Takahagi M, Shiba T, Nakata A, Shinagawa H. Escherichia coli RuvC protein is an endonuclease that resolves the Holliday structure. *EMBO J* 10, 4381-4389 (1991).
- James P, Halladay J, Craig EA. Genomic libraries and a host strain designed for highly efficient two-hybrid selection in yeast. *Genetics* 144, 1425-1436 (1996).
- Janke C, Magiera MM, Rathfelder N, Taxis C, Reber S, Maekawa H, Moreno-Borchart A, Doenges G, Schwob E, Schiebel E, Knop M. A versatile toolbox for PCR-based tagging of yeast genes: new fluorescent proteins, more markers and promoter substitution cassettes. *Yeast* 21, 947-962 (2004).
- Jasin M, Rothstein R. Repair of strand breaks by homologous recombination. *Cold Spring Harb Perspect Biol* 5, a012740 (2013).
- Jazayeri A, Falck J, Lukas C, Bartek J, Smith GC, Lukas J, Jackson SP. ATM- and cell cycle-dependent regulation of ATR in response to DNA double-strand breaks. *Nat Cell Biol* 8, 37-45 (2006).
- Johnson RD, Jasin M. Double-strand-break-induced homologous recombination in mammalian cells. *Biochem Soc Trans* 29, 196-201 (2001).
- Kadyk LC, Hartwell LH. Sister chromatids are preferred over homologs as substrates for recombinational repair in *Saccharomyces cerevisiae*. *Genetics* 132, 387-402 (1992).
- Kai M, Boddy MN, Russell P, Wang TS. Replication checkpoint kinase Cds1 regulates Mus81 to preserve genome integrity during replication stress. *Genes Dev* 19, 919-932 (2005).
- Kaliraman V, Mullen JR, Fricke WM, Bastin-Shanower SA, Brill SJ. Functional overlap between Sgs1-Top3 and the Mms4-Mus81 endonuclease. *Genes Dev* 15, 2730-2740 (2001).
- Kannouche PL, Wing J, Lehmann AR. Interaction of human DNA polymerase η with monoubiquitinated PCNA: a possible mechanism for the polymerase switch in response to DNA damage. *Mol Cell* 14, 491-500 (2004).
- Karras GI, Jentsch S. The RAD6 DNA damage tolerance pathway operates uncoupled from the replication fork and is functional beyond S phase. *Cell* 141, 255-267 (2010).
- Katou Y, Kanoh Y, Bando M, Noguchi H, Tanaka H, Ashikari T, Sugimoto K, Shirahige K. S-phase checkpoint proteins Tof1 and Mrc1 form a stable replication-pausing complex. *Nature* 424, 1078-1083 (2003).
- Keogh MC, Kim JA, Downey M, Fillingham J, Chowdhury D, Harrison JC, Onishi M, Datta N, Galicia S, Emili A, Lieberman J, Shen X, Buratowski S, Haber JE, Durocher D, Greenblatt JF, Krogan NJ. A phosphatase complex that dephosphorylates gammaH2AX regulates DNA damage checkpoint recovery. *Nature* 439, 497-501 (2006).
- Khidhir MA, Casaregola S, Holland IB. Mechanism of transient inhibition of DNA synthesis in ultraviolet-irradiated *E. coli*: inhibition is independent of recA whilst recovery requires RecA protein itself and an additional, inducible SOS function. *Mol Gen Genet* 199, 133-140 (1985).
- Kim Y, Spitz GS, Veturi U, Lach FP, Auerbach AD, Smogorzewska A. Regulation of multiple DNA repair pathways by the Fanconi anemia protein SLX4. *Blood* 121, 54-63 (2013).
- Kitao S, Ohsugi I, Ichikawa K, Goto M, Furuichi Y, Shimamoto A. Cloning of two new human helicase genes of the RecQ family: biological significance of multiple species in higher eukaryotes. *Genomics* 54, 443-452 (1998).
- Klein HL. Mutations in recombinational repair and in checkpoint control genes suppress the lethal combination of srs2Delta with other DNA repair genes in *Saccharomyces cerevisiae*. *Genetics* 157, 557-565 (2001).

REFERENCES

- Knop M, Siegers K, Pereira G, Zachariae W, Winsor B, Nasmyth K, Schiebel E. Epitope tagging of yeast genes using a PCR-based strategy: more tags and improved practical routines. *Yeast* 15, 963-972 (1999).
- Kogoma T. Recombination by replication. *Cell* 85, 625-627 (1996).
- Kondo T, Matsumoto K, Sugimoto K. Role of a complex containing Rad17, Mec3, and Ddc1 in the yeast DNA damage checkpoint pathway. *Mol Cell Biol* 19, 1136-1143 (1999).
- Kosugi S, Hasebe M, Tomita M, Yanagawa H. Systematic identification of cell cycle-dependent yeast nucleocytoplasmic shuttling proteins by prediction of composite motifs. *Proc Natl Acad Sci U S A* 106, 10171-10176 (2009).
- Kumagai A, Lee J, Yoo HY, Dunphy WG. TopBP1 activates the ATR-ATRIP complex. *Cell* 124, 943-955 (2006).
- Kunkel TA, Erie DA. DNA mismatch repair. *Annu Rev Biochem* 74, 681-710 (2005).
- Kuzminov A. Collapse and repair of replication forks in *Escherichia coli*. *Mol Microbiol* 16, 373-384 (1995).
- Lambert S, Watson A, Sheedy DM, Martin B, Carr AM. Gross chromosomal rearrangements and elevated recombination at an inducible site-specific replication fork barrier. *Cell* 121, 689-702 (2005).
- Lawrence C. The RAD6 DNA repair pathway in *Saccharomyces cerevisiae*: what does it do, and how does it do it? *Bioessays* 16, 253-258 (1994).
- Lee J, Kumagai A, Dunphy WG. The Rad9-Hus1-Rad1 checkpoint clamp regulates interaction of TopBP1 with ATR. *J Biol Chem* 282, 28036-28044 (2007).
- Lee JM, Greenleaf AL. CTD kinase large subunit is encoded by CTK1, a gene required for normal growth of *Saccharomyces cerevisiae*. *Gene Expr* 1, 149-167 (1991).
- Lehmann AR, Fuchs RP. Gaps and forks in DNA replication: Rediscovering old models. *DNA Repair (Amst)* 5, 1495-1498 (2006).
- Lemontt JF. Mutants of yeast defective in mutation induced by ultraviolet light. *Genetics* 68, 21-33 (1971).
- Lemontt JF. Pathways of ultraviolet mutability in *Saccharomyces cerevisiae*. II. The effect of rev genes on recombination. *Mutat Res* 13, 319-326 (1971).
- Leroy C, Lee SE, Vaze MB, Ochsenbein F, Guerois R, Haber JE, Marsolier-Kergoat MC. PP2C phosphatases Ptc2 and Ptc3 are required for DNA checkpoint inactivation after a double-strand break. *Mol Cell* 11, 827-835 (2003).
- Leung GP, Lee L, Schmidt TI, Shirahige K, Kobor MS. Rtt107 is required for recruitment of the SMC5/6 complex to DNA double strand breaks. *J Biol Chem* 286, 26250-26257 (2011).
- Li Q, Zhou H, Wurtele H, Davies B, Horazdovsky B, Verreault A, Zhang Z. Acetylation of histone H3 lysine 56 regulates replication-coupled nucleosome assembly. *Cell* 134, 244-255 (2008).
- Li X, Liu K, Li F, Wang J, Huang H, Wu J, Shi Y. Structure of C-terminal tandem BRCT repeats of Rtt107 protein reveals critical role in interaction with phosphorylated histone H2A during DNA damage repair. *J Biol Chem* 287, 9137-9146 (2012).
- Liao SM, Zhang J, Jeffery DA, Koleske AJ, Thompson CM, Chao DM, Viljoen M, van Vuuren HJ, Young RA. A kinase-cyclin pair in the RNA polymerase II holoenzyme. *Nature* 374, 193-196 (1995).
- Liberi G, Chiolo I, Pelliccioli A, Lopes M, Plevani P, Muzi-Falconi M, Foiani M. Srs2 DNA helicase is involved in checkpoint response and its regulation requires a functional Mec1-dependent pathway and Cdk1 activity. *EMBO J* 19, 5027-5038 (2000).
- Liberi G, Maffioletti G, Lucca C, Chiolo I, Baryshnikova A, Cotta-Ramusino C, Lopes M, Pelliccioli A, Haber JE, Foiani M. Rad51-dependent DNA structures accumulate at damaged replication forks in *sgs1* mutants defective in the yeast ortholog of BLM RecQ helicase. *Genes Dev* 19, 339-350 (2005).
- Lieber MR. The mechanism of double-strand DNA break repair by the nonhomologous DNA end-joining pathway. *Annu Rev Biochem* 79, 181-211 (2010).

REFERENCES

- Lisby M, Barlow JH, Burgess RC, Rothstein R. Choreography of the DNA damage response: spatiotemporal relationships among checkpoint and repair proteins. *Cell* 118, 699-713 (2004).
- Liu J, Kipreos ET. Evolution of cyclin-dependent kinases (CDKs) and CDK-activating kinases (CAKs): differential conservation of CAKs in yeast and metazoa. *Mol Biol Evol* 17, 1061-1074 (2000).
- Liu K, Paik JC, Wang B, Lin FT, Lin WC. Regulation of TopBP1 oligomerization by Akt/PKB for cell survival. *EMBO J* 25, 4795-4807 (2006).
- Longhese MP, Foiani M, Muzi-Falconi M, Lucchini G, Plevani P. DNA damage checkpoint in budding yeast. *EMBO J* 17, 5525-5528 (1998).
- Lopes M, Cotta-Ramusino C, Pelliccioli A, Liberi G, Plevani P, Muzi-Falconi M, Newlon CS, Foiani M. The DNA replication checkpoint response stabilizes stalled replication forks. *Nature* 412, 557-561 (2001).
- Lopes M, Foiani M, Sogo JM. Multiple mechanisms control chromosome integrity after replication fork uncoupling and restart at irreparable UV lesions. *Mol Cell* 21, 15-27 (2006).
- Lopez-Mosqueda J, Maas NL, Jonsson ZO, Defazio-Eli LG, Wohlschlegel J, Toczyski DP. Damage-induced phosphorylation of Sld3 is important to block late origin firing. *Nature* 467, 479-483 (2010).
- Lörincz AT, Reed SI. Primary structure homology between the product of yeast cell division control gene CDC28 and vertebrate oncogenes. *Nature* 307, 183-185 (1984).
- Lowery DM, Lim D, Yaffe MB. Structure and function of Polo-like kinases. *Oncogene* 24, 248-259 (2005).
- Luke B, Versini G, Jaquenoud M, Zaidi IW, Kurz T, Pintard L, Pasero P, Peter M. The cullin Rtt101p promotes replication fork progression through damaged DNA and natural pause sites. *Curr Biol* 16, 7867-92 (2006).
- Lyndaker AM, Goldfarb T, Alani E. Mutants defective in Rad1-Rad10-Slx4 exhibit a unique pattern of viability during mating-type switching in *Saccharomyces cerevisiae*. *Genetics* 179, 1807-1821 (2008).
- Manke IA, Lowery DM, Nguyen A, Yaffe MB. BRCT repeats as phosphopeptide-binding modules involved in protein targeting. *Science* 302, 636-639 (2003).
- Mankouri HW, Hickson ID. Top3 processes recombination intermediates and modulates checkpoint activity after DNA damage. *Mol Biol Cell* 17, 4473-4483 (2006).
- Mankouri HW, Ngo HP, Hickson ID. Shu proteins promote the formation of homologous recombination intermediates that are processed by Sgs1-Rmi1-Top3. *Mol Biol Cell* 18, 4062-4073 (2007).
- Mankouri HW, Hickson ID. The RecQ helicase-topoisomerase III-Rmi1 complex: a DNA structure-specific 'dissolvasome'? *Trends Biochem Sci* 32, 538-546 (2007).
- Masumoto H, Hawke D, Kobayashi R, Verreault A. A role for cell-cycle-regulated histone H3 lysine 56 acetylation in the DNA damage response. *Nature* 436, 294-298 (2005).
- Matos J, Blanco MG, Maslen S, Skehel JM, West SC. Regulatory control of the resolution of DNA recombination intermediates during meiosis and mitosis. *Cell* 147, 158-172 (2011).
- Matos J, Blanco MG, West SC. Cell-cycle kinases coordinate the resolution of recombination intermediates with chromosome segregation. *Cell Rep* 4, 76-86 (2013).
- Matos J, West SC. Holliday junction resolution: regulation in space and time. *DNA Repair (Amst)* 19, 176-181 (2014).
- McInerney P, O'Donnell M. Functional uncoupling of twin polymerases: mechanism of polymerase dissociation from a lagging-strand block. *J Biol Chem* 279, 21543-21551 (2004).
- McVey M. Strategies for DNA interstrand crosslink repair: insights from worms, flies, frogs, and slime molds. *Environ Mol Mutagen* 51, 646-658 (2010).
- Meister P, Taddei A, Vernis L, Poidevin M, Gasser SM, Baldacci G. Temporal separation of replication and recombination requires the intra-S checkpoint. *J Cell Biol* 168, 537-544 (2005).

REFERENCES

- Mendenhall MD, Hodge AE. Regulation of Cdc28 cyclin-dependent protein kinase activity during the cell cycle of the yeast *Saccharomyces cerevisiae*. *Microbiol Mol Biol Rev* 62, 1191-1243 (1998).
- Michel JJ, McCarville JF, Xiong Y. A role for *Saccharomyces cerevisiae* Cul8 ubiquitin ligase in proper anaphase progression. *J Biol Chem* 278, 22828-22837 (2003).
- Minca EC, Kowalski D. Multiple Rad5 activities mediate sister chromatid recombination to bypass DNA damage at stalled replication forks. *Mol Cell* 38, 649-661 (2010).
- Moldovan GL, Pfander B, Jentsch S. PCNA, the maestro of the replication fork. *Cell* 129, 665-679 (2007).
- Mordes DA, Nam EA, Cortez D. Dpb11 activates the Mec1-Ddc2 complex. *Proc Natl Acad Sci U S A* 105, 18730-18734 (2008).
- Morin I, Ngo HP, Greenall A, Zubko MK, Morrice N, Lydall D. Checkpoint-dependent phosphorylation of Exo1 modulates the DNA damage response. *EMBO J* 27, 2400-2410 (2008).
- Morrison AJ, Kim JA, Person MD, Highland J, Xiao J, Wehr TS, Hensley S, Bao Y, Shen J, Collins SR, Weissman JS, Delrow J, Krogan NJ, Haber JE, Shen X. Mec1/Tel1 phosphorylation of the INO80 chromatin remodeling complex influences DNA damage checkpoint responses. *Cell* 130, 499-511 (2007).
- Mullen JR, Kaliraman V, Ibrahim SS, Brill SJ. Requirement for three novel protein complexes in the absence of the Sgs1 DNA helicase in *Saccharomyces cerevisiae*. *Genetics* 157, 103-118 (2001).
- Mullen JR, Nallaseth FS, Lan YQ, Slagle CE, Brill SJ. Yeast Rmi1/Nce4 controls genome stability as a subunit of the Sgs1-Top3 complex. *Mol Cell Biol* 25, 4476-4487 (2005).
- Muñoz IM, Hain K, Déclais AC, Gardiner M, Toh GW, Sanchez-Pulido L, Heuckmann JM, Toth R, Macartney T, Eppink B, Kanaar R, Ponting CP, Lilley DM, Rouse J. Coordination of structure-specific nucleases by human SLX4/BTBD12 is required for DNA repair. *Mol Cell* 35, 116-127 (2009).
- Navadgi-Patil VM, Burgers PM. Yeast DNA replication protein Dpb11 activates the Mec1/ATR checkpoint kinase. *J Biol Chem* 283, 35853-35859 (2008).
- Nedelcheva MN, Roguev A, Dolapchiev LB, Shevchenko A, Taskov HB, Shevchenko A, Stewart AF, Stoyanov SS. Uncoupling of unwinding from DNA synthesis implies regulation of MCM helicase by Tof1/Mrc1/Csm3 checkpoint complex. *J Mol Biol* 347, 509-521 (2005).
- Nelson SW, Benkovic SJ. Response of the bacteriophage T4 replisome to noncoding lesions and regression of a stalled replication fork. *J Mol Biol* 401, 743-756 (2010).
- Nigg EA. Cellular substrates of p34(cdc2) and its companion cyclin-dependent kinases. *Trends Cell Biol* 3, 296-301 (1993).
- Ogi T, Limsirichaikul S, Overmeer RM, Volker M, Takenaka K, Cloney R, Nakazawa Y, Niimi A, Miki Y, Jaspers NG, Mullenders LH, Yamashita S, Foustieri MI, Lehmann AR. Three DNA polymerases, recruited by different mechanisms, carry out NER repair synthesis in human cells. *Mol Cell* 37, 714-727 (2010).
- Ohouo PY, Bastos de Oliveira FM, Almeida BS, Smolka MB. DNA damage signaling recruits the Rtt107-Slx4 scaffolds via Dpb11 to mediate replication stress response. *Mol Cell* 39, 300-306 (2010).
- Ohouo PY, Bastos de Oliveira FM, Liu Y, Ma CJ, Smolka MB. DNA-repair scaffolds dampen checkpoint signalling by counteracting the adaptor Rad9. *Nature* 493, 120-124 (2013).
- O'Neill BM, Szyjka SJ, Lis ET, Bailey AO, Yates JR 3rd, Aparicio OM, Romesberg FE. Pph3-Psy2 is a phosphatase complex required for Rad53 dephosphorylation and replication fork restart during recovery from DNA damage. *Proc Natl Acad Sci U S A* 104, 9290-9295 (2007).
- Osman F, Dixon J, Doe CL, Whitby MC. Generating crossovers by resolution of nicked Holliday junctions: a role for Mus81-Eme1 in meiosis. *Mol Cell* 12, 761-774 (2003).
- Osman F, Whitby MC. Exploring the roles of Mus81-Eme1/Mms4 at perturbed replication forks. *DNA Repair (Amst)* 6, 1004-1017 (2007).

REFERENCES

- Ozdemir A, Spicuglia S, Lasonder E, Vermeulen M, Campsteijn C, Stunnenberg HG, Logie C. Characterization of lysine 56 of histone H3 as an acetylation site in *Saccharomyces cerevisiae*. *J Biol Chem* 280, 25949-25952 (2005).
- Papamichos-Chronakis M, Peterson CL. The Ino80 chromatin-remodeling enzyme regulates replisome function and stability. *Nat Struct Mol Biol* 15, 338-345 (2008).
- Paulovich AG, Hartwell LH. A checkpoint regulates the rate of progression through S phase in *S. cerevisiae* in response to DNA damage. *Cell* 82, 841-847 (1995).
- Pfander B, Diffley JF. Dpb11 coordinates Mec1 kinase activation with cell cycle-regulated Rad9 recruitment. *EMBO J* 30, 4897-4907 (2011).
- Pfander B, Moldovan GL, Sacher M, Hoege C, Jentsch S. SUMO-modified PCNA recruits Srs2 to prevent recombination during S phase. *Nature* 436, 428-433 (2005).
- Prakash L. Characterization of postreplication repair in *Saccharomyces cerevisiae* and effects of rad6, rad18, rev3 and rad52 mutations. *Mol Gen Genet* 184, 471-478 (1981).
- Puddu F, Granata M, Di Nola L, Balestrini A, Piergiovanni G, Lazzaro F, Giannattasio M, Plevani P, Muzi-Falconi M. Phosphorylation of the budding yeast 9-1-1 complex is required for Dpb11 function in the full activation of the UV-induced DNA damage checkpoint. *Mol Cell Biol* 28, 4782-4793 (2008).
- Puranam KL, Blackshear PJ. Cloning and characterization of RECQL, a potential human homologue of the *Escherichia coli* DNA helicase RecQ. *J Biol Chem* 269, 29838-29845 (1994).
- Putnam CD, Jaehnig EJ, Kolodner RD. Perspectives on the DNA damage and replication checkpoint responses in *Saccharomyces cerevisiae*. *DNA Repair (Amst)* 8, 974-982 (2009).
- Rass U, Compton SA, Matos J, Singleton MR, Ip SC, Blanco MG, Griffith JD, West SC. Mechanism of Holliday junction resolution by the human GEN1 protein. *Genes Dev* 24, 1559-1569 (2010).
- Rass U. Resolving branched DNA intermediates with structure-specific nucleases during replication in eukaryotes. *Chromosoma* 122, 499-515 (2013).
- Recht J, Tsubota T, Tanny JC, Diaz RL, Berger JM, Zhang X, Garcia BA, Shabanowitz J, Burlingame AL, Hunt DF, Kaufman PD, Allis CD. Histone chaperone Asf1 is required for histone H3 lysine 56 acetylation, a modification associated with S phase in mitosis and meiosis. *Proc Natl Acad Sci U S A* 103, 6988-6993 (2006).
- Robert T, Dervins D, Fabre F, Gangloff S. Mrc1 and Srs2 are major actors in the regulation of spontaneous crossover. *EMBO J* 25, 2837-2846 (2006).
- Roberts TM, Kobor MS, Bastin-Shanower SA, Ii M, Horte SA, Gin JW, Emili A, Rine J, Brill SJ, Brown GW. Slx4 regulates DNA damage checkpoint-dependent phosphorylation of the BRCT domain protein Rtt107/Esc4. *Mol Biol Cell* 17, 539-548 (2006).
- Roberts TM, Zaidi IW, Vaisica JA, Peter M, Brown GW. Regulation of rtt107 recruitment to stalled DNA replication forks by the cullin rtt101 and the rtt109 acetyltransferase. *Mol Biol Cell* 19, 171-180 (2008).
- Robu ME, Inman RB, Cox MM. RecA protein promotes the regression of stalled replication forks in vitro. *Proc Natl Acad Sci U S A* 98, 8211-8218 (2001).
- Rodriguez M, Yu X, Chen J, Songyang Z. Phosphopeptide binding specificities of BRCA1 COOH-terminal (BRCT) domains. *J Biol Chem* 278, 52914-52918 (2003).
- Rosche WA, Foster PL. Determining mutation rates in bacterial populations. *Methods*, 20, 4-17 (2000).
- Rouse J. Esc4p, a new target of Mec1p (ATR), promotes resumption of DNA synthesis after DNA damage. *EMBO J* 23, 1188-1197 (2004).
- Rouse J. Control of genome stability by SLX protein complexes. *Biochem Soc Trans* 37, 495-510 (2009).
- Rouse J, Jackson SP. Lcd1p recruits Mec1p to DNA lesions in vitro and in vivo. *Mol Cell* 9, 857-869 (2002).
- Rudolph CJ, Upton AL, Lloyd RG. Replication fork stalling and cell cycle arrest in UV-irradiated *Escherichia coli*. *Genes Dev* 21, 668-681 (2007).

REFERENCES

- Sambrook J, Russell DW. Molecular cloning : a laboratory manual, 3rd edn (Cold Spring Harbor, N.Y., Cold Spring Harbor Laboratory Press) (2001).
- Sanchez Y, Bachant J, Wang H, Hu F, Liu D, Tetzlaff M, Elledge SJ. Control of the DNA damage checkpoint by chk1 and rad53 protein kinases through distinct mechanisms. *Science* 286, 1166-1171 (1999).
- Santocanale C, Diffley JF. A Mec1- and Rad53-dependent checkpoint controls late-firing origins of DNA replication. *Nature* 395, 615-618 (1998).
- Santocanale C, Sharma K, Diffley JF. Activation of dormant origins of DNA replication in budding yeast. *Genes Dev* 13, 2360-2364 (1999).
- Saponaro M, Callahan D, Zheng X, Krejci L, Haber JE, Klein HL, Liberi G. Cdk1 targets Srs2 to complete synthesis-dependent strand annealing and to promote recombinational repair. *PLoS Genet* 6, e1000858 (2010).
- Sarbajna S, Davies D, West SC. Roles of SLX1-SLX4, MUS81-EME1, and GEN1 in avoiding genome instability and mitotic catastrophe. *Genes Dev* 28, 1124-1136 (2014).
- Sassanfar M, Dosanjh MK, Essigmann JM, Samson L. Relative efficiencies of the bacterial, yeast, and human DNA methyltransferases for the repair of O6-methylguanine and O4-methylthymine. Suggestive evidence for O4-methylthymine repair by eukaryotic methyltransferases. *J Biol Chem* 266, 2767-2771 (1991).
- Sassanfar M, Samson L. Identification and preliminary characterization of an O6-methylguanine DNA repair methyltransferase in the yeast *Saccharomyces cerevisiae*. *J Biol Chem* 265, 20-25 (1990).
- Schärer OD. Nucleotide excision repair in eukaryotes. *Cold Spring Harb Perspect Biol* 5, a012609 (2013).
- Schneider J, Bajwa P, Johnson FC, Bhaumik SR, Shilatifard A. Rtt109 is required for proper H3K56 acetylation: a chromatin mark associated with the elongating RNA polymerase II. *J Biol Chem* 281, 37270-37274 (2006).
- Scholes DT, Banerjee M, Bowen B, Curcio MJ. Multiple regulators of Ty1 transposition in *Saccharomyces cerevisiae* have conserved roles in genome maintenance. *Genetics* 159, 1449-1465 (2001).
- Schwartz EK, Wright WD, Ehmsen KT, Evans JE, Stahlberg H, Heyer WD. Mus81-Mms4 functions as a single heterodimer to cleave nicked intermediates in recombinational DNA repair. *Mol Cell Biol* 32, 3065-3080 (2012).
- Schwartz MF, Duong JK, Sun Z, Morrow JS, Pradhan D, Stern DF. Rad9 phosphorylation sites couple Rad53 to the *Saccharomyces cerevisiae* DNA damage checkpoint. *Mol Cell* 9, 1055-1065 (2002).
- Schwob E, Böhm T, Mendenhall MD, Nasmyth K. The B-type cyclin kinase inhibitor p40SIC1 controls the G1 to S transition in *S. cerevisiae*. *Cell* 79, 233-244 (1994).
- Sebastian J, Kraus B, Sancar GB. Expression of the yeast PHR1 gene is induced by DNA-damaging agents. *Mol Cell Biol* 10, 4630-4637 (1990).
- Segurado M, Tercero JA. The S-phase checkpoint: targeting the replication fork. *Biol Cell* 101, 617-627 (2009).
- Seki M, Yanagisawa J, Kohda T, Sonoyama T, Ui M, Enomoto T. Purification of two DNA-dependent adenosinetriphosphatases having DNA helicase activity from HeLa cells and comparison of the properties of the two enzymes. *J Biochem* 115, 523-531 (1994).
- Shi Y, Dodson GE, Mukhopadhyay PS, Shanware NP, Trinh AT, Tibbetts RS. Identification of carboxyl-terminal MCM3 phosphorylation sites using polyreactive phosphospecific antibodies. *J Biol Chem* 282, 9236-9243 (2007).
- Shimada K, Oma Y, Schleker T, Kugou K, Ohta K, Harata M, Gasser SM. Ino80 chromatin remodeling complex promotes recovery of stalled replication forks. *Curr Biol* 18, 566-575 (2008).

REFERENCES

- Shirahige K, Hori Y, Shiraishi K, Yamashita M, Takahashi K, Obuse C, Tsurimoto T, Yoshikawa H. Regulation of DNA-replication origins during cell-cycle progression. *Nature* 395, 618-621 (1998).
- Sikorski RS, Hieter P. A system of shuttle vectors and yeast host strains designed for efficient manipulation of DNA in *Saccharomyces cerevisiae*. *Genetics* 122, 19-27 (1989).
- Simon M, Seraphin B, Faye G. KIN28, a yeast split gene coding for a putative protein kinase homologous to CDC28. *EMBO J* 5, 2697-2701 (1986).
- Smits VA, Klompmaker R, Arnaud L, Rijkse G, Nigg EA, Medema RH. Polo-like kinase-1 is a target of the DNA damage checkpoint. *Nat Cell Biol* 2, 672-676 (2000).
- Smolka MB, Albuquerque CP, Chen SH, Zhou H. Proteome-wide identification of in vivo targets of DNA damage checkpoint kinases. *Proc Natl Acad Sci U S A* 104, 10364-10369 (2007).
- Sogo JM, Lopes M, Foiani M. Fork reversal and ssDNA accumulation at stalled replication forks owing to checkpoint defects. *Science* 297, 599-602 (2002).
- Stelter P, Ulrich HD. Control of spontaneous and damage-induced mutagenesis by SUMO and ubiquitin conjugation. *Nature* 425, 188-191 (2003).
- Strebhardt K. Multifaceted polo-like kinases: drug targets and antitargets for cancer therapy. *Nat Rev Drug Discov* 9, 643-660 (2010).
- Stucki M, Clapperton JA, Mohammad D, Yaffe MB, Smerdon SJ, Jackson SP. MDC1 directly binds phosphorylated histone H2AX to regulate cellular responses to DNA double-strand breaks. *Cell* 123, 1213-1226 (2005).
- Sugawara N, Wang X, Haber JE. In vivo roles of Rad52, Rad54, and Rad55 proteins in Rad51-mediated recombination. *Mol Cell* 12, 209-219 (2003).
- Suter B, Fetchko MJ, Imhof R, Graham CI, Stoffel-Studer I, Zbinden C, Raghavan M, Lopez L, Beneti L, Hort J, Fillingham J, Greenblatt JF, Giaever G, Nislow C, Stagljar I. Examining protein protein interactions using endogenously tagged yeast arrays: the cross-and-capture system. *Genome Res* 17, 1774-1782 (2007).
- Svendsen JM, Smogorzewska A, Sowa ME, O'Connell BC, Gygi SP, Elledge SJ, Harper JW. Mammalian BTBD12/SLX4 assembles a Holliday junction resolvase and is required for DNA repair. *Cell* 138, 63-77 (2009).
- Szakal B, Branzei D. Premature Cdk1/Cdc5/Mus81 pathway activation induces aberrant replication and deleterious crossover. *EMBO J* 32, 1155-1167 (2013).
- Szankasi P, Smith GR. A role for exonuclease I from *S. pombe* in mutation avoidance and mismatch correction. *Science* 267, 1166-1169 (1995).
- Szostak JW, Orr-Weaver TL, Rothstein RJ, Stahl FW. The double-strand-break repair model for recombination. *Cell* 33, 25-35 (1983).
- Szyjka SJ, Aparicio JG, Viggiani CJ, Knott S, Xu W, Tavaré S, Aparicio OM. Rad53 regulates replication fork restart after DNA damage in *Saccharomyces cerevisiae*. *Genes Dev* 22, 1906-1920 (2008).
- Tay YD, Wu L. Overlapping roles for Yen1 and Mus81 in cellular Holliday junction processing. *J Biol Chem* 285, 11427-11432 (2010).
- Tanaka S, Umemori T, Hirai K, Muramatsu S, Kamimura Y, Araki H. CDK-dependent phosphorylation of Sld2 and Sld3 initiates DNA replication in budding yeast. *Nature* 445, 328-332 (2007).
- Taylor WR, Stark GR. Regulation of the G2/M transition by p53. *Oncogene* 20, 1803-1815 (2001).
- Tercero JA, Diffley JF. Regulation of DNA replication fork progression through damaged DNA by the Mec1/Rad53 checkpoint. *Nature* 412, 553-557 (2001).
- Thaminy S, Newcomb B, Kim J, Gatlinton T, Foss E, Simon J, Bedalov A. Hst3 is regulated by Mec1-dependent proteolysis and controls the S phase checkpoint and sister chromatid cohesion by deacetylating histone H3 at lysine 56. *J Biol Chem* 282, 37805-37814 (2007).
- Thomas BJ, Rothstein R. Elevated recombination rates in transcriptionally active DNA. *Cell* 56, 619-630 (1989).

REFERENCES

- Toczyski DP, Galgoczy DJ, Hartwell LH. CDC5 and CKII control adaptation to the yeast DNA damage checkpoint. *Cell* 90, 1097-1106 (1997).
- Toh GW, Sugawara N, Dong J, Toth R, Lee SE, Haber JE, Rouse J. Mec1/Tel1-dependent phosphorylation of Slx4 stimulates Rad1-Rad10-dependent cleavage of non-homologous DNA tails. *DNA Repair (Amst)* 9, 718-726 (2010).
- Toh-e A, Tanaka K, Uesono Y, Wickner RB. PHO85, a negative regulator of the PHO system, is a homolog of the protein kinase gene, CDC28, of *Saccharomyces cerevisiae*. *Mol Gen Genet* 214, 162-164 (1988).
- Tomlinson CG, Attack JM, Chapados B, Tainer JA, Grasby JA. Substrate recognition and catalysis by flap endonucleases and related enzymes. *Biochem Soc Trans* 38, 433-437 (2010).
- Torres-Ramos CA, Johnson RE, Prakash L, Prakash S. Evidence for the involvement of nucleotide excision repair in the removal of abasic sites in yeast. *Mol Cell Biol* 20, 3522-3528 (2000).
- Torres-Rosell J, Machín F, Farmer S, Jarmuz A, Eydmann T, Dalgaard JZ, Aragón L. SMC5 and SMC6 genes are required for the segregation of repetitive chromosome regions. *Nat Cell Biol* 7, 412-419 (2005).
- Trenz K, Smith E, Smith S, Costanzo V. ATM and ATR promote Mre11 dependent restart of collapsed replication forks and prevent accumulation of DNA breaks. *EMBO J* 25, 1764-1774 (2006).
- Ubersax JA, Woodbury EL, Quang PN, Paraz M, Blethrow JD, Shah K, Shokat KM, Morgan DO. Targets of the cyclin-dependent kinase Cdk1. *Nature* 425, 859-864 (2003).
- Ulrich HD, Jentsch S. Two RING finger proteins mediate cooperation between ubiquitin-conjugating enzymes in DNA repair. *EMBO J* 19, 3388-3397 (2000).
- Umezū K, Nakayama K, Nakayama H. *Escherichia coli* RecQ protein is a DNA helicase. *Proc Natl Acad Sci U S A* 87, 5363-5367 (1990).
- Vaze MB, Pellicioli A, Lee SE, Ira G, Liberi G, Arbel-Eden A, Foiani M, Haber JE. Recovery from checkpoint-mediated arrest after repair of a double-strand break requires Srs2 helicase. *Mol Cell* 10, 373-385 (2002).
- Wang H, Elledge SJ. Genetic and physical interactions between DPB11 and DDC1 in the yeast DNA damage response pathway. *Genetics* 160, 1295-1304 (2002).
- Waters LS, Minesinger BK, Wiltrout ME, D'Souza S, Woodruff RV, Walker GC. Eukaryotic translesion polymerases and their roles and regulation in DNA damage tolerance. *Microbiol Mol Biol Rev* 73, 134-154 (2009).
- Waters LS, Walker GC. The critical mutagenic translesion DNA polymerase Rev1 is highly expressed during G(2)/M phase rather than S phase. *Proc Natl Acad Sci U S A* 103, 8971-8976 (2006).
- Witkin EM, Roegner-Maniscalco V, Sweasy JB, McCall JO. Recovery from ultraviolet light-induced inhibition of DNA synthesis requires umuDC gene products in recA718 mutant strains but not in recA⁺ strains of *Escherichia coli*. *Proc Natl Acad Sci U S A* 84, 6805-6809 (1987).
- Wu L, Hickson ID. The Bloom's syndrome helicase suppresses crossing over during homologous recombination. *Nature* 426, 870-874 (2003).
- Wyatt HD, Sarbajna S, Matos J, West SC. Coordinated actions of SLX1-SLX4 and MUS81-EME1 for Holliday junction resolution in human cells. *Mol Cell* 52, 234-247 (2013).
- Yamaguchi T, Goto H, Yokoyama T, Silljé H, Hanisch A, Uldschmid A, Takai Y, Oguri T, Nigg EA, Inagaki M. Phosphorylation by Cdk1 induces Plk1-mediated vimentin phosphorylation during mitosis. *J Cell Biol* 171, 431-436 (2005).
- Yang J, Bachrati CZ, Ou J, Hickson ID, Brown GW. Human topoisomerase III α is a single-stranded DNA decatenase that is stimulated by BLM and RMI1. *J Biol Chem* 285, 21426-21436 (2010).
- Yang W, Woodgate R. What a difference a decade makes: insights into translesion DNA synthesis. *Proc Natl Acad Sci U S A* 104, 15591-15598 (2007).
- Yao S, Neiman A, Prelich G. BUR1 and BUR2 encode a divergent cyclin-dependent kinase-cyclin complex important for transcription in vivo. *Mol Cell Biol* 20, 7080-7087 (2000).
- Yeeles JT, Poli J, Marians KJ, Pasero P. Rescuing stalled or damaged replication forks. *Cold Spring Harb Perspect Biol* 5, a012815 (2013).

REFERENCES

- Yoo HY, Shevchenko A, Shevchenko A, Dunphy WG. Mcm2 is a direct substrate of ATM and ATR during DNA damage and DNA replication checkpoint responses. *J Biol Chem* 279, 53353-53364 (2004).
- You Z, Harvey K, Kong L, Newport J. Xic1 degradation in *Xenopus* egg extracts is coupled to initiation of DNA replication. *Genes Dev* 16, 1182-1194 (2002).
- Yu CE, Oshima J, Fu YH, Wijsman EM, Hisama F, Alisch R, Matthews S, Nakura J, Miki T, Ouais S, Martin GM, Mulligan J, Schellenberg GD. Positional cloning of the Werner's syndrome gene. *Science* 272, 258-262 (1996).
- Yu X, Chini CC, He M, Mer G, Chen J. The BRCT domain is a phospho-protein binding domain. *Science* 302, 639-642 (2003).
- Yuen KW, Warren CD, Chen O, Kwok T, Hieter P, Spencer FA. Systematic genome instability screens in yeast and their potential relevance to cancer. *Proc Natl Acad Sci U S A* 104, 3925-3930 (2007).
- Zaidi IW, Rabut G, Poveda A, Scheel H, Malmström J, Ulrich H, Hofmann K, Pasero P, Peter M, Luke B. Rtt101 and Mms1 in budding yeast form a CUL4(DDB1)-like ubiquitin ligase that promotes replication through damaged DNA. *EMBO Rep* 9, 1034-1040 (2008).
- Zegerman P, Diffley JF. Phosphorylation of Sld2 and Sld3 by cyclin-dependent kinases promotes DNA replication in budding yeast. *Nature* 445, 281-285 (2007).
- Zegerman P, Diffley JF. Checkpoint-dependent inhibition of DNA replication initiation by Sld3 and Dbf4 phosphorylation. *Nature* 467, 474-478 (2010).
- Zhang T, Nirantar S, Lim HH, Sinha I, Surana U. DNA damage checkpoint maintains CDH1 in an active state to inhibit anaphase progression. *Dev Cell* 17, 541-551 (2009).
- Zhou BB, Elledge SJ. The DNA damage response: putting checkpoints in perspective. *Nature* 408, 433-439 (2000).
- Zhu Z, Chung WH, Shim EY, Lee SE, Ira G. Sgs1 helicase and two nucleases Dna2 and Exo1 resect DNA double-strand break ends. *Cell* 134, 981-994 (2008).
- Zou L, Elledge SJ. Sensing DNA damage through ATRIP recognition of RPA-ssDNA complexes. *Science* 300, 1542-1548 (2003).
- Zou L, Liu D, Elledge SJ. Replication protein A-mediated recruitment and activation of Rad17 complexes. *Proc Natl Acad Sci U S A* 100, 13827-13832 (2003).

8 ABBREVIATIONS

2D	two-dimensional
4-NQO	4-Nitroquinoline 1-oxide
aa	amino acid
AAD	ATR-activating domain
AD	Gal4 activation domain
Ade	adenine
APS	ammonium persulfate
Arg	arginine
Asp	aspartate
BD	Gal4 binding domain
BER	base excision repair
bp	base pair
BRCT	BRCA1 carboxy terminal
BTR	BLM-TOPOIII α -RMI1 complex
C	Celsius
C-terminal	carboxy terminal
C-terminus	carboxy terminus
CAN	canavanine
CDK	cyclin-dependent kinase
CMK	chloromethylketone
CO	crossover
CoIP	co-immunoprecipitation
CPT	camptothecin
DDR	DNA damage response
DDT	DNA damage tolerance
DMSO	dimethylsulfoxide
DNA	deoxyribonucleic acid
dNTP	deoxynucleoside triphosphate
DSB	double-strand break
dsDNA	double-stranded DNA
DTT	dithiothreitol
EDTA	ethylenediaminetetraacetic acid
FACS	fluorescence-activated cell sorting
g	gram
G1	gap 1 phase of the cell cycle
G2	gap 2 phase of the cell cycle
G418	geneticin
GAL	galactose
Glu	glutamine
h	hour(s)
H3	histone 3
His	histidine
HJ	Holiday junction
HO	HO endonuclease
Hph	hygromycin
HR	homologous recombination

ABBREVIATIONS

HU	hydroxyurea
INT	integrative
IP	immunoprecipitation
JM	joined molecule
K	lysine
kb	kilo base pairs
l	liter
LB	Luria-Bertani
leu	leucine
log	logarithmic
Lys	lysine
M	molar
m	milli ($\times 10^{-3}$)
μ	micro ($\times 10^{-6}$)
M-phase	mitosis phase of the cell cycle
min	minute(s)
MMR	mismatch repair
MMS	methyl methanesulfonate
MRX	Mre11-Rad50-Xrs2 complex
MS	mass spectrometry
n	nano ($\times 10^{-9}$)
N-terminal	amino terminal
N-terminus	amino terminus
NAT	noursethricin
NCO	non-crossover
NER	nucleotide excision repair
NHEJ	non-homologous end joining
NLS	nuclear localization signal
OD	optical density
ON	over night
ORF	open reading frame
P	proline
PAGE	polyacrylamide gel electrophoresis
PBD	Polo-box domain
PCNA	proliferating cell nuclear antigen
PCR	polymerase chain reaction
PEG	polyethylene glycol
PFGE	pulsed-field gel electrophoresis
Phe	phenylalanine
PLK	Polo-like kinase
pS	phosphorylated serine
pT	phosphorylated threonine
PTM	post-translational modification
RNase	ribonuclease
rNMP	ribonucleotide monophosphates
RPA	replication protein A
rpm	rounds per minute
PRR	post-replication repair
S	serine
s	second(s)

ABBREVIATIONS

S-phase	synthesis phase of the cell cycle
SC	synthetic complete
SDS	sodium dodecylsulfate
Ser	serine
SLIC	sequence- and ligation-independent cloning
Smc	structural maintenance of chromosome
SSA	single-strand annealing
ssDNA	single-stranded DNA
STR	Sgs1-Top3-Rmi1 complex
T	threonine
TBST	tris-buffered saline with Tween-20
TCA	trichloroacetic acid
TE	Tris-EDTA
TEMED	tetramethylethylenediamine
Thr	threonine
TLS	translesion synthesis
Top3	topoisomerase 3
Tris	Tris(hydroxymethyl)aminomethane
Tyr	tyrosine
UV	ultraviolet light
V	Volt
Val	valine
v/v	volume per volume
WT	wild type
w/v	weight per volume
Y2H	yeast two hybrid
YPD	yeast bacto-peptone dextrose

9 ACKNOWLEDGEMENTS

First, I would like to express my deep gratitude to Boris Pfander, my research supervisor, for his patient guidance, enthusiastic encouragement and useful critiques of this research work. One simply could not wish for a better or friendlier supervisor.

I would also like to express my very great appreciation to Stefan Jentsch, my “Doctorvater” and TAC member, for being generous, kind and inspiring.

Moreover, I would like to thank Aloys Schepers, my TAC member, for his great interest in my project and helpful advice.

I would like to offer my special thanks to the members of the doctoral thesis committee for refereeing my thesis.

I thank our collaborators, Dana Branzei, Barnabas Szakal, Michael Lisby, Joao Matos, for a significant contribution to the success of this project.

Furthermore, I would like to kindly acknowledge Lissa N. Prinz for a great work on the project together.

I would also like to extend my thanks to Uschi Kagerer, the technician of the laboratory, and Jochen Rech, Alexander Strasser, Ulla Cramer, Massimo Bossi and Ruzica, the technicians of the department, for their valuable technical support.

I wish to thank to Klara Schwander for her help and assistance in administrative work.

Special thanks should be given to IMPRS coordination office, Hans-Joerg, Ingrid and Maxi, for their enormous help in all aspects during PhD.

In addition, I say thank you to all members of Pfander, Jentsch and Storchova labs for a friendly and cheerful atmosphere in the department.

I would like to express my sincere gratitude to Sean, Flo and Ivan for being friendly and supportive from the start of my PhD.

I would also like to thank Susi and Fabi for fruitful discussions with a cup of coffee.

Finally, I wish to thank my parents and my all family for their support and encouragement throughout my PhD.

10 CURRICULUM VITAE

Name Dalia Gritenaite
Date/Place of birth 14.03.1985, Panevezys, Lithuania
Address Klarastr. 22, 80636 Munich, Germany

Higher Education

Since 2011 **PhD** studies, Max Planck Institute of Biochemistry,
Martinsried/Munich, Germany
Thesis: “Characterization of the Dpb11-Slx4
complex and its role in DNA repair”
Supervisor: Dr. Boris Pfander

2008 – 2010 **M.Sc.** Genetics, Vilnius University,
Vilnius, Lithuania
GPA: 9.66 (10 is the highest, less than 5 - fail)
Thesis: “Development of a system for the expression of
Influenza virus neuraminidase proteins in yeast
Pichia pastoris”
Supervisor: Prof. Kestutis Sasnauskas

2004 – 2008 **B.Sc.** Molecular Biology, Vilnius University,
Vilnius, Lithuania
GPA: 9.27 (10 is the highest, less than 5 - fail)
Thesis: “Development of a system for the production of
chimeric nucleocapside-like particles in yeast”
Supervisor: Prof. Kestutis Sasnauskas

Publications

Gritenaite D. *, Princz L.N. *, Szakal B., Bantele S.C.S., Wendeler L., Schilbach S., Habermann B.H., Matos J., Lisby M., Branzei D. and Pfander B. (2014). A cell cycle-regulated Slx4-Dpb11 complex promotes the resolution of DNA repair intermediates linked to stalled replication. *Genes Dev.* 28, 1604-19 *equal contribution

Princz L.N.*, **Gritenaite D.***, Pfander B. (2014). The Slx4-Dpb11 scaffold complex: coordinating the response to replication fork stalling in S-phase and the subsequent mitosis. *Cell Cycle.* 14, 488-494 *equal contribution

Zvirbliene A., Kucinskaite-Kodze I., Juozapaitis M., Lasickiene R., **Gritenaite D.**, Russell G., Bingham J., Michalski W.P., Sasnauskas K. (2010). Novel monoclonal antibodies against Menangle virus nucleocapsid protein. *Arch Virol.* 155, 13-8